MOLECULAR BASIS OF CARDIAC FIBROBLAST RESISTANCE TO OXIDATIVE STRESS

A THESIS PRESENTED BY

LINDA PHILIP

TO

SREE CHITRA TIRUNAL INSTITUTE FOR MEDICAL SCIENCES AND TECHNOLOGY

TRIVANDRUM 695011

IN PARTIAL FULFILLMENT OF THE REQUIREMENTS FOR THE AWARD OF

DOCTOR OF PHILOSOPHY

2013

CERTIFICATE

I, Linda Philip, hereby certify that I had personally carried out the work depicted in the thesis entitled **"Molecular basis of cardiac fibroblast resistance to oxidative stress"**. No part of the thesis has been submitted for the award of any other degree or diploma prior to this date.

Date Linda Philip

Dr K Shivakumar
Division of Cellular and Molecular Cardiology
Sree Chitra Tirunal Institute for Medical Sciences and Technology
Thiruvananthapuram-695 011, India.

CERTIFICATE

This is to certify that Linda Philip, in the Division of Cellular & Molecular Cardiology of this Institute, has fulfilled the requirements of the regulations relating to the nature and prescribed period of research for the PhD degree of the Sree Chitra Tirunal Institute for Medical Sciences and Technology, Thiruvananthapuram. The study titled **"Molecular Basis of Cardiac Fibroblast Resistance to Oxidative Stress"** was carried out under my direct supervision. No part of the thesis has been submitted for the award of any other degree or diploma prior to this date.

Clearance was obtained from the Institutional Animal Ethics Committee for carrying out the study.

Date Dr K Shivakumar

The thesis entitled

MOLECULAR BASIS OF CARDIAC FIBROBLAST RESISTANCE TO OXIDATIVE STRESS

Submitted by

LINDA PHILIP

For the degree of

Doctor of Philosophy

of

SREE CHITRA TIRUNAL INSTITUTE FOR MEDICAL SCIENCES AND TECHNOLOGY
TRIVANDRUM

is evaluated and approved by

Dr K Shivakumar (Guide) (Examiner)

Acknowledgement

I consider myself privileged to have had the opportunity to carry out my doctoral studies in the Division of Cellular and Molecular Cardiology, Sree Chitra Tirunal Institute for Medical Sciences and Technology, Thiruvananthapuram, India. I thank Dr. K Radhakrishnan, Director, for extending support and excellent facilities required for research programs in this institute. I acknowledge the financial support received from the Council of Scientific and Industrial Research, India.

I owe a huge depth of gratitude to my mentor, Dr. K Shivakumar for his continued encouragement and constant support in my research program, which has helped me greatly in the successful completion of my studies. I consider it as a great opportunity to do my doctoral programme under his guidance and to learn from his research expertise.

I express my sincere thanks to Dr. Renuka Nair, Head of the Division of Cellular and Molecular Cardiology for her encouragement and advice. I wish to take this opportunity to thank all the members of my department for their kind support.

I warmly thank Dr. T R Santhosh Kumar and Dr. N Jayakumari, the members of my Doctoral Advisory Committee for their help and co-operation. A special thanks to Dr. Jackson James and Dr. Ruby John Anto of Rajiv Gandhi Centre for Biotechnology, Thiruvananthapuram for the help extended to me during the course

of my work. My sincere thanks are due to Ms. Vasanthi and Mr. Liji of the Medical Illustration Unit, SCTIMST.

I appreciate the goodwill extended to me by all my friends and a word of thanks would be far too inadequate to express the gratitude I have for them. I am extremely fortunate to have a loving family that was a pillar of strength and support to me at all occasions, which has been crucial in the progress of my studies. Above all, I owe it to the Lord Almighty for granting me this opportunity and enabling me to achieve this goal.

Contents

List of Figures

ABBREVIATIONS

AIF	Apoptosis-inducing factor
Ang II	Angiotensin II
APAF-1	adaptor molecule protease-activating factor 1
AT1 receptor	Angiotensin II type 1 receptor
bFGF	Basic fibroblast growth factor
BSA	Bovine serum albumin
BIR	baculoviral repeat domain
CARD	caspase recruitement domain
(c-FLIP)	cellular FLICE (FADD-like IL-1beta-converting enzyme)-inhibitory protein
cIAP-2	cellular inhibitor of apoptosis protein-2
DEPC	Diethyl pyrocarbonate
DMSO	Dimethyl sulfoxide
DDR2	Discoidin domain receptor 2
DNase	deoxyribonuclease
ECM	Extracellular matrix
ECs	Endothelial cells
EMSA	Electrophoretic mobility shift assay
EMT	Epithelial-to-mesenchymal transformation
EndoG	Endonuclease G
eNOS	endothelial nitric oxide synthase
ET 1	Endothelin 1
EPDCs	Epicardial-derived cells
ERK1/2	Extracellular signal regulated kinase 1/2
FITC	Fluorescein isothiocyanate
HRP	Horse Radish peroxidase
Hsp	Heat shock protein
JNK	Jun-N-terminal kinase
IAP	Inhibitor of apoptosis protein
IGF	Insulin-like growth factor
iNOS	inducible nitric oxide synthase
IκB	Inhibitory-kappa B
IL	Interleukin
MAPK	Mitogen-activated protein kinase
MEM	Minimal essential medium
MMPs	Matrix metalloproteinases
MPT	mitochondrial permeability transition
NAIP	Neuronal apoptosis inhibitory protein
NF-κB	Nuclear factor-kappa B
NIK	NF-κB-inducing kinase
PARP	Poly(ADP ribose) polymerase
pCMV	Cytomegalovirus plasmid
PEO	Proepicardial organ
PI	Propidium iodide
PI3K	Phosphoinositide 3-kinase

RING	really interesting new gene
ROS	Reactive oxygen species
Smac/DIABLO	Second mitochondrial derived activator of caspases/ direct IAP-binding protein with low pI
TIMPs	tissue inhibitors of matrix metalloproteinases
TGF-β	Transforming growth factor-β
TNF-α	Tumour necrosis factor-α
TNFR	Tumour necrosis factor receptor
VEGF	Vascular endothelial growth factor
VSMCs	Vascular smooth muscle cells
XIAP	X-linked inhibitor of apoptosis protein

SYNOPSIS

Cardiac fibroblasts, the principal stromal cell type in the heart, are a major source of extracellular matrix proteins like collagen types I and III, fibronectin, matrix metalloproteinase, growth factors and cytokines. Unlike myocytes that have limited replicative capacity, cardiac fibroblasts retain their proliferative potential throughout life. Under conditions of myocardial injury, quiescent cardiac fibroblasts get transformed into a myofibroblast phenotype that is equipped with enhanced proliferative, migratory and secretory properties, which enable them to orchestrate wound healing *post injury*. This implies that cardiac fibroblasts are uniquely programmed to survive cell death signals that compromise viability of co-resident cells in the heart. In all organs, apoptosis of activated myofibroblasts marks the culmination of the healing response but, surprisingly, apoptosis of activated myofibroblasts fails to occur in the heart. This results in disproportionate stromal accumulation that compromises ventricular compliance and contributes to the onset and progression to heart failure. Further, several *in vitro* studies show that cardiac fibroblasts are relatively refractory to pro-apoptotic stimuli like staurosporine, hypoxia and nutrient deprivation.

Barring a single study that links cardiac fibroblast resistance to constitutively expressed Bcl-2, the factors and mechanisms that contribute to the survival of cardiac fibroblasts under stress conditions remain obscure. In this regard, recent studies from our laboratory stress the pro-survival role of Nuclear factor-κB (NF-κB) in hypoxic cardiac fibroblasts via induction of anti-apoptotic cIAP-2, a member of the Inhibitor of apoptosis family of proteins. Against this backdrop, this study focused on the molecular basis of cardiac fibroblast resistance to oxidative stress, a

major component of ischemia-reperfusion injury and congestive heart failure. The study focused on the regulation and role of cIAP-2 in apoptosis resistance in cardiac fibroblasts exposed to H_2O_2, which is a widely used experimental model to study oxidative stress. It was found that cIAP-2 is strikingly up-regulated in cardiac fibroblasts in response to H_2O_2-mediated oxidative stress. Further, ERK1/2 may mediate activation of NF-κB-dependent up-regulation of cIAP-2 to constitute a potent anti-apoptotic mechanism in cardiac fibroblasts under oxidative stress.

Methods

Cardiac fibroblasts were isolated from the ventricular tissue of young adult Sprague Dawley (2-3 months) rats by a series of enzymatic digestions using collagenase, trypsin, pancreatin and DNase. Confluent cultures of cardiac fibroblasts exposed to hydrogen peroxide were used as the experimental model. Viability analysis, ROS measurement by H_2DCFDA, western blot, electrophoretic mobility shift assay, Taqman quantitative real-time PCR analyses, gene knockdown by RNA interference and forced expression of cIAP-2 using a pCMV promoter system were performed following standard protocols. Statistical significance was assessed using Student's *t*-test and $p \leq 0.05$ was considered significant.

Major findings

Cardiac fibroblasts are relatively resistant to oxidative stress-mediated injury

In the initial experiments, the response of cardiac fibroblasts to H_2O_2-mediated oxidative stress was compared with that of pulmonary fibroblasts (used as a reference). Cell viability analysis by Hoechst/Annexin/PI staining showed about 3%

and 10% viability loss at 25 µM and 50 µM H_2O_2, respectively, in cardiac fibroblasts. On the other hand, viability loss observed in pulmonary fibroblasts was 10% and 54% at 25 µM and 50 µM H_2O_2, respectively. Further, H_2DCFDA measurement of intracellular reactive oxygen species showed 2-fold and 3-fold increase in ROS generation in response to 25 µM and 50 µM H_2O_2 while in pulmonary fibroblasts, the increase was 40% and 80%, respectively.

cIAP-2 mediates apoptosis resistance in cardiac fibroblast exposed to H_2O_2

The relative resistance of cardiac fibroblasts to oxidative stress led to studies to probe the activation of anti-apoptotic mechanisms in cardiac fibroblasts. Constitutive levels of Bcl-2 were found in cardiac fibroblasts, which remain unchanged upon exposure to oxidative stress. But, interestingly, cIAP-2 expression was found to be strikingly up-regulated in response to H_2O_2. Real time PCR analysis revealed a 3-fold increase in cIAP-2 mRNA levels, which showed that cIAP-2 is transcriptionally up-regulated under conditions of oxidative stress. cIAP-2 knockdown by RNA interference compromised cardiac fibroblast viability significantly, as shown by Hoechst/PI staining. Enhanced PARP cleavage in cIAP-2-silenced cardiac fibroblasts further confirmed occurrence of apoptosis.

NF-κB-mediated cIAP-2 up-regulation promotes cardiac fibroblast resistance to oxidative stress-induced apoptosis

NF-κB is a stress-activated redox-sensitive transcription factor, which is known to regulate anti-apoptotic molecules, including cIAP-2, in different cell types. In the present study, H_2O_2-mediated oxidative stress was found by electrophoretic mobility

shift assay, to induce NF-κB activation in cardiac fibroblasts. Further, NF-κB inhibition resulted in 21% increase in Annexin/PI uptake, which was further confirmed by appearance of cleaved PARP. NF-κB inhibition significantly attenuated cIAP-2 mRNA transcript and protein expression levels, suggesting that the pro-survival role of NF-κB may be mediated by cIAP-2.

Forced expression of cIAP-2 in NF-κB-inhibited cardiac fibroblasts exposed to oxidative stress attenuates viability loss

Since cIAP-2 induction in cardiac fibroblasts is NF-κB-dependent, strong constitutive expression of cIAP-2 under a pCMV promoter was induced in NF-κB-inhibited cells to confirm the pro-survival role of cIAP-2 in cardiac fibroblasts under oxidative stress. Over-expression of cIAP-2 attenuated loss of viability in NF-κB-inhibited cardiac fibroblasts substantially, stressing the centrality of cIAP-2 in cardiac fibroblast survival under stress.

ERK1/2 MAPK as modulator of cardiac fibroblast survival

ERK1/2 has been implicated in the regulation of cell proliferation, meiosis, mitosis and apoptosis in many cell types. In this study, significant loss of viability upon ERK1/2 inhibition was observed in cardiac fibroblasts exposed to H_2O_2, pointing to a role for ERK1/2 in regulating cell survival in cardiac fibroblasts exposed to oxidative stress. Activation of ERK1/2 was observed as early as 5 minutes following exposure to H_2O_2, which peaked at 15 minutes and was sustained upto 12 hours. cIAP-2 levels were down-regulated in ERK1/2-inhibited cells, clearly showing that ERK1/2 has a positive regulatory role on cIAP-2.

ERK1/2 phosphorylation leads to NF-κB activation and regulates cIAP-2 expression in response to oxidative stress

Inhibition of H_2O_2-induced NF-κB DNA binding activity in ERK1/2-inhibited cardiac fibroblasts exposed to H_2O_2 revealed that NF-κB activation is ERK-dependent. Inhibition of ERK1/2 also attenuated H_2O_2-induced IκBα degradation, indicating that IκBα-mediated NF-κB activation is ERK1/2-dependent. As it was also shown that ERK has a positive regulatory effect on cIAP-2, it can be concluded that cIAP-2 is up-regulated in cardiac fibroblasts by ERK1/2-dependent-NF-κB signaling pathway under conditions of oxidative stress.

Significance of the findings

This study throws light on the less-explored subject of apoptosis resistance in cardiac fibroblasts, which, in the short-term, enables these cells to resist death signals and play a central role in tissue repair following myocyte loss, but, in the long-term, may contribute to disproportionate stromal growth and consequent pump dysfunction.

I. Introduction

The heart is a highly organized structure made up of parenchyma and stroma. Cardiac parenchyma comprises cardiomyocytes that are capable of phasic contractility. Cardiomyocytes are terminally differentiated cells that constitute one-third of the myocardial cell population. The stromal compartment, on the other hand, is a dynamic metabolic entity composed of a complex network of structural extracellular matrix (ECM) proteins and non-myocytes, including endothelial cells (ECs), vascular smooth muscle cells (VSMCs) and fibroblasts (Laurent, 1987; Weber *et al.*, 1995). Cardiac fibroblasts constitute about 90% of stroma and two-thirds of the myocardial population. They are organized in a lamellar fashion, surrounding groups of myocytes and maintain contacts with each other, with cardiac myocytes and the ECM (Goldsmith *et al*., 2004). Such an arrangement equips cardiac fibroblasts to establish cell–cell and cell–ECM interactions and respond to diverse stimuli arising during several pathophysiological states within the myocardium (Kakkar *et al*., 2010). Cardiac fibroblasts are primarily responsible for the homeostatic maintenance of the ECM (Porter *et al*., 2009). They are the only intra-cardiac source of fibrillar collagen types I and III, and are a major source of matrix metalloproteinases (MMPs) and tissue inhibitors of matrix metalloproteinases (TIMPs). Over the years, it has become increasingly evident that they synthesize and secrete an array of bioactive molecules like growth factors, cytokines and immunomodulatory factors, which orchestrate wound healing *post injury* and act as an important determinant of myocardial remodeling in several cardiac pathologies (Brown *et al.*, 2005, Baudino *et al*., 2006, Porter *et al*., 2009).

I.1 Identification of the problem

I.1.1 Cardiac fibroblast resistance to apoptosis

In response to myocyte loss in the heart in several disease states, normally quiescent fibroblasts get activated to myofibroblasts, which converge on the site of myocyte injury to facilitate tissue healing *post injury* (Van den Borne *et al*., 2010). Activated myofibroblasts proliferate and mediate the deposition of ECM components such as collagen, fibronectin and laminin resulting in the formation of a scar (Sun *et al*., 2000). In non-cardiac tissues, wound repair is terminated by the orchestrated removal of activated myofibroblasts by programmed cell death, which underlies the progression of granulomatous tissue into a mature scar. However, myofibroblasts in the heart are reported to persist in the infarct scar long after the healing phase is completed (Sun *et al*., 2000). Several *in vitro* studies show that cardiac fibroblasts are relatively resistant to a variety of apoptotic stimuli like staurosporine, nutrient deprivation, hypoxia and oxidative stress (Zhang *et al*., 2001, Mayorga *et al*., 2004, Sangeetha *et al*., 2011). The relative resistance of cardiac fibroblasts to apoptosis may, in the short-term, enable these cells to resist death signals and play a central role in tissue repair following cardiomyocyte loss, but, in the long-term, the persistent population of myofibroblasts may act as an active "secretome" that generates angiotensin II (Ang II), angiotensin type 1 (AT1) receptor and fibrogenic growth factors like TGF-β1. These factors may act in tandem to promote excessive type 1 collagen deposition, resulting in fibrosis, which has serious adverse outcomes on contractility, arrythmogenecity and coronary vasomotor reactivity (Weber *et al*., 2013). Disproportionate stromal growth alters the vital balance between stroma and parenchyma (Takeda *et al*., 2010), which progressively leads to pump dysfunction.

Surprisingly, mechanisms underlying the relative resistance of cardiac fibroblasts to diverse death stimuli in the diseased heart remain largely unclear. In this regard, Mayorga *et al.,* 2004 examined the involvement of several pro- and anti-apoptotic factors, including Bcl-2, Bcl-X_L, Bid, Bax, Bak, Bim, XIAP and other apoptosis regulators in fibroblasts of cardiac and non-cardiac origin exposed to different apoptotic stimuli and concluded that Bcl-2 plays a predominant role in apoptosis resistance in cardiac fibroblasts under ambient stress (Mayorga *et al*., 2004). Notably, the study did not examine the role of cIAP-2 (Inhibitor of apoptosis-2) in cardiac fibroblast resistance to apoptosis. Given the plethora of pro-death signals that can prevail in the diseased heart, it is likely that cardiac fibroblast resistance to death signals may involve multiple factors and mechanisms. Consistent with such a postulation, recent studies in this laboratory demonstrated that Nuclear factor-κB (NF-κB) protects cardiac fibroblasts from hypoxic injury and presented correlation-based evidence that cIAP-2 may mediate the pro-survival role of NF-κB (Sangeetha *et al*., 2011). Against this backdrop, the present study was undertaken to evaluate the role and regulation of cIAP-2 in cardiac fibroblasts exposed to oxidative stress, which is a major stress stimulus associated with multiple pathological states of the heart.

I.1.2 Oxidative stress in the heart

The term oxidative stress is used to imply a condition in which the cell encounters excessive levels of molecular oxygen or chemical derivatives of oxygen called reactive oxygen species (ROS). Oxidative stress is implicated in the heart under several pathological conditions like left ventricular hypertrophy, myocardial infarction, reperfusion injury, congestive heart failure and also in cardiomyopathies like anthracycline-induced cardiomyopathy and lethal dilated cardiomyopathy (Mallat *et al*., 1998, Sabri *et al*., 2003, Misra *et al*., 2009). Notably, cardiac myocytes are susceptible to oxidative injury (Zhang *et al*., 2001),which can be a causal component of decompensatory remodeling, contributing to the progression to heart failure (Foo *et al*., 2005). In contrast, cardiac fibroblasts are shown to be relatively resistant to oxidative injury (Zhang *et al*., 2001).

Whether a cell succumbs to a stress condition or recruits survival mechanisms that enable it to tide over the stress stimuli depends entirely upon the cellular milieu that determines its apoptotic threshold, intensity of the stress stimulus and activation of survival pathways (Kracikova *et al*., 2013). Survival signaling may either be by the down-regulation of pro-apoptotic factors or recruitment of anti-apoptotic factors that specifically target the apoptotic machinery at different points.

I.1.3 Apoptotic pathways

Apoptosis or programmed cell death is an essential physiological process that plays cardinal role in tissue patterning during embryogenesis, programmed removal of damaged cells and in determining the fate of end-stage differentiated cells as part of

physiological turnover of cells (William *et al*., 2002). However, dysregulated apoptosis is implicated in diverse pathological conditions. At the molecular level, apoptosis is executed by a class of enzymes called caspases, cysteinyl aspartate-specific proteases (Earnshaw *et al*., 1999), which may be activated either by the death receptor-mediated (extrinsic) pathway or mitochondria-mediated (intrinsic) pathway (Yigong *et al*., 2004, Empel *et al*., 2005).

I.1.4 Anti-apoptotic mechanisms activated upon exposure to ambient stress

Anti-apoptotic mechanisms may interfere with the apoptotic machinery at multiple points. Anti-apoptotic molecules can exert their action by binding to components of the apoptosome complex in the intrinsic mode of apoptosis and blocking the activation of procaspase 9 or by blocking the release of pro-apoptotic factors from mitochondria into cytosol or may act as endogenous modulators of caspases (Beere *et al*., 2000, Crow *et al.*, 2004, Hunter *et al*., 2007). In this regard, the IAP family of proteins are dynamic regulators of apoptosis that act by inhibiting caspases 3, 7 and 9 and blocking both the extrinsic and intrinsic pathways of apoptosis. The IAPs are characterized by one or more 70–80 amino-acid baculoviral IAP repeat (BIR) domains at the N-terminal domain, which is essential to mediate its anti-apoptotic effects (Silke & Meier, 2013). IAPs also possess E3 ubiquitin ligase activity (Mace *et al*., 2010), which mediates the proteolytic degradation of apoptogenic factors like Smac/DIABLO released into cytosol as a result of any apoptotic stimuli.

It has been shown that IAP is under the regulatory control of NF-κB, which is a stress-activated transcription factor (Lee *et al*., 2001, Salvesan *et al*., 2002). NF-κB

is activated in the heart in response to various stimuli including ischemia, ROS and inflammatory cytokines during heart failure (Frantz *et al*., 2006). NF-κB regulates genes involved in the synthesis of cytokines and chemokines associated with inflammation, cell cycle progression, apoptosis and cell survival (Chin *et al*., 1999, Lin & Karin, 2003). Depending on the cell type and stress stimuli, NF-κB mediates expression of pro- or anti-apoptotic proteins. The NF-κB family comprises five major members: RelA (p65), NF-κB1 (p50/p105), NF-κB2 (p52/p100), c-Rel and RelB. Each member of the NF-κB family, except RelB, can form homodimers as well as heterodimers with one another. NF-κB dimers are localized cytosolically by its inhibitory binding with a class of molecules called Inhibitor of κB proteins (IκB). Upon activation, IκB gets proteolytically cleaved, allowing NF-κB to translocate to the nucleus and mediate transcriptional regulation of its target genes.

NF-κB activation is regulated by mitogen-activated protein kinases (MAPKs), a class of protein kinases that integrate signals from diverse stimuli and elicit appropriate physiological responses like proliferation, differentiation, survival or apoptosis. Three MAPK families have been clearly characterized: namely, classical MAPK (also known as ERK1/2-extracellular signal-regulated kinase or p44/42 MAPK), c-Jun N-terminal kinase/ stress-activated protein kinase (JNK/SAPK) and p38 MAPK. MAPKs are reported to mediate post-translational modification of NF-κB that modulates its DNA binding and oligomerization properties (Jeffries *et al*., 2000). ERK1/2-dependent NF-κB activation is known to regulate expression of cell cycle protein, GADD45β (Wang *et al*., 2005), and anti-apoptotic Bcl-2 (Kurland *et al*., 2003). Further, phosphoinositide 3-kinase (PI3K) is implicated in the regulation of

XIAP (Dan *et al*., 2004). MAPKs like ERK1/2, JNK and p38 MAPK are reported to regulate cIAP-1 and cIAP-2 in human endothelial cells in response to TNF-α by an NF-κB-independent mechanism (Furusu *et al*., 2007). ERK1/2, which is mainly involved in the regulation of cell proliferation and other post-mitotic functions in differentiated cells, translationally up-regulates cIAPs by blocking the mitochondrial release of Smac/DIABLO in small cell lung cancer cells (Pardo *et al*., 2003). However, a role for ERK1/2 in NF-κB-mediated transcriptional up-regulation of cIAP-2 has not been reported.

I.2 Broad objective of the study

Against this backdrop, the major goal of this study was to delineate the survival mechanisms recruited in adult rat cardiac fibroblasts *in vitro* in response to H_2O_2-mediated oxidative stress, focusing on the pro-survival role of cIAP-2 and its regulation by NF-κB and ERK1/2.

I.3 Specific questions addressed in the study:

- Are cardiac fibroblasts relatively resistant to oxidative stress compared to fibroblasts of non-cardiac origin?
- Does cIAP-2 play a pro-survival role in cardiac fibroblasts exposed to oxidative stress?
- Does NF-κB play a role in apoptosis resistance in cardiac fibroblasts exposed to oxidative stress? If so, what are the underlying mechanisms?
- Does ERK1/2 have a pro-survival role in cardiac fibroblasts under oxidative stress? If so, what are the underlying mechanisms?

I.4 Major finding:

Using a combination of Real Time PCR, western blot analysis and knockdown and knock-in strategies, this study shows for the first time that ERK1/2-dependent activation of NF-κB and consequent induction of cIAP-2 protects cardiac fibroblasts from oxidative damage.

II. Review of Literature

Myocardial function is regulated by the co-ordinated and dynamic interaction between two inter-dependent compartments of the heart, parenchyma and stroma. Parenchyma comprises the functional cell type of the heart, the myocyte, while stroma is the connective tissue scaffold in which the non-myocytes reside (Nag, 1980, Harvey &Rosenthal, 1999, Camelliti *et al*., 2005, Baudino *et al.*, 2006). Generally, cardiac myocytes account for one-third of the cell population in the heart and are responsible for its contractile function (Walker *et al*., 1999). Stroma, on the other hand, constitutes two-thirds of the cell population of the heart, which comprises non-myocytes like fibroblasts, ECs, monocytes and VSMCs embedded in the framework of structural proteins of cardiac interstitium (Weber *et al*., 1995, Souders *et al*., 2009). Notably, more than 90% of the non-myocyte population is formed of cardiac fibroblasts.

II.1.Cardiac fibroblasts

Cardiac fibroblasts are cells of mesenchymal origin (Porter *et al*., 2009) that produce a variety of ECM components, including collagen types I, III, IV and VI and fibronectin (Eghbali *et al*., 1989, Gabbiani, 1998). They play an essential role under diverse pathophysiological states of the myocardium by contributing to cardiac growth, maintenance of myocardial structure and electro-mechanical function in the healthy and diseased myocardium (Camelliti *et al*., 2005).

II.1.1 Origin of cardiac fibroblasts

There are two major sources of cardiac fibroblasts: embryonic proepicardial organ (PEO) and circulating progenitor cells derived from adult bone marrow stem cells (Porter & Turner, 2009, Amerongen *et al*., 2008). The PEO is a sac-like vascular structure derived from coelomic mesothelium, located at the venous inlet (sinuatrial) pole of the heart (Wessels *et al.,* 2004). Cells originate from the PEO and form the embryonic epicardium, which later undergoes epithelial-to-mesenchymal transformation (EMT) to form epicardial-derived cells (EPDCs), the immediate progenitors of cardiac fibroblasts. Apart from EPDCs, cardiac fibroblasts also originate from postnatal recruitment of circulating fibroblast progenitor stem cells into the ventricular myocardium (Visconti *et al*., 2006).

II.1.2 Structural organization of cardiac fibroblasts

Cardiac fibroblasts lie within the endomysial collagen network surrounding groups of myocytes in a lamellar fashion (Camelliti *et al*., 2005). Such an arrangement helps maintain structural and functional integrity through cell-cell and cell-ECM interactions (Kanekar *et al.,* 1998). This enables cardiac fibroblasts to contract the endomysial collagen network, exerting force on myocytes. Cardiac fibroblast-ECM interaction is established through integrins and discoidin domain receptor 2 (DDR2), a collagen receptor specifically expressed in cardiac fibroblasts (Goldsmith *et al*., 2004) while intercellular communication occurs through two families of cell surface proteins – connexins (Cx) and cadherins. Heterotypic interactions between fibroblasts and myocytes are mediated through Cx43 while fibroblast-fibroblast

(homotypic) interactions are through Cx45 (Camelliti *et al.*, 2005, Banerjee *et al.*, 2006).

II.1.3 Functions of cardiac fibroblasts in the myocardium

II.1.3.1 Cardiac fibroblasts in the normal myocardium

In the normal heart, cardiac fibroblasts are primarily responsible for steady state turnover of ECM by controlling the synthetic and degradative aspects of ECM metabolism. Cardiac fibroblasts are the only intra-cardiac source of fibrillar collagen types I and III along with smaller amounts of other collagens (IV, V, VI), elastin, proteoglycans, glycoproteins, cytokines, growth factors, and proteases (Corda *et al*., 2000; Bowers *et al*., 2009). Collagen serves to maintain normal cardiac architecture that assists in coordinating the contractile capacity of myocytes. In the normal heart, synthesis of collagen is low but is markedly up-regulated in the failing heart (Weber, 1989). Cardiac fibroblasts are also a major source of MMPs (proteolytic enzymes that degrade collagen) and TIMPs that are involved in ECM turnover within the heart (Weber *et al*., 1995).

Cardiac fibroblasts also serve as transitional sensors and amplifiers of stimuli originating from other cells of the myocardium, including myocytes and infiltrating immune cells (Zhao &Eghbali, 2001). Pro-inflammatory cytokines, mechanical stretch and altered oxygen levels act as stimuli for the production of growth factors (VEGF, bFGF, IGF-1), cytokines (IL-1β, IL-6, TNF-α, TGF-β), and other signaling molecules (Ang II, ET-1) by cardiac fibroblasts (Baudino *et al*., 2006; Porter & Turner, 2009; Souders *et al*., 2009).

II.1.3.2 Fibroblasts in cardiac pathology - role in myocardial remodeling

Cardiac remodeling, induced upon conditions of myocardial injury, refers to a sequence of events that trigger changes at the molecular, cellular and interstitial levels, resulting in alterations in ventricular shape and size (Kehat & Molkentin, 2010). A common type of myocardial remodeling triggered by different stress stimuli is myocyte hypertrophy, defined as increase in individual cell mass. Myocyte hypertrophy can be physiological, resulting from normal growth and exercise, or pathological, associated with various pathological states like chronic hypertension, valvular disease and ischemia (Weber *et al*., 1995, Bosman &Stamenkovic, 2003). However, pathological remodeling is not limited to hypertrophy of myocytes but encompasses the interstitial compartment of the myocardium as well. Myofibroblast proliferation in a setting of myocyte death leads to concomitant fibrosis and associated changes in the ECM (Konstam *et al*., 2011). Recent studies indicate that cardiac fibroblast, the principal stromal cell, is uniquely programmed to be at the centre of myocardial structural remodeling following injury (Porter *et al*., 2009).

- *Cardiac fibroblasts in wound healing*

Cardiac fibroblasts are key participants in the wound healing response, which includes hemostasis, inflammatory phase and formation of granulomatous scar that eventuates to a mature scar (Brown *et al.*, 2005). In the early adaptive phase of wound healing response, MMP/TIMP balance is altered that leads to changes in net proteolytic activity (Spinale, 2000), which in turn leads to ECM degradation. This allows the infiltration of inflammatory cells into the site of injury and clears the wound of dead myocytes and remnant cellular debris. In response to TGF-β1-

released at the site of injury by macrophages as part of the inflammatory response, cardiac fibroblasts undergo transition to myofibroblasts, characterized by increased expression of α-smooth muscle actin (Desmouliere *et al*., 1993). Cardiac fibroblasts chemotactically migrate from the wound margin into the zone of injury (Porter *et al*., 2009), and studies point to expression of frizzled-2 (fz2), a transmembrane protein that regulates tissue polarity and determines migration to the infarct area (Blankesteijn *et al.*, 1997). Fibrogenic phase ensues, which is characterized by accelerated synthesis of ECM proteins such as collagen types I and III, fibronectin and laminin resulting in scar formation.

- *Persistence of cardiac fibroblasts in mature infarct scar post repair*

Normally, culmination of the wound healing response process in non-cardiac tissues is associated with myofibroblast apoptosis, leading to the progression of granulomatous tissue to a mature scar (Gurtner *et al*., 2008). However, in the heart, myofibroblasts are reported to persist in the mature scar long after the tissue healing process is completed (Souders *et al*., 2009, Krenning *et al*., 2010). When cardiac fibroblasts do not get eliminated from the mature infarct scar after repair, deposition of ECM components continues, which finally alters the relative proportions of parenchyma and stroma that reduces ventricular compliance (Souders *et al*., 2009, Krenning *et al*., 2010) and leads to pump dysfunction. In this regard, a large number of *in vitro* studies show that cardiac fibroblasts are relatively resistant to pro-apoptotic stimuli that are known to prevail in pathophysiologic states of the myocardium (Zhang *et al*., 2001, Mayorga *et al*., 2004). Surprisingly, mechanisms

underlying the resistance of cardiac fibroblasts to several pro-death signals and their insensitivity to apoptosis regulatory mechanisms remain unclear (Krenning *et al*., 2010).

II.2 Cell death

Cell survival is determined by an intrinsic balance between factors contributing to survival and death. Cell death associated with embryonic development is essential for successful organogenesis. Programmed death of cells in adult organisms helps maintain cellular homeostasis. However, pathological situations also trigger cell death, which may significantly impact organ function.

There are three morphologically and biochemically distinct forms of cell death (Mani, 2008), namely autophagic cell death, necrosis and apoptosis.

II.2.1 Autophagic cell death

Autophagy is an evolutionarily conserved self-digesting mechanism for cellular components (Scarlatti *et al*., 2009). Autophagy is primarily cytoprotective in nature as it aids in clearing out misfolded, damaged proteins and yields new pools of amino acids, fatty acids, nucleosides for anabolic processes and drives a continuous flow of material in the cell in a degradation-regeneration cycle. It also serves to provide energy under conditions of nutrient starvation. The cytoplasmic contents are sequestered within double-membrane vacuoles called autophagosomes, which are subsequently delivered to lysosomes that contain acidic hydrolases like peptidases,

lipases and nucleases (Wirawan *et al*., 2012). However, loss of regulation of bulk macroautophagy can prime self-destruction by cells.

Autophagy employs 2 conjugation systems: Atg12-Atg5 and Atg8 (microtubule-associated protein 1 light chain 3 [LC3])–phosphatidylethanolamine system. Formation of autophagosomes depends on(1) the assembly of a lipid kinase signaling complex comprising class III PI3K that mediates nucleation of the pre-autophagosomal membrane (phagophore or isolation membrane) and (2) two ubiquitin-like conjugation pathways that stimulate expansion of the isolation membrane (Klionsky, 2005).

II.2.2 Necrotic cell death

The hallmark of necrosis is the loss of membrane integrity and spillage of intracellular contents into the surrounding mileu, usually triggering an inflammatory response (Schweichel & Merker, 1973). It occurs generally in response to physico-chemical stress like ischemia/reperfusion injury and nutrient deprivation. Massive degree of necrosis takes place at the core of myocardial infarct. Catastrophic energy depletion, Ca^{2+} accumulation and increase in availability of ROS are the stimuli that trigger necrosis. Execution of necrosis is mediated by calpains and lysosomal cathepsins that cause proteolysis and cellular destruction (Mani *et al.*, 2008).

II.2.3 Apoptotic cell death

Apoptosis is an evolutionarily conserved, energy-consuming process aimed at eliminating cells in an organized manner without eliciting an inflammatory response (Mani *et al*., 2008). It is essential for embryo development, maintenance of immune-tolerance and tissue remodeling. Morphologically, apoptosis is characterized by membrane blebbing, chromatin condensation and nuclear margination (Kerr, 1971). Finally, the cytosolic and organellar remnants are pinched off into membrane-enclosed apoptotic bodies that are phagocytosed by either macrophages or neighboring cells and degraded within their phagolysosomes. Notably, every cell possesses apoptotic machinery and is capable of undergoing self-destruction in the event of an irreparable injury incurred during any disease condition (Mani *et al*., 2008).

II.2.3.1 Apoptosis in the heart

- *Under physiological conditions (during development)*

During the early stages of heart development, there are two main foci of apoptosis: outflow tract and atrioventricular endocardial cushions. Apoptosis at these sites contributes to the formation of septa and valves of the mature heart (Keyes *et al*., 2002). Regulated occurrence of apoptosis leads to the formation of cardiac chambers and correct routing of blood vessels. Post-natally, apoptosis of myocytes in outflow tract facilitates the transition from fetal to post-natal circulation. During the course of embryonic growth, apoptosis of small round pacemaker cells occurs, the delay or failure of which can lead to life-threatening conditions like arrhythmias. On the other

hand, excessive apoptosis can lead to sudden cardiac death due to bradyarrhythmias (Kam *et al.*, 2000).

- *Under pathophysiological conditions*

Evidence from both human and animal studies shows that apoptosis is an important mode of cell death under conditions of anthracycline-induced cardiotoxicity (Montaigne *et al*., 2012) and heart failure. Studies in animal models of ischemia, ischemia–reperfusion as well as human myocardial infarction demonstrate apoptosis in 5–30% of cells in the infarct zone and the immediate peri-infarct penumbra (Wencker *et al*., 2003). The overloading of adult myocytes induces hypertrophic response as an initial compensatory response associated with up-regulation of c-myc and c-fos, which are also known to trigger apoptosis. This eventually leads to progressive functional deterioration of the hypertrophied left ventricle. Thus, apoptosis is a key modulator in the transition from compensatory hypertrophy to heart failure (Empel & Windt, 2005).

II.2.3.2 Molecular machinery of apoptosis

The key to understanding apoptosis is the activation and function of caspases, a group of cysteinyl aspartate-directed proteases. Caspases are synthesized either by scaffold-mediated trans-activation or upon cleavage by upstream proteases in an intracellular cascade (Earnshaw *et al*., 1999). These enzymes cleave intracellular proteins that disrupt survival pathways and disassemble the architectural components of the cell.

Caspases can be broadly classified into 2 major subfamilies: apoptotic caspases and inflammatory caspases. Inflammatory caspases are associated with immune responses to pathogens. They include caspase 1 and caspase 5, which get activated in response to assemblage of a complex called inflammasome (Martinon &Tschopp, 2007). These caspases mediate proteolytic activation of inflammatory cytokines like IL-1β and IL-18 (Martinon &Tschopp, 2004). On the other hand, apoptotic caspases orchestrate apoptotic events.

Cells undergoing apoptosis exhibit several changes like DNA cleavage, chromatin condensation, loss of mitochondrial membrane potential, changes in plasma membrane composition and formation of apoptotic bodies. Apoptotic caspases can be broadly classified into upstream initiator caspases (caspases 2, 8, 9, 10 and 12) and downstream effector caspases (caspases 3, 6, and 7). The activation of effector caspases is considered the final commitment step in the apoptotic cascade (Burguillos *et al.*, 2011). The proteolytic cascade is initiated either by ligation of death receptors exposed at cell surface (extrinsic pathway) or by intracellular death signals (intrinsic pathway) (Figure 1).

The major cytoplasmic targets of caspases include nuclear lamins, actin and actin-regulatory proteins like α-fodrin, spectrin and gelsolin, proteins involved in DNA synthesis and repair, like nuclear replication factor MCM3, the large subunit of DNA replication factor C and human Rad51, a protein involved in checkpoint activating in response to DNA damage (Rheaume *et al.*, 1997, Pest *et al.*, 2003). Further, the

nuclease DFF40/CAD, which cleaves the DNA into internucleosomal fragments (Sakahira *et al*., 1998), is also activated upon caspase activation.

The extrinsic pathway

The extrinsic/death receptor-mediated pathway is mediated by tumour necrosis factor (TNF)/ nerve growth factor receptor superfamily of proteins. These transmembrane proteins possess an extracellular ligand-interacting domain, a transmembrane domain and an intracellular death domain (Thorburn, 2004). Successful binding of ligand to extracellular domain causes oligomerization and activation of the receptor. Upon activation, the intracellular domain assembles with procaspase 8 to activate caspase 8. Activated caspase 8 propagates the apoptoic signal by stimulating downstream executioner caspases. The best-characterized death receptors are Fas (also called CD95 or Apo1) and TNFR1. Both receptors are present in cardiac myocytes (Ferrari *et al.,* 1995) and have been implicated in extensive cell death, which contributes to cardiovascular disease. Patients with end-stage congestive heart failure have also been shown to have elevated circulating levels of TNF-α, the ligand for TNFR1 (Testa *et al*., 1996).

The intrinsic pathway

Intracellular stress conditions like oxidative stress, serum deprivation and DNA damage trigger the intrinsic/mitochondrial mode of cell death. In this pattern of cellular death, multimerization on the adaptor molecule protease-activating factor 1 (APAF-1) within a multiprotein complex called apoptosome takes place that results in the activation of upstream caspase, caspase 9 (Shi, 2004). APAF-1 pre-exists in

the cytosol as a monomer, and its activation depends on the presence of cytochrome c (Jiang *et al*., 2004) and ATP/dATP (Rodriguez *et al*., 2002). The release of cytochrome c, which normally resides only in the inter-membrane space where it functions as an electron shuttle in the respiratory chain, is the rate-limiting step for the generation of the apoptosome. Hence, mitochondrial membrane permeabilization is the critical event responsible for caspase activation in the intrinsic pathway (Tait *et al*., 2010).

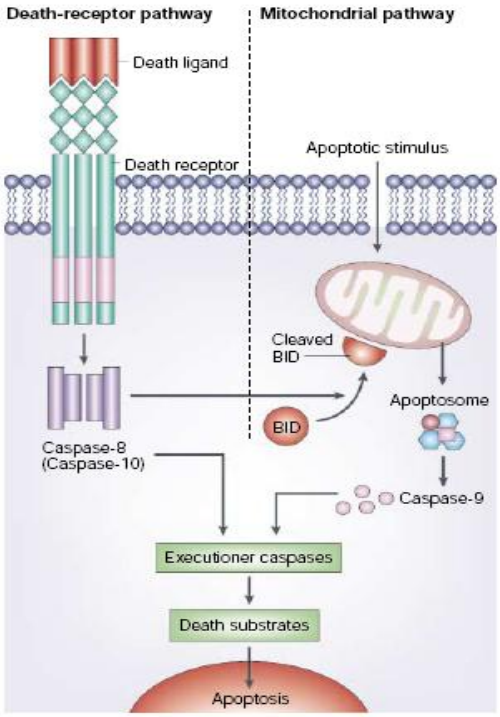

Ref: Igney FH and Krammer PH (2002) Death and anti-death: Tumour resistance to apoptosis, *Nature ReviewsCancer* 2: 277-288.

Figure 1: Illustration of the death-receptor-mediated (extrinsic) and mitochondrial (intrinsic) modes of apoptosis

The endoplasmic reticulum (ER) stress-mediated pathway

Stress conditions in the myocardium, like oxidative stress and ischemia, lead to accumulation of unfolded proteins that trigger unfolded protein response (UPR) in the endoplasmic reticulum. For instance, Okada *et al*., 2004 found that pressure overload by aortic constriction induced extensive ER stress during progression from cardiac hypertrophy to heart failure (Okada *et al*., 2004). The UPR reduces the accumulation of unfolded proteins by increasing ER-resident chaperones, inhibiting protein translation and accelerating the degradation of unfolded proteins. However, if stress is severe and/or prolonged, the ER finally initiates apoptotic signalling (Minamino &Kitakaze, 2010). Under ER stress, apoptosis may be triggered either via activated caspase 12 that can induce downstream caspase 3 (Szegezdi *et al*., 2006) or by the activation of a transcriptional program involving CHOP/GADD. CHOP activates transcription of genes encoding pro-apoptotic proteins including the BH3-only protein Puma (Breckenridge *et al*., 2003).

Cross-talk between apoptotic pathways

Activation of caspase 8 by the death receptor pathway directly activates executioner caspase 3, but also cleaves the BH3-only protein Bid at aspartate 60 position to generate a 15 kDa truncated form (tBid) that facilitates release of cytochrome c from the mitochondria (Luo *et al.*, 1998). The release of cytochrome c causes activation of caspase 9, which in turn activates caspase 3, thus amplifying the death signal from the plasma membrane.

Caspase-independent apoptotic pathways

The release of apoptosis inducing factor (AIF), AIF-homologous mitochondrion-associated inducer of death (AMID), cyclophilin D and endonuclease G (Endo G) have been shown to initiate caspase-independent mechanisms of cell death (Lorenzo & Susin, 2004). AIF and Endo G are located within the inter-mitochondrial membrane, which are released in response to apoptotic stimulus (Norberg *et al*., 2008). Once released into the cytosol, they directly/indirectly mediate DNA degradation. Granzymes, released by T-cells and natural killer cells cause cleavage of DNA, nuclear lamins and histones directly.microRNA, which are single stranded RNAs of 20-25 nucleotides transcribed from DNA, directly bind to functional mRNAs and block the translation of survival proteins, causing apoptosis (Crow *et al*., 2004).

II.2.3.3 Endogenous modulators of caspases

FLIP

Cellular FLICE (FADD-like IL-1beta-converting enzyme)-inhibitory protein (c-FLIP) is a catalytically inactive procaspase-8/10 homologue that associates with the signalling complex downstream of death-receptors and negatively interfering with apoptotic signalling (Scaffidi *et al*., 1999). Three c-FLIP splice variants have been identified: c-$FLIP_L$, c-$FLIP_S$ and c-$FLIP_R$, with all three functioning as apoptosis inhibitors involved in modulation of caspase 8/10 activity in both physiologic and pathologic contexts (Bagnoli *et al*., 2010). c-FLIP is also found to activate NF-κB and ERK by binding to adaptor proteins like TNFR-associated factors (TRAF1 and TRAF2), receptor-interacting protein 1(RIP) and Raf-1.

Heat shock proteins

Heat shock proteins are highly conserved proteins, which include both constitutively expressed forms like Hsp90, Hsp70 and Hsp60 and the induced forms like Hsp70 and Hsp27. They may have anti- and pro-apoptotic properties. Hsp70, for instance, can inhibit the formation of apoptosome by directly associating with Apaf-1 to prevent the recruitment and activation of the pro-caspase-9 (Beere *et al*., 2000). Hsp27 binds to cytochrome c released from the mitochondria to the cytosol and prevents cytochrome c-mediated interaction of Apaf-1 with procaspase-9. Thus, Hsp27 interferes specifically with the mitochondrial pathway of apoptosis (Bruey *et al*., 2000). Pandey *et al*., 2000 have reported that Hsp27 can also bind to procaspase-3 to prevent activation by caspase-9 (Pandey *et al*., 2000).

Bcl-2 family of proteins

Bcl-2 and Bcl-X_L are the two well studied anti-apoptotic members of the Bcl-2 family of proteins involved in programmed cell survival. Bcl-2 is constitutively localized in the outer mitochondrial membrane facing the cytoplasm, while a significant pool of Bcl-X_L is not membrane-bound. The ratio of anti-apoptotic Bcl-2 to pro-apoptotic Bax/Bak determines whether a cell lives or dies. Bcl-2/Bcl-X_L sequesters pro-apoptotic Bid from activating Bax/Bak and blocks these pro-apoptotic members from forming pores in the outer mitochondrial membrane and prevents release of apoptotic Smac/DIABLO/AIF/cytochrome C into the cytoplasm (Crow *et al.*, 2004). A certain threshold of growth factors is reported to sustain up-regulation of Bcl-2/Bcl-X_L expression within cells to prevent the early onset of death. Bcl-

2/Bcl-X_L is also reported to prevent cell death-induced by hypoxia by decreasing the production and action of ROS within cells (Shimizu *et al*., 1995).

Inhibitor of apoptosis family of proteins (IAP)

The inhibitor of apoptosis family of proteins is characterized by two defining features, namely

- BIR (Baculoviral Inhibitor of apoptosis repeat) domain at the amino terminal (Birnbaum *et al*., 1994) The BIR domains are multifaceted protein-protein interaction domains that facilitate binding to caspases and other proteins. BIR domains comprise 3 short β-strands and 4 α-helices that fold into a compact domain that includes a co-ordinated Zn ion. BIRs can be grouped into type-I and type-II domains based on the presence of a deep peptide-binding groove (Silke & Meier, 2013).
  - type-I BIR domains lack a peptide-binding groove
  - type-II BIR domains carry a hydrophobic cleft through which they bind to IAP-binding motifs (IBMs) present in caspases and IAP-inhibitory molecules like mammalian Smac/DIABlO and Omi/HtrA2 or Drosophila Reaper, Grim and Head Involution Defective (Hid), collectively known as IAP-antagonists.
- RING (Really Interesting New Gene) Zn finger domain at the carboxyl terminus. The RING Zn finger domain acts like an E3-ubiquitin ligase, transferring ubiquitin to several substrate proteins (Mace *et al*., 2010).

To date, 8 human IAP family members have been identified that have been classified into 3 classes - 1, 2 and 3 based on presence/absence of RING finger and homology of BIR domains (Schimmer *et al*., 2004).

a. Class I IAPs possess homologous BIR domains and a RING finger Zn motif. e.g., XIAP, cIAP-1, cIAP-2

b. Class II IAPs possess 3 BIR domains and no RING finger Zn motif. e.g., NAIP

c. Class III IAPs possess only one BIR domain and no RING finger Zn motif. e.g., Survivin

In addition to these, cIAP-1 and cIAP-2 possess an evolutionarily conserved caspase recruitement domain (CARD) between their 3 BIR domains and the RING finger domain. Recent studies show that the CARD domain can inhibit the intrinsic E3 ligase activity of IAP (Dueber *et al*., 2011; Lopez *et al*., 2011).

Functions of IAPs

1. Caspase inhibition

IAPs inhibit executioner caspases and suppress both mitochondria-dependent and -independent apoptosis (Hunter *et al*., 2007) and are a dynamic regulator of apoptosis in cells under conditions of ambient stress. IAPs have been shown to directly inhibit activated caspases 3 and 7. IAP is also known to inhibit procaspase 9 activation but not caspase 8. Interestingly, cIAP-1 and cIAP-2 protect cells from TNF-α-induced cell death by reducing the amount of caspase 8. Although caspase 8 is not a direct target of IAP, it is suggested that cIAP-1 and 2 could inhibit downstream caspases 3 and 7, thus blocking the feedback loop inhibiting further activation of caspase 8 (Verhagen e*t al*., 2001). Apart from its interaction with caspases, IAPs also serve to block apoptosis through their interaction with pro-apoptotic proteins like Hid, Reaper, Grim and Doom. IAPs are also involved in signal transduction pathways

activating NF-κB and JNK, thus sub-serving a pro-survival role (Silke& Meier, 2013).

Structural basis of caspase inhibition by XIAP

Many studies have focused on XIAP, as it can be produced in recombinant form and crystallized. Its BIR-2 domain with its NH_2-terminal extension inhibits caspases 3 and 7, whereas its BIR-3 domain inhibits caspase 9. A "hook, line and sinker" model has been proposed to explain how XIAP inhibits caspase 3 (Fig. 2). The "hook" (residues 138–146 of the NH_2 terminus) inhibits caspase 3 by lying across the active site of the caspase, thereby blocking the substrate-binding pocket of active caspase 3. The "line" represents two peptide bonds on Val147 that connect the hook to the sinker. The "sinker" (residues 148–150) stabilizes the interaction between XIAP and caspase 3. In this model, XIAP inhibits caspase 3 through steric hindrance. On the other hand, the BIR3 domain of XIAP forms a heterodimer with monomeric caspase 9, thereby preventing caspase 9 dimerization and activation (Shiozaki *et al*., 2003). In addition to trapping caspase 9 in a monomeric form, it also keeps the active site of caspase 9 in an inactive conformation (Shiozaki *et al*., 2003). Thus, it is interesting to note that XIAP inhibits caspase 9 without physically touching the active site.

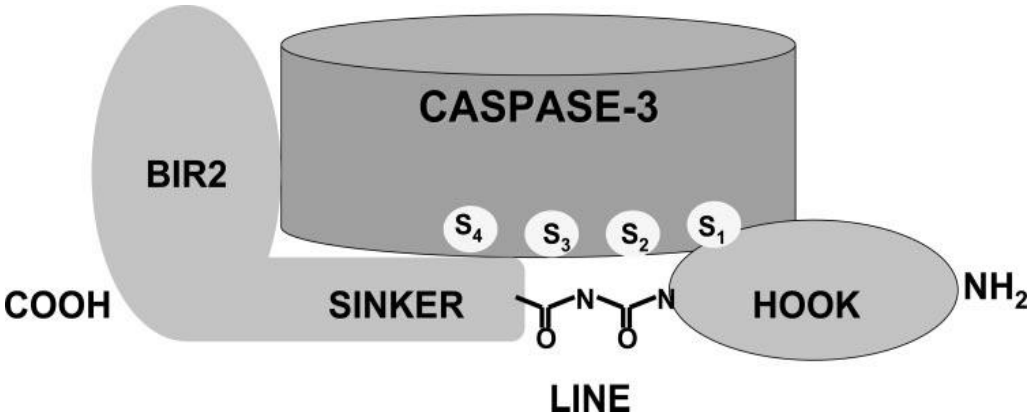

Ref: Schimmer AD (2004) Inhibitor of Apoptosis Proteins: Translating basic knowledge into clinical practice Cancer Research 64, 7183–7190.

Figure 2: Hook, line and sinker model showing interaction between XIAP and caspase 3

2. Beyond caspase inhibition

IAPs can inhibit apoptosis also through effects on cell cycle progression, cell division and signal transduction pathways.

IAPs regulate cell division: In mammalian cells, survivin co-localizes with the mitotic apparatus including β-tubulin and kinetochores. Silencing survivin results in delayed mitosis and produces shorter and less dense mitotic spindles (Temme *et al*., 2003).

IAPs regulate cell cycle progression*:* Ectopic expression of XIAP arrests cells in G_0/G_1 phase that is associated with down-regulation of cyclin A and D1 and further induction of cyclin-dependent kinase inhibitors like p27 and p21 (Levkau *et al*., 2001).

IAPs regulate survival-related cell signaling*:* A large panel of evidence points to involvement of IAPs in modulating NF-κB activation by regulating RIP1 (receptor

interacting protein) polyubiquitination and destabilization of NIK1 (NF-κB inducing kinase 1). XIAP and NAIP form a complex with the TAK1 kinase and its cofactor, TAB1, which leads to activation of JNK (Sanna *et al.*, 2002).

II.3 Nuclear Factor-kappa B

NF- κB is a stress-activated transcription factor that plays a major role in inflammatory response, embryonic development, apoptosis, cell survival and cell cycle progression. NF-κB comprises a family of evolutionarily conserved, redox-sensitive family of transcription factors. This family consists of five members: p50, p52, p65 (Rel A), Rel B, c-Rel encoded by NF-κB1, NF-κB2, Rel A, Rel B and Rel C, respectively. These proteins share an N-terminal Rel homology (RHD) responsible for DNA binding, homo/hetero-dimerization and the interaction with IκB, the intracellular inhibitor of NF-κB. Hydrophobic residues at the C-terminal end constitute the transactivation domain (TAD) necessary for positive regulation of gene expression present in p65, c-Rel and RelB. As, p50 and p52 lack TAD, they may repress transcription unless associated with TAD-containing NF-κB family member. Binding of IκBs to NF-κB dimers keeps the latter in the cytoplasm. When bound to RelA: p50, IκBα masks the RelA nuclear localization signal (NLS) but not the p50 NLS. However, owing to the presence of a strong nuclear export signal (NES) in IκBα, the IκBα: RelA: p50 trimer is mainly cytoplasmic, although a constant shuttling between cytoplasm and nucleus has been documented (Ghosh & Karin, 2002). Upon activation, NF-κB dimers bind to a cognate 10 bp DNA binding site called the κB site and directly regulate gene transcription. NF-κB DNA binding

shows great degeneracy, generally the sequence preferred is 5'-GGGRNNYYCC-3' (where R is a purine, Y is a pyrimidine and N indicates any base).

II.3.1 Activation of NF-κB

II.3.1.1 Canonical/Classical pathway

This pathway mainly impinges on activation of Inhibitory kappa B kinase (IκK) complex comprising catalytic subunits, IκKα and IκKβ and the regulatory subunit NEMO (NF-κB essential modulator)/ IκKγ (Hacker & Karin, 2006). Successful receptor-ligand binding results in IκK activation. Activated IκK phosphorylates Ser 32 and Ser 36 residues on IκBα, leading to its polyubiquitination by Skp1, Cdc53/Cullin 1 and F box protein β-transducer repeat containing protein (βTRCP), $SCF^{I\kappa B}$ E3 ubiquitin ligase complex (Perkins, 2006). Ubiquitylated IκBα is directed for degradation by 26S proteasome, thereby exposing NLS in RelA and directing RelA: p50 dimer towards nucleus.

II.3.1.2 Non-canonical pathway

In this pathway, NIK-activated IκKα phosphorylates p100 precursor at its C-terminal serine residues. Once phosphorylated, $SCF^{I\kappa B}$ E3 ligase recognizes p100 resulting in its proteasomal degradation (Liang *et al.,* 2006). Owing to the presence of a stop signal located between p52 N-terminal portion and p100 C-terminal ankyrin repeat domain, ubiquitylated p100 undergoes only partial degradation, resulting in release of p52/RelB dimer, which is free to translocate to the nucleus.

Activity of NF-κB is also regulated through covalent modifications, like phosphorylation by mitogen- and stress-activated protein kinase 1/2 (MSK1/2), protein kinase A, GSK3β, AKT/PI3K and NF-κB- activating kinases, acetylation or methylation of dimer complex or the histones surrounding NF-κB target genes. Such modifications alter its ability to bind to DNA, recruit co-activators to enhancer regions and its interactions with IκBα. Differences in the pattern of phosphorylation and acetylation lead to recruitment of different transcription cofactors resulting in distinct profiles of gene expression (Huang *et al*., 2010).

II.3.2 NF-κB and cell fate

NF-κB can be pro- or anti-apoptotic, depending on the cell type, extent of NF-κB activation and nature of the apoptotic stimulus. (Sarnico *et al*., 2009).

In RelA-deficient mice, embryonic lethality was observed, indicating that NF-κB has a predominant role to play in development (Beg *et al*., 1996). Further, another study found over-expression of anti-apoptotic Bcl-2 insufficient to prevent hepatocyte apoptosis in RelA-knockout mice (Gugasyan *et al*., 2006). NF-κB mediates cytoprotection by suppressing JNK, which is known to mediate apoptosis (Tang *et al*., 2001).

In addition to the role of NF-κB as a survival factor, its pro-apoptotic role is also reported (Fujioka *et al.*, 2004, Chen *et al*., 1999). NF-κB is known to transcriptionally regulate about eight pro-apoptotic genes like TNF-α, Fas, FasL and c-myc (Chen *et al*., 1999). NF-κB is also found to potentiate H_2O_2-induced cell death in mouse embryonic fibroblasts (Ho *et al*., 2011). In addition, nuclear translocation

of NF-κB by AMPA (a-amino 3-hydroxy-5-methyl-4-isoxazolepropionic acid) receptors leads to transcription of p53, resulting in death of dopaminergic neurons (Erausquin, 2003). It has also been reported that doxycycline, an anti-cancer agent, generates superoxide within cells that subsequently stimulates NF-κB-dependent p53 up-regulation, leading to apoptosis (Fujioka *et al*., 2004).

II.3.3 NF-κB in the heart

Cardiac myocyte apoptosis was found to be significantly enhanced in transgenic mice that have defective nuclear translocation of NF-κB due to cardiac-restricted over-expression of dominant negative IκBα construct that retains NF-κB in cytoplasm in inactive form (Misra e*t al*., 2003). This study also suggests roles for Bcl-2 and cIAP-1 in mediating the pro-survival effect of NF-κB. In patients with heart failure, the functional deterioration of the heart is associated with a p50 gene polymorphism (Santos *et al*., 2010). The protective role of NF-κB was further supported by the observations of Kratsios *et al*., 2010, who showed in mice model that cardiac-specific deletion of NEMO gene led to the onset of cardiomyopathy (Kratsios *et al*., 2010). However, *in vivo* studies show that cardiac-specific over-expression of IκBα super-repressor reduces Ang II- or isoproterenol-induced hypertrophic phenotype of cardiomyocytes (Freund *etal*., 2005, Zelarayan *et al*., 2009). The molecular mechanisms underlying NF-κB-mediated hypertrophic response remain largely unknown. To date, binding sites of NF-κB in promoter sites of cardiac growth-related adult or fetal genes have not been identified (Gordon *et al*., 2011).

Although a large panel of evidence pointing to a cardioprotective role of NF-κB exists, there are several other findings too that support the hypothesis that chronic activation of NF-κB could mediate an inflammatory response, increased apoptosis and consequent heart failure (Hamid *et al.,* 2011). In this context, Gordon *et al.,* 2011 provide a possible, rather interesting, explanation to the dichotomous action of NF-κB in the heart, which needs further experimental validation. They speculate that early activation of NF-κB following myocardial injury may be adaptive in effect as it mediates cardioprotective effects like attenuation of apoptosis and maintaining the myocyte population. However, chronic activation may mediate inflammatory processes and be deleterious (Gordon *et al*., 2011).

II.4 MAPKs - Mitogen-activated protein kinases

Multi-cellular organisms possess 3 well-defined families of mitogen-activated protein kinases (MAPK) that control a vast array of physiological processes - extracellular signal-regulated kinases (ERK 1 & 2), c-Jun NH_2-terminal kinases (JNK 1, 2 and 3), p38-p38α, p38β, p38y, and p38δ. MAPKs comprise protein kinases that attach phosphate group to the target molecule in the cell and thereby alter its function. Substrates include other protein kinases, phospholipases, transcription factors and cytoskeletal proteins. Such phosphorylation events may be coupled to dephosphorylation by phosphatases, which eventually culminates in altered cell behavior, equipping it to respond to external stimuli.

II.4.1 ERK1/2 MAPK

6 different isoforms of ERK have been identified: ERK 1-5 and ERK 7/8 of which ERK1/2 are involved in the regulation of meiosis, mitosis and post-mitotic functions in differentiated cells. ERK1/2 is ubiquitously expressed in all tissues. In fibroblasts, it is mainly activated by growth factors, ligands that stimulate G protein-coupled receptors, cytokines and TGF-β. Activation of ERK occurs by phosphorylation of threonine and tyrosine residue by MEK1/2, which employs Ras-Raf axis to transduce signal to ERK1/2. Apart from Ras, ERK1/2 may be activated by other signaling molecules like Raf, protein kinase C and mixed lineage kinase3 (MLK3) (Zhimin & Shuichin, 2006). Following activation by several initiating stimuli, ERKs phosphorylate multiple targets like 90 kDa ribosomal S6 protein kinase ($pp90^{rsk}$), cytosolic phospholipase C and transcription factors like c-Myc, Elk-1, Ets-2 and STAT.

II.4.1.1 ERK1/2 and cell fate

Many cancer-associated lesions lead to constitutive activation of ERK, which is correlated to uncontrolled cell proliferation. In a few types of cancers, ERK1/2 is found to be localized to mitochondria where it inhibits phosphorylation of cyclophilin D, rendering cells more refractory to mitochondrial pore opening and consequent cell death (Rasola *et al*., 2009). Further, ERK1 plays a dispensable role in embryonic development owing to the presence of ERK2 that may in fact compensate for the deficiency of ERK1. But, ERK2-deficient embryos fail to form mesoderm and the ectoplacental cone, thus severely impacting the development of fetal portion of the placenta leading to embryonic lethality (Hatano *et al*., 2003).

ERK has been shown to mediate survival by the phosphorylation and consequent degradation of Bim, a pro-apoptotic member of Bcl-2 family that is known to mediate ER stress-induced apoptosis (Tay *et al*., 2012). Activated ERK1/2 signaling cascade phosphorylates pro-apoptotic Bad (Datta *et al*., 1997) and causes it to bind to 14-3-3, which further sequesters it away from its mitochondrial target (Zha *et al*., 1996). Further, activated ERK1/2 promotes conformational change of Bax and prevents apoptosis (Tsuruta *et al*., 2002). Moreover, ERK1/2 is also known to inhibit caspase-3 activation in haematopoietic cells (Terada *et al*., 2000). Apart from attenuating the actions of pro-apoptotic molecules, ERK1/2 promotes survival by up-regulating activity of anti-apoptotic molecules like Mcl-1, c-FLIP and IEX-1 (Domina *et al*., 2004, Garcia *et al*., 2002). ERK1/2 also facilitates survival upon DNA damage by up-regulating the activity of DNA repair enzymes like ATM and Rad 3-related kinase (Wu D *et al*., 2006).

Though a pro-survival factor, ERK1/2 is reported to mediate cell death as well (Cheung & Slack, 2004, Cagnol *et al.*, 2010). It has been suggested that ERK could be involved in neurodegeneration, possibly by causing plasma membrane rupture (Cheung *et al*., 2004). ERK signaling potentiates activation of death receptors by increasing levels of death ligands like FasL, TNF-α or death receptors like Fas, DR4, DR5 (Cagnol *et al.*, 2010). ERK modulates binding of FADD to death receptor complex leading to activation of caspase 8. Further, ERK activation could lead to mitochondrial membrane disruption and subsequent cytochrome c release. The differential response of ERK activation to cell viability can be attributed to several

factors like time of activation and subcellular localization of ERK determined by docking phosphatases and scaffold proteins.

II.4.1.2 ERK1/2 in the heart

ERK1/2 has been reported to exert both beneficial and deleterious effects upon the heart (Bottcher & Niehrs, 2005, Thum *et al*., 2008, Kovacs *et al*., 2009, Rose *et al*., 2010). ERK1/2 pathway has been implicated in the development of heart due to its role in growth factor signaling, mainly initiated by fibroblast growth factor (FGF) (Bottcher *et al*., 2005). Several lines of evidence show that ERK1/2 has important roles to play in hypertrophy and cardioprotection. Interestingly, two classes of drugs used to treat cardiac diseases, Ca^{+2} channel blockers and β-adrenergic receptor blockers, have been reported to sub-serve their protective effects, in part, through the ERK1/2 pathway (Kovacs *et al*., 2009). Doxorubicin, a drug known to induce myocardial damage, is reported to mediate its cyototoxic effects mainly by down-regulating ERK1/2 activity (Su *et al*., 2006). Further, a large number of reports point to the role of ERK1/2 signaling in preventing ischemia-reperfusion-induced injury (Hausenloy & Yellon, 2007).

Apart from these protective aspects, dysregulated ERK1/2 is also shown to contribute to hypertrophy and pathological remodeling in the heart. ERK pathway can induce contractile defects and sudden cardiac arrest prevalent in hypertrophic cardiomyopathy by modulating ion channels and triggering sarcoplasmic reticulum calcium defects and arrhythmias (Rose *et al*., 2010). Additionally, mechanical unloading achieved by the use of left ventricular-assist device (LVAD) is associated

with reverse remodeling and attenuation of hypertrophic response. Of note, the post-LVAD heart is related to decreased ERK activity (Flesch *et al*., 2001). Correlating with this observation, Huebert *et al*., 2004 found elevated levels of Sprouty-1, an inhibitor of the ERK pathway, in human hearts following LVAD support during hypertrophy regression (Huebert *et al*., 2004). Interestingly, Sprouty-1 expression is also found to be markedly up-regulated in cardiac fibroblasts of the failing heart. The *in vivo* silencing of miR-21, micoRNA targeting Sprouty -1 in a mouse pressure-overload-induced disease model, attenuates ERK1/2 activity and inhibits interstitial fibrosis (Thum *et al*., 2008). Taken together, ERK1/2 can mediate cardiac hypertrophy as well as interstitial fibrosis and modulate remodeling of heart under disease conditions.

Crosstalk between ERK and NF-κB

Ghoda *et al.,* 1997 have identified 90kDa ribosomal S6 kinase ($pp90^{rsk}$) as a downstream target of ERK-activated signaling pathway. Upon activation, pp90rsk phosphorylates the regulatory N-terminus of IκBα on Ser-32 and triggers its degradation (Ghoda *et al*., 1997). ERK-mediated NF-κB induction has been reported to regulate the cell cycle-related molecule, GADD45β (Wang *et al*., 2005), and also Bcl-2 (Kurland *et al.,* 2003). In primary cultures of rat aortic VSMCs, ERK1/2 was reported to activate NF-κB in a differential manner. Persistent activation of NF-κB was observed in the presence of ERK1/2, which became transient when ERK1/2 was inhibited (Jiang *et al*., 2004). The ERK1/2-mediated persistent activation of NF-κB was observed to be via an IκBβ-degradation-mediated manner (Xu *et al.,* 2006).

Primary skeletal muscle cells adapt to hypoxia by activating both ERK1/2 and NF-κB but by independent mechanisms (Osorio-Fuentealba *et al*., 2009).

II.5 Oxygen and the life-death balance: Redox homeostasis

The redox system plays a crucial role in the maintenance of cellular oxygen homeostasis. Under physiologic conditions, cells maintain redox balance through generation and elimination of reactive oxygen/nitrogen species (ROS/RNS). But when the redox homeostasis is altered, oxidative stress builds up, which can lead to cell death and contribute to disease development. However, intracellular ROS levels can also elicit signaling that equips cells to survive under conditions of oxidative stress (Schroder & Eaton, 2008).

II.5.1 Oxidative stress

Reactive oxygen species include a group of molecules like hydrogen peroxide (H_2O_2), superoxide anion (O_2^-), singlet oxygenand hydroxyl radical (OH). Optimal levels of ROS are principally involved in physiological metabolism. In order to maintain the concentrations of ROS within the physiological range of 1-700 nM (Stone *et al*., 2006), cells are equipped with an antioxidant system comprising ascorbic acid, α-tocopherol, glutathione and several enzymes like catalase, glutathione peroxidase and superoxide dismutase. The state of oxidative stress results when ROS concentration exceeds the antioxidant capacity within the cell (Ray *et al*., 2012). High levels of ROS may be generated by NADPH oxidase, xanthine/xanthine oxidase, arachidonic acid monooxygenases, and diminution in intracellular anti-oxidant defense or mitochondrial respiratory chain.

The mitochondrial electron transport chain reduces 95% of available oxygen but the remaining 5% is reduced by the univalent pathway that leads to the generation of free radicals (Becker, 2004). When O_2 accepts an electron, superoxide anion (O_2^-) is formed, which is in equilibrium with its protonated form, •HO. Under conditions of ischemia, the protonated form is favoured, which is dismutated to H_2O_2 by the activity of superoxide dismutase. H_2O_2 is further reduced to H_2O by catalase or glutathione system (Griendling *et al*., 2003). Under pathological conditions that erode the antioxidant system, H_2O_2 can generate the more destructive hydroxyl radical (•OH) in the presence of endogenous iron by Fenton chemistry (Hess *et al*., 1984). The nature of response elicited upon increased levels of ROS may be proliferation, growth arrest, cell death or transformation, depending on a wide array of factors like stress stimuli, time of exposure and type of cell.

II.5.2 Cellular signaling pathways regulated by ROS

Under normal conditions, low levels of ROS can drive several physiological processes. ROS can interact with critical signaling molecules and modulate a variety of cellular processes like proliferation, metabolism, differentiation and survival. An example of ROS-mediated regulation of apoptosis is through ASK1 (apoptosis signal-regulated kinase-1), an upstream MAPKKK that is reported to control JNK and p38 MAPK pathways (Ichijo *et al*., 1997). However, ROS-activated ASK1-mediated p38 signaling may trigger non-apoptotic outcomes as well, like differentiation and immune signaling (Matsuzawa *et al*., 2005). Interestingly, the PI-3K pathway that mediates cell proliferation and survival is also modulated by ROS.

PI3K pathway is negatively regulated by the phosphatase and tensin homology (PTEN) phosphatase (Leslie *et al*., 2002), which, upon ROS generation, gets oxidized and inactivated (Kwas et al., 2004). It is noteworthy that sources of ROS can activate an array of antioxidant genes mediated by PI3K-NFE2-like 2 (Nrf2)-antioxidant response element (ARE) mechanism (Ray *et al*., 2012).

Of particular interest in the realm of cellular signaling triggered by ROS is ischemic preconditioning. Cardiomyocytes constitutively express eNOS (endothelial nitric oxide synthase), which sub-serves a cardioprotective role by opening mitoK_{ATP} (Davidson & Duchen, 2006) channel that inhibits mitochondrial permeability transition (MPT), up-regulates transcription of iNOS, a mediator of the late phase of ischemic preconditioning, and also activates antioxidant defense comprising NF-κB and manganese superoxide dismutase (Bolli *et al*., 2007). Cardiomyocyte-restricted expression of iNOS is found to decrease free radical generation during reperfusion, which in turn prevents MPT and helps mediate a cardioprotective role (Zhang *et al*., 2012).

II.5.3 Cardiovascular response to oxidative stress

Oxidative stress has been implicated in myocardial dysfunction associated with several cardiovascular pathologies (Mallat *et al*., 1998), like ventricular hypertrophy (Sabri *et al*., 2003), myocardial ischemia (Misra *et al*., 2009) and atrial fibrillation (Dudley *et al*., 2005). iNOS, under pathological conditions, increases cytokine levels in both macrophages and vascular smooth muscle cells and leads to an inflammatory response, resulting in production of $NO^{\cdot}$, which in turn can mediate endothelial

vasodilation (Griendling *et al*., 2003). *In vitro* observations show that VSMCs have a differential response to oxidative stress. In response to high levels of H_2O_2, VSMCs undergo apoptosis while at lower concentrations, they undergo cell cycle arrest (Deshpande *et al*., 2002). ECs undergo apoptosis in response to H_2O_2-induced oxidative stress (Niwa *et al*., 2002).

Oxidative stress has several detrimental effects on the myocardium, like cardiac stunning, arrhythmia, reduction in contractility, elevated diastolic Ca^{+2}, intracellular ATP depletion, myocyte hypertrophy and apoptosis (Mike *et al*., 2007), fibrosis and ventricular dysfunction and dilatation (Grieve & Shah, 2003). Several lines of evidence show that Nox2, a potent source of superoxide in cardiomyocytes, has a role in the pathogenesis of remodeling. In contrast to wild-type mice, markedly less cardiomyocyte hypertrophy and apoptosis, interstitial fibrosis and ventricular dysfunction is observed in Nox2-deficient ($Nox2^{-/-}$) mice after myocardial infarction (Looi *et al*., 2008). Notably, cardiac myocytes are susceptible to oxidative injury, which is significant because cardiomyocyte apoptosis can be a causal component of lethal dilated cardiomyopathy and heart failure (Foo *et al*., 2005).

II.5.4 Response of cardiac fibroblasts to oxidative stress

ROS can impact several aspects of cardiac fibroblast biology, like collagen metabolism and proliferation. Cucoranu *et al*., 2005 have described a role for NADPH oxidase in TGF-β-induced transformation of cardiac fibroblast to myofibroblast (Cucoranu *et al*., 2005). In correlation with *in vivo* observations that up-regulated levels of ROS can trigger interstitial fibrosis in the heart, *in vitro*

studies have shown that Ang II-mediated ROS generation can increase collagen biosynthesis (Lijnen *et al*., 2006). In contrast to its co-residents in the myocardium, cardiac fibroblasts are shown to be relatively resistant to oxidative injury (Zhang *et al*., 2001), which facilitates a role for cardiac fibroblasts in wound healing. However, the molecular mechanisms underlying cardiac fibroblast resistance to oxidative injury-mediated cell death remain unclear.

Cardiac fibroblast resistance to apoptosis

Several *in-vitro* studies show that cardiac fibroblasts are more resistant than cardiomyocytes and fibroblasts of non-cardiac origin to apoptotic stimuli such as staurosporine, etoposide, serum deprivation and simulated ischemia (Mayorga *et al*., 2004). Cardiac fibroblasts from neonatal rats are reported to be resistant to hypoxic injury, unlike cardiac myocytes. Further, in contrast to cardiac myocytes, cardiac fibroblasts have also been shown to be resistant to H_2O_2-mediated oxidative stress (Xiling *et al*., 1997). The differential expression of anti-apoptotic Bcl-2 and pro-apoptotic Bax in cardiac myocytes and fibroblasts is reported to contribute to the differential susceptibility of these major cell types to oxidative stress (Zhang *et al*., 2001). Consistent with the relative resistance of cardiac fibroblasts with respect to myocytes to hypoxia, Shivakumar *et al*., 2007 observed that hypoxic cardiac fibroblast-conditioned medium (HFCM) enhances the susceptibility of cardiac myocytes to ROS-induced MPT. This study also identified increased TNF-α in hypoxic-fibroblast conditioned medium to be responsible for mediating apoptosis in myocytes via a paracrine effect (Shivakumar *et al*., 2007). Notably, *in vivo* studies show that myofibroblasts persist in the mature infarct scar long after the culmination

of the wound healing response due to their resistance to several apoptotic signals like Fas, TGF-β1 and AT1 receptor (Van den Borne *et al*., 2010).

However, mechanisms underlying cardiac fibroblast resistance to apoptosis remain largely unclear. Mayorga *et al.,* 2004 ascribe a predominant role to Bcl-2 in apoptosis resistance in cardiac fibroblasts in response to several pro-apoptotic stimuli (Mayorga *et al*., 2004). The study screened pro-apoptotic and anti-apoptotic members of the Bcl-2 family of proteins as well as XIAP, a member of the IAP family of proteins in fibroblasts of cardiac and non-cardiac origin, like dermal and pulmonary fibroblasts. Of the multiple proteins checked, the study found that Bcl-2 was expressed in cardiac fibroblasts alone but not in other fibroblasts. Cardiac fibroblast resistance to apoptosis may, however, be dynamic and multifactorial and not limited to constitutively expressed Bcl-2. In this context, Sangeetha *et al*., 2011 have shown NF-κB to be a major player in mediating protection to cardiac fibroblasts in response to hypoxia. The study provided preliminary evidence that cIAP-2 may mediate the pro-survival role of NF-κB (Sangeetha *et al.,* 2011).

III. Materials and Methods

III.1. Materials

III.1.1. Fine chemicals

M199, Opti-MEM, FBS, BSA, collagenase type IA, trypsin, pancreatin, DNase I, HEPES, EDTA, DMSO, amphotericin B, glucose, calcium chloride, disodium hydrogen phosphate, magnesium chloride, potassium chloride, potassium dihydrogen phosphate, sodium bicarbonate, sodium chloride, sodium dihydrogen phosphate, 2',7'-dichlorodihydrofluorescein diacetate (H_2DCFDA), Bay 11-7085, PD 98059, RNase A, propidium iodide, Hoechst 33342, Tri-reagent, DEPC, DNase I (amplification grade), aprotinin, pepstatin A, SDS, trizma base, agarose, glycine, acrylamide, bis-acrylamide, β-mercaptoethanol, TEMED, ammonium per sulphate, Ponceau S, ColorBurst electrophoresis marker, anti-desmin antibody, anti-von Willebrand antibody, immunostaining kit for vimentin, anti-β-actin primary antibody, anti-rabbit and anti-mouse secondary antibodies (FITC-labelled and HRP-conjugated) were purchased from Sigma-Aldrich, USA. cIAP-2, Bcl-2, total IκBα primary antibodies were from Santa Cruz Biotechnology, USA. Cleaved PARP, ERK1/2 (phospho and total forms) antibodies and cell lysis buffer were obtained from Cell Signaling Technology, USA. Fine chemicals for cDNA synthesis including RT buffer, RNase inhibitor, random primers, dNTPs and M-MLV Reverse Transcriptase were purchased from Promega Corporation, Madison, USA. LightShift Chemiluminesent EMSA kit, NE-PER nuclear and cytoplasmic extraction reagents, Biotin 3'end DNA Labeling kit, Biodyne nylon membrane and DAB substrate, SuperSignal West Femto substrate kit, SuperSignal West Pico Chemiluminescent kit were from ThermoScientific,USA. Taqman gene expression assay was procured from Applied Biosystems, USA. Alexa Flour 488 annexin V/Dead Cell Apoptosis

Kit was obtained from Invitrogen, USA. Lipofectamine 2000, Birc 2 SilencerSelect pre-designed siRNAs (siRNAs14 & 15) were procured from Ambion, USA. Nitrocellulose membrane was from Millipore, USA. Native ORF cIAP-2 clone in pCMV vector and turbofectin were purchased from Origene, Rockville, USA. The study had the approval of the Institutional Animal Ethics Committee (B29112005 VII).

III.1.2. Routine Chemicals

Chloroform, isopropanol, hydrochloric acid, ethanol, ether, glycerol and phenol red were purchased from Sisco Research Laboratories, India. Skim milk was obtained from Himedia, Mumbai, India. Hydrogen peroxide (30% purified) and methanol were from Merck, India. Gentamicin and benzyl-penicillin were from Cadila pharmaceuticals, India and Alembic Limited, India, respectively.

III.1.3. Cell culture ware

35mm and 100mm cell culture-treated dishes were from Becton Dickinson, USA. Cell culture filter ware was procured from Millipore, USA. Cell scrapers were from Nunc, USA.

III.1.4. Equipments used

ELISA reader (Bio-Tek instruments, USA), UV-visible spectrophotometer (Shimadzu, Japan), high speed refrigerated centrifuge (Hitachi, Japan), weighing balance (Sartorius, Germany), water bath (LKB, Sweden), ice-flaker (Hoshizaki, Japan), pH meter (Labindia, India), CO_2 incubator (Sanyo, Japan), phase-contrast microscope (Nikon, Japan), fluorescence microscope (Zeiss Axioskop 2 Plus), laminar flow hood (CLAS, India), magnetic stirrer (Schott, Germany), EASY pure UV/UF compact reagent grade water system (Barnstead, USA), electrophoresis unit

(Biorad laboratories, USA), Mini Blot (Biorad laboratories, USA), Programmable Thermal Cycler (MJ Research Inc, USA), Syngene Bio Imaging (Ingenius, Canada), UV-Trans-illuminator (Bangalore Genei, India), 7900 Real-Time PCR System (Applied Biosystems, USA).

III.2. Composition of Media, Reagents and Buffers

III.2.1 Acrylamide 30%

29% (w/v) acrylamide and 1% (w/v) N, N'-methylene bisacrylamide in deionized water

III.2.2 Agarose gel (1%) for electrophoresis of DNA or RNA samples

For RNA – 200 mg agarose in 20 ml of 0.5X TBE

III.2.3 Bis-benzimide H 33324 (Hoechst 33342)

Dissolved 10mg Hoechst 33324 powder in 5ml sterile distilled water to get a final concentration of 10mM. A working concentration of 10μM was used for the experiments.

III.2.4 Blocking solution

5% (w/v) skim milk or BSA in TBST containing 0.1% Tween-20

III.2.5 Buffer P1 (resuspension buffer)

50 mM Tris HCl (pH 8.0), 10 mM EDTA, 100 μg/ml RNase A

III.2.6 Buffer P2 (lysis buffer)

200 mM MaOH, 1% SDS (w/v)

III.2.7 Buffer P3 (neutralization buffer)

3 M potassium acetate, pH 5.5

III.2.8 Buffer QBT (equilibration buffer)

750 mM NaCl, 50 mM MOPS, (pH 7.0), 15% isopropanol (v/v), 0.15% Triton X-100 (v/v)

III.2.9 Buffer QC (wash buffer)

1.0 M NaCl, 50 mM MOPS, pH (7.0), 15% isopropanol (v/v)

III.2.10 Buffer QN (elution buffer)

1.6 M NaCl, 50 mM MOPS (pH 7.0), 15% isopropanol (v/v)

III.2.11 Cardiac fibroblast growth medium (pH 7.4)

M199 with Earle's salts containing FBS (10%), benzyl penicillin (50 U/ml) and gentamycin (0.04 mg/ml)

III.2.12 Cell Lysis buffer for westerns (1X)

20 mM Tris-HCl (pH 7.5), 150 mM NaCl, 1 mM Na_2EDTA, 1 mM EGTA, 1% Triton, 2.5 mM sodium pyrophosphate, 1 mM β-glycerophosphate, 1 mM Na_3VO_4, 1 μg/ml leupeptin

III.2.13 DEPC-treated deionized water

1 ml of DEPC in one litre of deionized water, stirred overnight at room temperature and autoclaved

III.2.14 Dissociation medium for cardiac fibroblast isolation

The medium consisted of sodium chloride (116.4 mM), HEPES (20 mM), sodium dihydrogen phosphate (1.15 mM), glucose (5.55 mM), potassium chloride (5.37 mM), magnesium sulfate (0.81 mM), BSA (1 mg/ml) and $CaCl_2$ (1 mM). pH was adjusted to 7.4. Deoxyribonuclease I (5.5 μg/ml), amphotericin B (10 mg/l) and antibiotics (50 U/ml penicillin and 0.04 mg/ml gentamicin) were added to the medium under sterile conditions at the time of

isolation. The dissociation medium had collagenase type IA (0.5 mg/ml), trypsin 1:250 (1 mg/ml) and pancreatin (0.020 mg/ml).

III.2.15 Dissociation medium for pulmonary fibroblast isolation

The medium consisted of sodium chloride (116.4 mM), HEPES (20 mM), sodium dihydrogen phosphate (1.15 mM), glucose (5.55 mM), potassium chloride (5.37 mM), magnesium sulfate (0.81 mM), BSA (1 mg/ml) and $CaCl_2$ (1 mM). pH was adjusted to 7.4. Deoxyribonuclease I (5.5 μg/ml), amphotericin B (10 mg/l) and antibiotics (50 U/ml penicillin and 0.04 mg/ml gentamicin) were added to the medium under sterile conditions at the time of isolation. The dissociation medium had collagenase type IA (0.75 mg/ml), trypsin 1:250 (1 mg/ml) and 0.025 mg/ml pancreatin.

III.2.16 DNA/RNA gel-loading dye

Bromophenol blue (0.25%); xylene cyanol (0.25%); EDTA (1mM); glycerol (50%) in DEPC-treated deionized water

III.2.17 Electrode buffer (pH 8.3) for SDS–polyacrylamide gel electrophoresis (SDS-PAGE)

Tris base (25 mM), glycine (192 mM), SDS (0.1%) in deionized water

III.2.18 Ethidium bromide (Stock solution)

1 mg in 1 ml deionized water, 5 μl of this stock solution was added to 20 ml of 1% agarose gel for DNA/RNA electrophoresis

III.2.19 EDTA (0.5 M, pH 8.0)

Dissolve 7.3 g EDTA tetra-acetic acid (anhydrous) in 30 ml de-ionized water. Adjust the pH to 8, using NaOH at which EDTA would dissolve and then make up the volume to 50 ml.

III.2.20 LB medium

Dissolve 10 g tryptone, 5 g yeast extract and 10 g NaCl in 800 ml distilled water. The pH was adjusted to 7.0 with 1 N NaOH. Adjust the volume to 1 litre with distilled water. Sterilize by autoclaving.

III.2.21 Non-denaturing gel (6%)

5.93 ml water, 2 ml 30% acrylamide, 2 ml 5X TBE, 35 µl 20% APS, 10 µl TEMED

III.2.22 Paraformaldehyde (4%)

Dissolve 4 g paraformaldehyde in 100 ml PBS by keeping at 60ºC

III.2.23 Phosphate-buffered saline (PBS) (pH 7.4)

Sodium chloride (137 mM), potassium chloride (2.7 mM), disodium hydrogen phosphate (10.14 mM), potassium dihydrogen phosphate (1.76 mM)

III.2.24 Resolving gel buffer (pH 8.8)

Dissolve 18.165 g of Tris base in 80 ml deionized water. pH was adjusted to 8.8 using HCl and made upto 100 ml and stored at room temperature.

III.2.25 Resolving Gel for SDS–PAGE (10%)

2.7 ml 30% acrylamide, 2.5 ml 1.5M Tris (pH 8.8), 0.1 ml 10% SDS, 0.1 ml 10% ammonium persulfate and 6 µl TEMED were added to 4.6 ml of deionized water.

III.2.26 Resolving Gel for SDS–PAGE (12%)

4 ml 30% acrylamide, 2.5 ml 1.5M Tris (pH 8.8), 0.1 ml 10% SDS, 0.1 ml 10% ammonium persulfate and 4 µl TEMED were added to 3.3 ml of deionized water.

III.2.27 Resolving Gel for SDS–PAGE (15%)

5 ml 30% acrylamide, 2.5 ml 1.5 M Tris (pH 8.8), 0.1 ml 10% SDS, 0.1 ml 10% APS and 4 µl TEMED were added to 2.3 ml of deionized water.

III.2.28 SDS gel-loading buffer (6X)

Dissolve SDS (9% w/v), bromophenol blue (0.03%), β-mercaptoethanol (9%), glycerol (50% v/v) in 18.75 ml 1M Tris HCl- pH 6.8 (0.375 M).

III.2.29 Serum-free medium

M199 containing antibiotics (50 U/ml penicillin and 0.04 mg/ml gentamycin)

III.2.30 Stacking gel buffer (pH 6.8)

30 ml from resolving buffer was measured, adjusted pH to 6.8 using HCl and was made up to 45ml. Stored at room temperature.

III.2.31 Stacking gel for SDS – PAGE (5%)

0.33 ml 30% acrylamide, 0.25 ml 1 M Tris (pH 6.8), 0.02 ml 10%SDS, 0.02 ml 10% ammonium persulfate and 2 µl TEMED were added to 1.4 ml of deionized water.

III.2.32 Towbin's buffer (Transfer buffer)

3.027 g Tris base, 14.4 g glycine, 200 ml methanol made up to 1L with deionized water

III.2.33 Tris borate EDTA buffer (TBE) (5X, pH 8.3)

54 g Tris base; 27.5 g boric acid; 20 ml EDTA (0.5 M, pH 8.0) made up to 1L with deionized water.

III.2.34 Tris-buffered saline (TBS) (10X, pH 7.6)

24.2 g Tris base, 80 g sodium chloride in 1L deionized water

III.2.35 Tris-buffered saline with Tween-20 (TBST) [1X]

1X TBS containing 0.1% Tween-20

III.2.36 Trypsin-EDTA solution

2.5 mg/ml trypsin and 0.38 mg/ml EDTA in PBS (pH 7.4)

The study had the approval of the Institutional Animal Ethics Committee (B29112005).

II.3. Methodology

III.3.1 Isolation, Culture and Characterization of Cardiac Fibroblasts

III.3.1.1 Isolation of cardiac fibroblasts

Cardiac fibroblasts were isolated from young adult male Sprague-Dawley rats following the method of Kumaran and Shivakumar, 2002 with some modifications (Kumaran & Shivakumar, 2002). Rats (2-3 months old) were anaesthetized with ether. Heart was excised and collected in PBS (Ref.III.2.23) containing antibiotics (50 U/ml penicillin and 0.04 mg/ml gentamycin) and amphotericin B (10mg/l). The atria were removed and the ventricular tissue was washed in PBS, minced into bits of approximately 1 mm^3 size and subjected to a series of digestions in dissociation medium (Ref. III.2.14) containing collagenase type IA (0.5 mg/ml), trypsin 1:250 (1mg/ml) and pancreatin (0.020 mg/ml). Digestion was aided by gentle shaking of the flask containing tissue bits on an orbital shaker maintained at 37°C. The supernatants were centrifuged at 1500 rpm for 5 minutes. The cell pellets were pooled, re-suspended in M199 supplemented with 10% FBS, seeded in two 35mm cell culture dishes and incubated in a humidified CO_2 incubator for 150 minutes at 37ºC in 95%, air and 5% CO_2. At the end of this period, the supernatant containing

unattached cells and debris was discarded, the dishes with the adherent fibroblasts were rinsed 3-4 times and incubated with M199 containing 10% FBS. The pre-plating step ensured preferential attachment of cardiac fibroblasts. At 24 hours after isolation, the dishes were washed and incubated with M199 containing 10% FBS (Ref. III.2.11) and maintained in a CO_2 incubator at 37ºC.

III.3.1.2. Sub-culture of cardiac fibroblasts

At confluence, the culture supernatant was removed, cells were washed with PBS (Ref. III.2.23) and trypsinized at 37ºC in trypsin-EDTA solution (Ref. III.2.36). Trypsinization was stopped by addition of M199 containing 10% FBS (Ref. III.2.11) and the detached cells were collected immediately by centrifugation at 1500 rpm for 5 minutes. The cell pellet was suspended in M199 containing 10% FBS (Ref. III.2.11) and seeded in fresh culture dishes at a split ratio of 1:3.

III.3.1.3. Characterization of cardiac fibroblasts in culture

Fibroblastic nature of the cells in culture was ascertained by morphology and immunocytochemistry.

- Analysis of morphology

Sub-confluent and confluent cultures were examined under an inverted phase contrast microscope for morphologic characteristics.

- Immunocytochemical analysis for vimentin, desmin and von Willebrand factor

Immunocytochemical staining was done as described by Willingham, 1994 with certain modifications. Cells from passage 2 or 3 grown to 60-70% confluence were washed with PBS (Ref. III.2.23) and fixed in 4% ice-cold paraformaldehyde (Ref.

III.2.22) for 20 minutes. The fixed cells were blocked with PBS containing 5% FBS and 0.2% Triton for 30 minutes. The cells were then incubated overnight in primary antibody diluted in blocking solution. Following PBS wash, cells were incubated in FITC-labelled secondary antibody at room temperature for 90 minutes. After PBS wash to remove unbound stain, nuclei were counterstained with Hoechst 33342 and observed under a fluorescence microscope. Anti-desmin and anti-von Willebrand factor were diluted 1:500 while immunostaining for anti-vimentin was done using a commercially available kit.

III.3.1.4 Isolation, culture and characterization of lung fibroblasts

Lung tissues were excised from young adult male Sprague-Dawley rats (2-3 months) after cervical dislocation. The isolation procedure was essentially the same as that for cardiac fibroblasts. The fibroblastic nature of the isolated cells was ascertained as described for cardiac fibroblasts.

III.3.2 Transfection of cardiac fibroblasts

$8x10^4$ cells were seeded per well into 12-well plates. 24 hours post-subculture, cells were incubated in Opti-MEM containing Ambion cIAP-2 pre-designed Silencer - Select siRNA (5 pmol) and Lipofectamine (2 µl) for 19 hours. Cells were then incubated with M199 containing 10% FBS (Ref. III.2.11) for 15 hours. This was followed by incubation in M199 with/without H_2O_2 for 12 hours. Cell lysate was prepared in SDS lysis buffer and denatured in boiling water bath for 5 minutes and stored at -20ºC. For cell viability analysis, the treatment duration with/without H_2O_2 was 3 hours.

III.3.3 Assessment of cell viability by Hoechst 33342/ Annexin-PI staining

Cultures of cardiac fibroblasts or pulmonary fibroblasts in M199 with 10% FBS were subjected to the required experimental conditions and incubated for 10 minutes with Hoechst 33342 (10 µM) (Ref. III.2.3) at 37ºC, followed by annexin V for 15 minutes. Following incubation in the dark, propidium iodide (PI) was added (0.25 µg/ml) and cultures were visualized under a fluorescence microscope (Zeiss Axioskop 2 Plus) at excitation wavelengths of 352 nm, 488 nm and 538 nm for Hoechst 33342, Annexin V and PI, respectively.

III.3.4 Intracellular ROS measurement (H_2DCFDA assay)

Intracellular ROS levels were measured by loading cardiac and pulmonary fibroblasts with 10 µM H_2DCFDA for 10 minutes and incubated with H_2O_2 at a range of concentrations from 1 µM to 50 µM for 15 minutes. Fluoresence was read at excitation and emission wavelengths of 485 nm and 530 nm respectively. Relative fluorescence was calculated as percentage of the untreated cells.

III.3.5 Electrophoretic Mobility Shift Assay (EMSA)

DNA-binding activity of NF-κB in cardiac fibroblasts was assessed by EMSA.

III.3.5.1 Preparation of nuclear extract

Nuclear extracts were prepared using NE-PER nuclear and cytoplasmic extraction kit (ThermoScientific) following manufacturer's instructions. Confluent cardiac fibroblast cultures in M199 containing 0.1% FBS were subjected to 30 or 60 minutes

treatment with H_2O_2 and were harvested by trypsinization as described earlier, washed in PBS (Ref. III.2.23) and pelleted. The cell pellet was re-suspended in 75–150 µl (depending on the pellet size) cytoplasmic extraction reagent I provided with the kit. The mixture was vortexed for 15 sec at high speed and incubated on ice for 30 minutes. After addition of cytoplasmic extraction reagent II, the mixture was vortexed again for 15 seconds at high speed and centrifuged at 16,000 x g for 5 min at 4^0C. The supernatant (the cytoplasmic fraction) was removed and stored at $–80^0$C until use. The pellet was re-suspended in nuclear extraction reagent, vortexed at high speed for 15 seconds, incubated on ice for 2 hours, vortexed again for 15 seconds at high speed and centrifuged at 16,000 x g for 10 minutes at 4^0C. The supernatant (nuclear fraction) was aliquoted and stored at $–80^0$C until use. Protein concentration of the nuclear extracts was determined by the Bradford assay (Bradford *et al*., 1976).

III.3.5.2 Primers

Single-stranded oligos containing the consensus sequence for the NF-κB binding site (-GGGGACTTTCC-) were obtained as a kind gift from Dr. Ruby John Anto, Rajiv Gandhi Centre for Biotechnology, Trivandrum.

III.3.5.2.1 Primer labeling

Single-stranded oligos for NF-κB were biotin-labelled using Biotin 3’ end DNA labeling kit. All reaction components were added in the following order:

Component	Volume	Final concentration
Ultrapure water	25 µl	

5X TdT reaction buffer	10 µl	1X
5 pmol 3'-OH ends of unlabelled DNA		
Biotin-11-UTP (5µM)	5 µl	0.5 µM
Diluted TdT (2U/µl)	5 µl	0.2 U/µl

Reaction components were incubated at 37ºC for 30 minutes. Following addition of 2.5 µl 0.2 M EDTA to stop the reaction, 50 µl of chloroform:isoamyl alcohol (24:1) was added to extract TdT and briefly centrifuged at high speed to separate the phases. The top aqueous phase containing the biotin-labelled oligo was collected.

III.3.5.2.2 Annealing of NF-κB oligos

1. Mixed equal volumes of both complimentary oligos at equimolar concentrations
2. Incubated on thermal block at 90ºC for ~2 minutes
3. Removed from thermal block and allowed to cool to room temperature for 1 hour
4. Stored at -20ºC until use

III.3.5.3 DNA binding

15 µg nuclear protein was incubated with 200 femtomoles of double-stranded biotinylated probes for NF-κB and other components of the Light Shift Chemiluminescent kit at 37ºC for 60 minutes in labeled vials. 5 µl loading dye was added to each vial and mixed gently. 20 µl of each sample was loaded on a 6% non-denaturing TBE gel and electrophoresed in TBE buffer at 100 V until the bromophenol blue moved more than 3/4th the gel. The run was stopped at this point as the free probe runs just below the bromophenol blue dye. Electrophoretic gel

transfer onto a nylon membrane was carried out at 380 mA for 80 minutes, followed by UV cross-linking at 254 nm for 10 minutes.

III.3.5.4 Detection of biotin-labeled oligos

After blocking for 15 minutes, the membrane was incubated in streptavidin-conjugated-HRP in blocking buffer (1:300) for 30 minutes with gentle shaking. Bands were visualised by application of chemiluminescent working solution, prepared by adding Luminol/Enhancer solution to stable peroxide solution in equal ratio.

III.3.5.5 Competition assay

Specificity of binding was examined by competition with excess unlabelled NF-κB oligonucleotides (200-fold).

III.3.6 Western blot analysis

Western blot analysis was carried out following standard protocol (Maniatis *et al*., 1982). Briefly, confluent cardiac fibroblast cultures in M199 containing 10% FBS (Ref. III.2.11) were exposed to H_2O_2 for the indicated durations and lysed in cell lysis buffer (Ref. III.2.12) followed by incubation at 4ºC for 30 minutes. The lysates were centrifuged at 13,000 rpm for 30 minutes to remove cell debris, and the supernatant was aliquoted and stored at –80ºC until use. Protein was quantified by the Bradford assay (Bradford *et al*., 1976). The lysates were denatured by incubation with SDS-gel loading buffer (Ref. III.2.28) at 100ºC for 5 minutes. 20 µg of protein was electrophoretically fractionated on 10% or 12% or 15% SDS-PAGE minigels

and electroblotted onto nitrocellulose membrane for 90 minutes at 100V. The membrane with the transferred proteins (ascertained by Ponceau S staining) was blocked for 1 hour with 5% skim milk or BSA (in case of phosphoproteins) (Ref. III.2.4) and incubated overnight at 4ºC with primary antibodies prepared at a dilution of 1:1000 (anti-cIAP2, anti Bcl-2, anti-total IκBα, anti-phospho-ERK1/2, anti-ERK1/2) in TBST containing 5% BSA (Ref. III.2.4). Unbound primary antibody was removed by washing (5x5' times) with TBST (Ref. III.2.35). Immunoblots were exposed for 1 hour to HRP-conjugated anti-mouse/anti-rabbit secondary antibody at 1:10000 dilution in 5% BSA-containing TBST (Ref. III.2.4). The ECL detection system was used to detect the antigen-antibody complexes, with average exposure time of 5–60s. Duration of exposure of the membrane to X-ray film ranged from 30 seconds to 15 minutes. The membrane was then stripped overnight by washing with TBST (Ref. III.2.35) on a rocking platform, re-probed with anti-β actin antibody (1:1000) and developed as described above. Protein expression was quantified by densitometric scanning (Syngene gel documentation system).

III.3.7 Real time PCR analysis

III.3.7.1 Isolation of total RNA

Glasswares used for RNA isolation were DEPC-treated and autoclaved. All reagents were prepared with DEPC-treated water (Ref. III.2.13). Total RNA was isolated using Tri reagent (5ml/100mm culture dish) from confluent cultures of cardiac fibroblasts exposed to H_2O_2 for 6 hours, according to the manufacturer's instructions. Following phase separation with chloroform, RNA was precipitated

from the aqueous phase using isopropanol and was dissolved in DEPC-treated water (Ref. III.2.13).

III.3.7.2 Assessment of isolated RNA

The yield and purity of the isolated RNA was determined spectrophotometrically at A_{260} and $A_{260/280}$, respectively. The intactness was ascertained by 1% agarose gel (Ref. III.2.2) electrophoresis.

III.3.7.3 DNase treatment of isolated RNA

The isolated RNA samples were subjected to DNase I (amplification grade) treatment, as per manufacturer's instructions, to remove any genomic DNA contamination. This was further validated by PCR analysis of the DNase I treated-RNA using G3PDH primers.

III.3.7.4 cDNA synthesis

Following DNase I treatment, 2 µg of total RNA was reverse transcribed to cDNA by the following procedure. The cDNA synthesizing mixture consisted of:

5X RT buffer	6.0 µl
dNTPs	2.5 µl
Random primers	3.0 µl
RNase inhibitor	0.5 µl
M-MLV RT	2.0 µl
Total RNA	10.0 µl
DEPC-treated water	6.0 µl
---	---
	30 µl

1 µg total RNA, 10 µl of DEPC-treated water (Ref. III.2.12) and 3.0 µl random primers were initially mixed and heated at 70ºC for 5 minutes. The heated mixture was then snap-cooled on ice and mixed with the remaining constituents listed above. The reaction mixture was incubated at 37ºC for 60 minutes, heated at 90ºC for 5 minutes and then cooled on ice to inactivate M-MLV reverse transcriptase. The cDNA preparations were stored at -20ºC until use.

III.3.7.5 Real time PCR analysis

Taqman quantitative real-time PCR analysis was carried out using the ABI Prism 7900 Sequence Detection System (Applied Biosystems, CA) with specific FAM-labelled probes. The oligonucleotide primers and probes for cIAP-2 mRNA (Assay ID, Rn00572734_m1) and 18S rRNA (4333760T) were from Applied Biosystems. PCR reactions were performed as per the manufacturer's instructions. The following thermal cycling condition was used: 95°C for 10 min followed by denaturation at 95°C for 15s and annealing/extension at 60°C for 1 min for each of 40 cycles. cIAP-2 expression was quantified using $\Delta\Delta C_T$method with 18S rRNA as reference gene (Livak *et al.*, 2001).

<u>$\Delta\Delta C_T$ method to calculate relative fold of cIAP-2 with respect to 18S rRNA</u>

- Average C_T (The cycle in which the growth curve crosses the threshold which is indicative of the initial amount of cDNA) of each experimental group is recorded.
- Normalization of C_T (ΔC_T) was calculated for each sample. ΔCt is the difference between the average Ct of target gene and that of reference gene

$\Delta C_T = Ct_{target} - Ct_{reference\ gene}$

- Calculation of $\Delta\Delta C_T$: $\Delta\Delta C_T$ is the difference between ΔC_T of unknown and the ΔC_T of the calibrator

  $\Delta\Delta C_T = (Ct_{target} - Ct_{reference})_{sample} - (Ct_{target} - Ct_{reference})_{control}$

- Relative fold of target mRNA levels of treated with respect to control = $2^{-\Delta\Delta C_T}$

III.3.8 Forced expression of cIAP-2

Strong constitutive expression of cIAP-2 was achieved under a pCMV promoter, purchased as cDNA clone from Origene, Rockville, USA.

III.3.8.1 Plasmid amplification

1. 100 µl nuclease-free water was added to reconstitute the supplied 10 µg lyophilized DNA.
2. DH5-α strain was thawed from -80ºC, by keeping in ice. 1 µl from reconstituted plasmid DNAwas added into 100 µl DH5-α. Provide a gentle tap and incubate in ice for 30 minutes.
3. The vial was kept in water bath set at 42ºC for 40 seconds to provide a heat shock, which was immediately snap-cooled on ice and then mixed with 250 µl LB broth (without ampicillin) (Ref. III.2.20)
4. After incubation at 37ºC for 1 hour at 175 rpm, the broth was plated on kanamycin (50 µg/ml) containing medium that was again incubated at 37ºC overnight.

5. Post-incubation, one colony was inoculated into kanamycin (50 µg/ml) containing LB broth (5ml) and incubated at 37ºC for 6-8 hours at 175 rpm to set up a starter culture.
6. Further, 100 ml kanamycin (50 µg/ml) containing LB broth was inoculated with 500 µl of starter culture and incubated at 37ºC, 175 rpm for 12-16 hours.
7. *Preparation of glycerol stock:* 850 µl culture broth was added to 150 µl sterile glycerol and vortexed vigorously for 5 seconds and kept at -80ºC until use.

III.3.8.2 Plasmid isolation

Qiagen plasmid Midi kit was employed to isolate plasmid DNA.

1. Harvested bacterial cells by centrifugation at 6000 x *g* for 15 minutes at 4ºC.
2. Added the RNase A solution to buffer P1 (resuspension buffer) (Ref. III.2.5) to give a final concentration of 100 µg/ml. Resuspended the bacterial pellet in 4 ml Buffer P1.
3. Added 4ml Buffer P2 (lysis buffer) (Ref. III.2.6), mixed thoroughly to facilitate homogenous mixing and incubated at 25ºC for 5 minutes.
4. Added 4 ml pre-chilled Buffer P3 (neutralization buffer) (Ref. III.2.7), mixed thoroughly andincubated on ice for 15 minutes. Precipitation of genomic DNA, proteins, cell debris andpotassium dodecyl sulphate was facilitated by addition of buffer P3.
5. Centrifuged at ≥20000 x *g* for 30 minutes at 4ºC and removed the supernatant containing plasmid DNA.
6. Equilibrated a Qiagen-tip100 by applying 4 ml Buffer QBT (equilibration buffer) (Ref. III.2.8). The presence of detergent facilitated the flow of buffer through the

column. Applied the supernatant from step 5 to the Qiagen-tip and allowed it to enter the resin by gravity flow.

7. Washed the Qiagen-tip with 10 ml Buffer QC (wash buffer) (Ref. III.2.9), which wassufficient to remove all contaminants in plasmid DNA preparation.
8. Eluted the DNA with 5 ml Buffer QF (elution buffer) (Ref. III.2.10) into 15 ml centrifuge tube and precipitated by adding 3.5 ml isopropanol. Mixed and centrifuged immediately at ≥15000 x *g*. Washed the pellet with 2 ml 70% ethanol and centrifuged at ≥15000 x *g* for 10 minutes. Carefully decanted the supernatant without disturbing thepellet. Air-dried the pellet and redissolved the DNA in 250 µl nuclease-free water. Concentration of plasmid DNA and purity were assessed spectrophotometrically fromthe 260 nm and 280 nm readings.

III.3.8.3 Plasmid verification

i. Amplification of cIAP-2 ORF clone was carried out using forward and reverse DNA vector sequencing primers provided in the kit.

   Reaction was set using the following components

Water	18.5 µl
10X buffer	2.5 µl
Forward primer	0.25 µl
Reverse primer	0.25 µl
dNTP	0.5 µl
DNA template	1 µl
Sigma Taq polymerase	0.5 µl

   under the following conditions: 95ºC for 3 minutes followed by 95ºC for 30 seconds, 55ºC for 40 seconds and 72ºC for 2 minutes repeated over 27

cycles and final extension at 72ºC for 5 minutes. The amplification product was electrophoresed on 1.2% agarose gel.

ii. Restriction digestion

The cIAP-2 clone (1770 bp) is located within the Sgf-1 and Mlu-1 sites of the pCMV plasmid. Single site restriction digestion at Mlu-1 linearized the plasmid and its size was checked on 1.2% agarose gel. The restriction digestion mixture, consisting of

10X restriction buffer	2 µl
Plasmid	17.5 µl
Mlu-1	0.5 µl

was incubated at 37ºC for 2 hours. The post-restriction digestion product was electrophoresed on 1.2% agarose gel.

III.3.8.4 Transfection of NF-κB-inhibited cardiac fibroblasts with Native cIAP-2 ORF clone pCMV system

cIAP-2 over-expression plasmid cocktail was prepared with 1 µg plasmid and 3 µl turbofectin in 100 µl Opti-MEM, which was added to the cultures for incubation in M199+10% FBS for 4 hours. After a recovery period of 15 hours, cells were pre-treated with the NF-κB inhibitor, Bay 11-7085, followed by H_2O_2 treatment. Cell viability was checked by Hoechst/PI staining.

III.3.9 Statistical Analysis

Statistical significance was assessed using Student's *t*-test. $p \leq 0.05$ was considered significant. Values were expressed as Mean ± SD.

IV. Results

IV.1 Characterization of adult rat cardiac fibroblasts

1V.1.1 Morphological analysis

Cardiac fibroblasts isolated from adult rat ventricular tissue were grown in culture as described under 'Methods'. Pre-plating for 150 minutes following isolation ensured selective enrichment of fibroblasts, which constituted >99% of the cells in these cultures. Morphological analysis and immunocytochemical staining established the fibroblastic nature of the cells. At 150 minutes after isolation, the cells had a dense nest-like morphology and, by 24 hours, the cells attained spindle-like appearance (Figure 3). At confluence, the cultures exhibited a monolayer pattern (Figure 4). Absence of 'cobblestone' or 'hill and valley' pattern of morphology ruled out contamination of cultures by ECs and VSMCs respectively. Cells at passages 2 and 3 were used for the experiments.

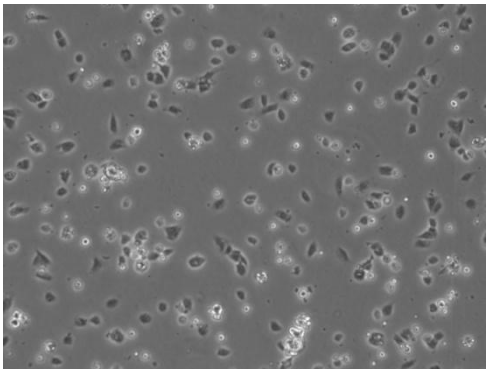

Figure 3: Phase contrast micrograph of adult rat cardiac fibroblasts at 150 minutes after isolation (100X magnification)

Cardiac fibroblasts, isolated as described under 'Methods', were pre-plated for 150 minutes in M199 containing 10% FBS. At the end of this period, cultures enriched with adherent fibroblasts were rinsed and incubated with M199 containing 10% FBS.

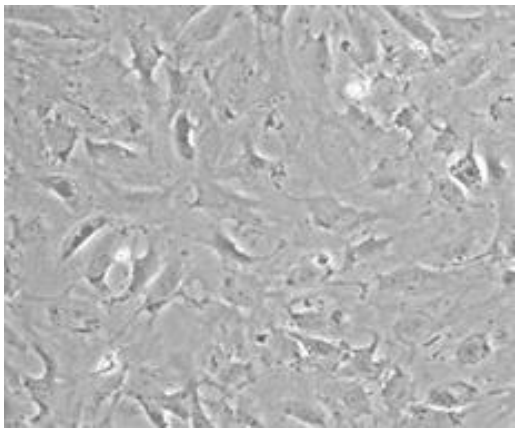

Figure 4: Phase contrast micrograph of adult rat cardiac fibroblasts at confluence (100X magnification)

Cardiac fibroblasts, isolated as described under 'Methods' were grown to confluence in M199 containing 10% FBS to form a monolayer with spindle-shaped morphology.

1V.1.2 Immunocytochemical staining

Cells were examined for immunoreactivity with antibodies against the cytoskeletal proteins, vimentin, desmin and von-Willebrand factor. The cells were positive for vimentin (Figure 5) but negative for desmin and von-Willebrand factor (Figures 6 & 7), confirming their fibroblastic nature and ruling out the presence of VSMCs and ECs, respectively, in the culture.

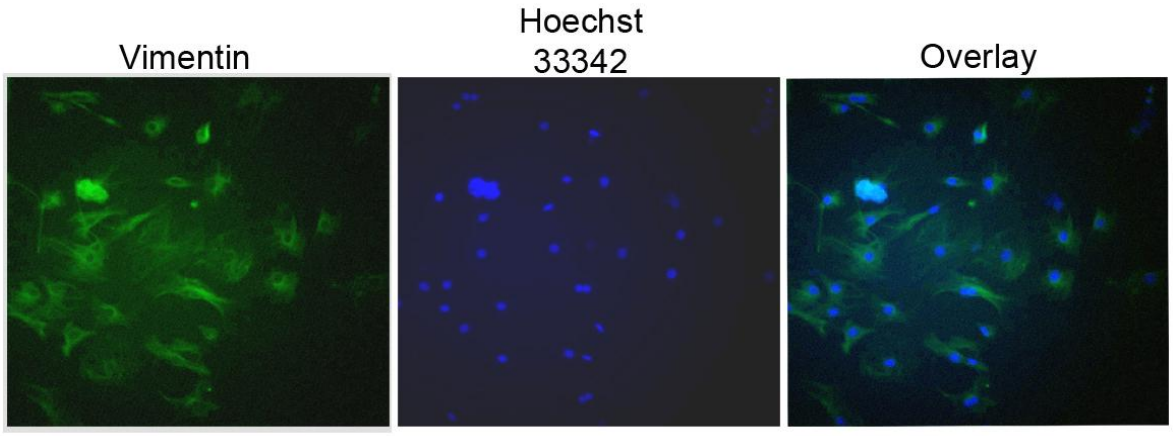

Figure 5: Fluorescent micrographs of vimentin-positive adult rat cardiac fibroblasts

Sub-confluent cultures were immunostained with anti-vimentin antibody. Nuclei were counter-stained with Hoechst 33342.

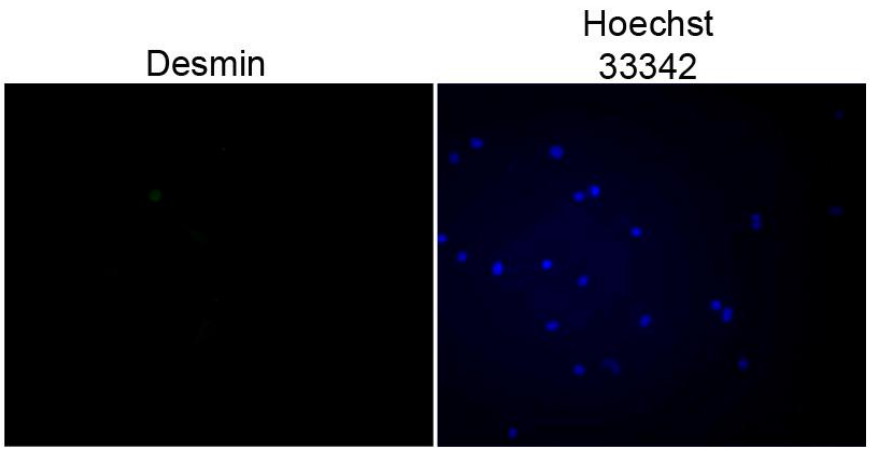

Figure 6: **Fluorescent micrographs of desmin-negative adult rat cardiac fibroblasts**

Sub-confluent cultures were immunostained with anti-desmin antibody. Nuclei were counter-stained with Hoechst 33342.

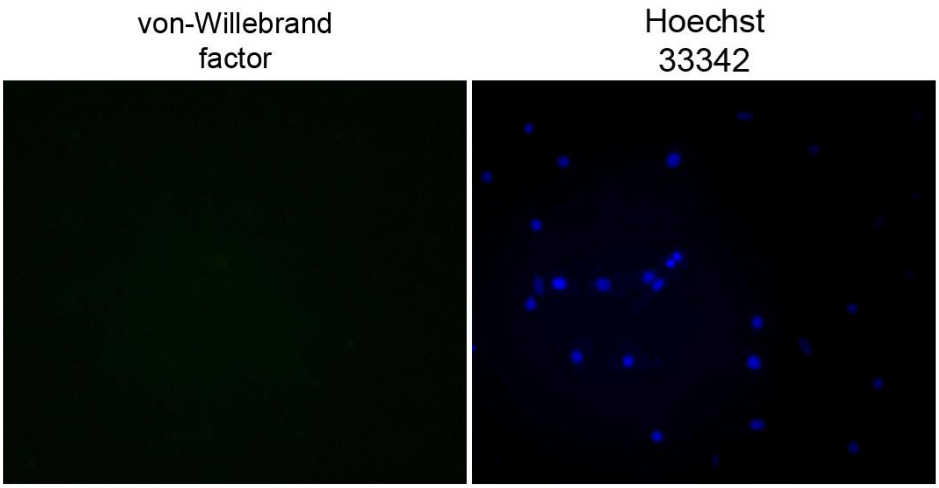

Figure 7: Fluorescent micrographs of von-Willebrand factor-negative adult rat cardiac fibroblasts

Sub-confluent cultures were immunostained with anti-von-Willebrand factor antibody. Nuclei were counter-stained with Hoechst 33342.

1V.2 The oxidative stress model

Cardiac fibroblasts from passage 2 or 3 exposed to H_2O_2 served as the experimental model.

1V.3 Effect of H_2O_2-mediated oxidative stress on cardiac fibroblasts

1V.3.1 Cardiac fibroblasts are relatively resistant to oxidative stress-mediated injury

In the first set of experiments, the effect of H_2O_2 on the viability of cardiac and pulmonary fibroblasts was examined to ascertain whether cardiac fibroblasts are more resistant than pulmonary fibroblasts to oxidative stress. Cardiac and pulmonary fibroblasts were exposed to a range of H_2O_2 concentrations and viability was

checked by Hoechst/Annexin V/PI staining. There was no significant loss of viability with 1 or 25 µM H_2O_2 in cardiac fibroblasts. Exposure to 50 µM H_2O_2 for 3 hours caused about 10% cell death (Figure 8). There was, however, no significant increase in cell death with extended exposure (24 hrs) to 50 µM H_2O_2. In pulmonary fibroblasts, viability loss was found to be 10% and 54% at 25 µM H_2O_2 and 50 µM H_2O_2, respectively (Figure 8). Pre-treatment with antioxidants, N-acetyl cysteine (5 µM), prevented cell death-associated with H_2O_2 treatment (Figure 9).

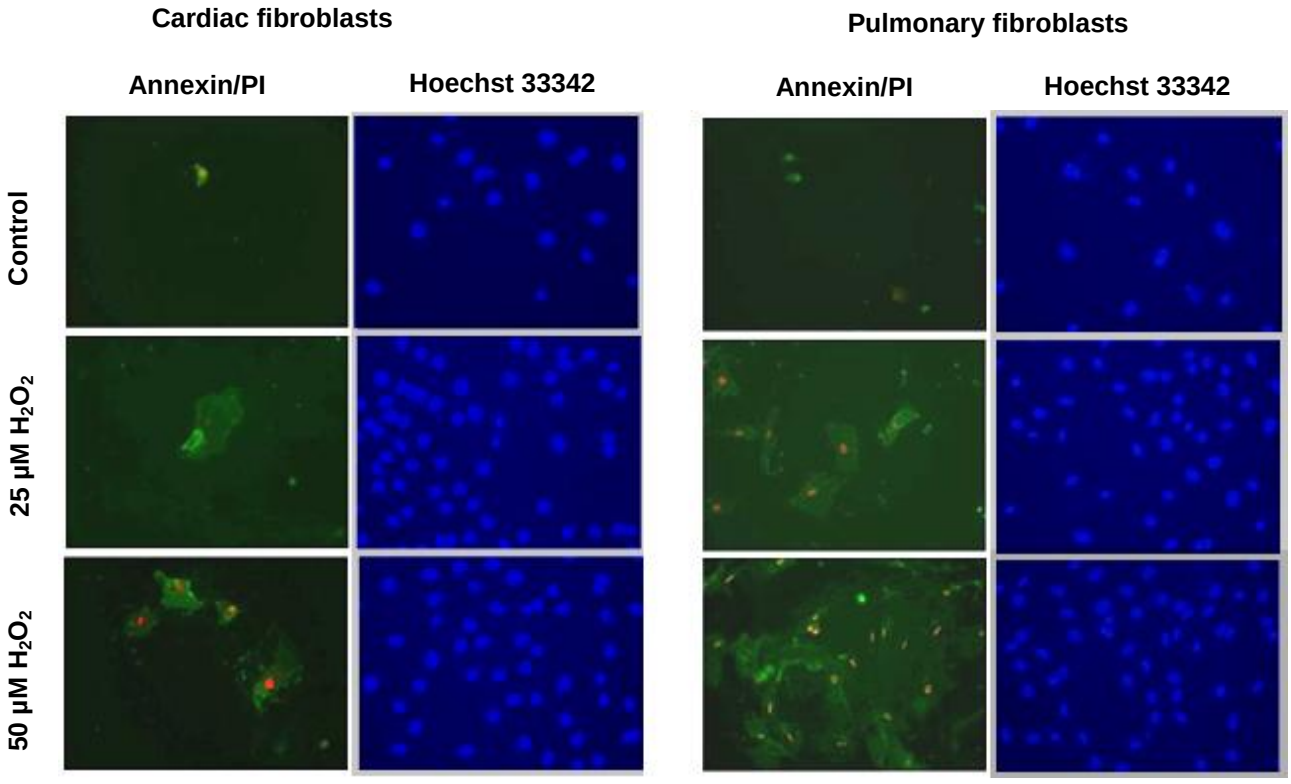

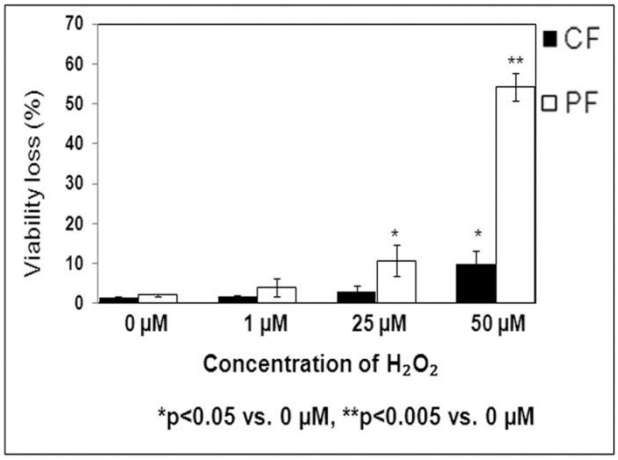

Figure 8: Effect of H_2O_2 on viability of cardiac and pulmonary fibroblasts

Percent loss of viability was assessed by Hoechst/Annexin/PI staining following exposure of cardiac fibroblasts (CF) and pulmonary fibroblasts (PF) to a range of concentrations of H_2O_2 upto 50 µM for 3 h. Values are expressed as Mean +/- SD, n=4, where n indicates total number of dishes and a minimum of 250 cells were counted per dish.

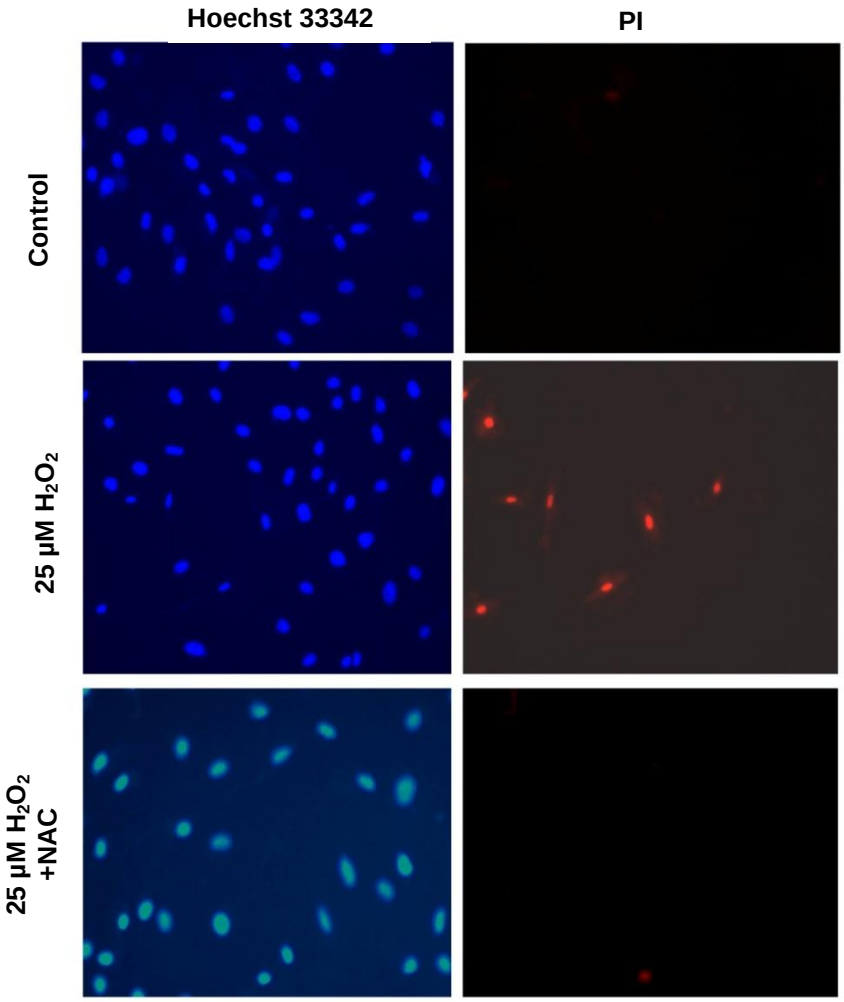

Figure 9: N-acetyl cysteine prevents H_2O_2-induced cell death in pulmonary fibroblasts

Loss of viability in pulmonary fibroblasts upon H_2O_2 treatment, observed by Hoechst/PI
staining, was reduced significantly upon pre-treatment with 5 µM N-acetyl cysteine (NAC). A minimum of 250 cells was counted per dish. Representative fluorescent micrographs from one of two experiments are shown.

1V.3.2 ROS generation occurs in cardiac fibroblasts in response to exposure to H_2O_2

To examine whether exposure to H_2O_2 results in generation of intracellular ROS, cells were loaded with H_2DCFDA and exposed to H_2O_2 for 10 minutes. A 2- and 3-fold increase in intracellular ROS levels was observed with 25 µM and 50 µM H_2O_2, respectively, in cardiac fibroblasts (Figure 10). In pulmonary fibroblasts exposed to 25 µM and 50 µM H_2O_2, a 40% and 80% increase in ROS levels was observed (Figure 10).

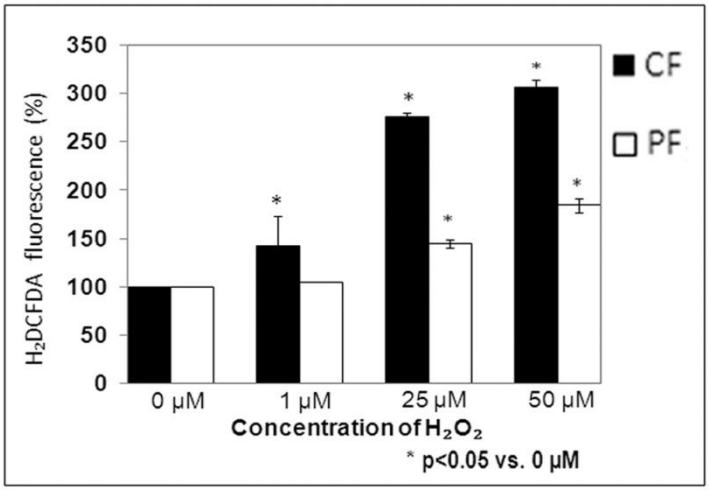

Figure 10: Effect of H_2O_2 on intracellular ROS levels in cardiac and pulmonary fibroblasts

Intracellular ROS in cardiac and pulmonary fibroblasts exposed to H_2O_2 was measured by pre-treatment of cells with 10 µM H_2DCFDA followed by treatment with the indicated concentrations of H_2O_2 for 10 min. Fluorescence was measured at excitation and emission wavelengths of 485 nm and 530 nm respectively. n=3.

Based on these observations, a concentration of 25 µM was chosen for subsequent experiments.

These preliminary observations pointed to significant differences between cardiac and non-cardiac fibroblasts in their susceptibility to oxidative stress. Hence, further studies examined the molecular mechanisms underlying the relative resistance of cardiac fibroblasts to oxidative stress. In this context, levels of anti-apoptotic proteins like Bcl-2 and cIAP-2 were probed in cardiac fibroblasts exposed to H_2O_2.

1V.4 Constitutive levels of Bcl-2 remained unchanged upon exposure to H_2O_2

To examine the levels of Bcl-2 in rat cardiac fibroblasts, cells were subjected to 12 and 24 hours of H_2O_2 exposure. Cell lysates for western blot analysis were prepared and blotting was carried out as explained under 'Methods'. Bcl-2 was found to be constitutively expressed in cardiac fibroblasts, which remained unaffected upon exposure to oxidative stress (Figure 11).

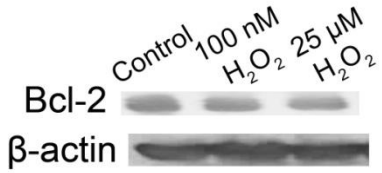

Figure 11: H_2O_2 does not affect constitutive expression of Bcl-2 in cardiac fibroblasts

Confluent cultures of cardiac fibroblasts in M199 with 10% FBS were treated with H_2O_2 (100 nM and 25 µM) for 12 h. Western blot analysis was performed as described under Methods, using polyclonal anti-Bcl-2 antibody. β-actin served as

loading control. Constitutive levels of Bcl-2 were observed, which remained unchanged upon exposure to H_2O_2.

1V.5 cIAP-2 is induced in cardiac fibroblasts exposed to H_2O_2

Cardiac fibroblasts were exposed to H_2O_2 for 12 or 24 hours and cIAP-2 levels were determined by western blot analysis, using β-actin as loading control. A significant increase in cIAP-2 protein expression was observed at a concentration of H_2O_2 as low as 100 nM (Figure 12). However, no significant expression of cIAP-2 was observed in pulmonary fibroblasts in response to H_2O_2 (Figure 13).

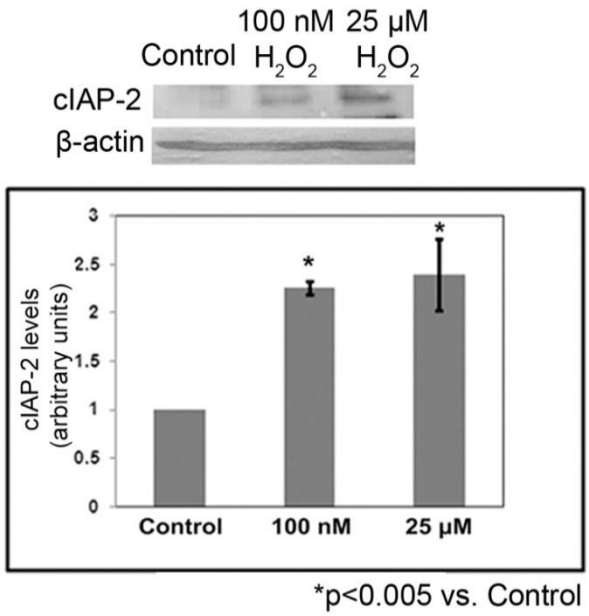

Figure 12: H_2O_2 induces cIAP-2 in cardiac fibroblasts

Confluent cultures of cardiac fibroblasts in M199 with 10% FBS were treated with H_2O_2 (100 nM and 25 μM) for 12 h. Western blot analysis was performed as described under Methods, using polyclonal anti-cIAP-2 antibody. β-actin served as loading control. H_2O_2 caused significant induction of cIAP-2 expression. A representative profile from one of three experiments is shown.

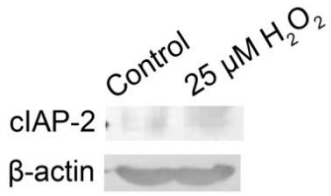

Figure 13: No cIAP-2 induction observed in response to H_2O_2 exposure in pulmonary fibroblasts

Confluent cultures of pulmonary fibroblasts in M199 with 10% FBS were treated with 25 μM H_2O_2 for 12 h. Western blot analysis was performed as described under Methods, using polyclonal anti-cIAP-2 antibody. β-actin served as loading control. H_2O_2 caused no induction of cIAP-2 expression. A representative profile from one of two experiments is shown.

1V.6 RNA interference-mediated cIAP-2 knockdown compromises cell viability in presence of H_2O_2

To ascertain if cIAP-2 plays a pro-survival role in cardiac fibroblasts exposed to H_2O_2, cell death was examined in cardiac fibroblasts exposed to H_2O_2 following cIAP-2 knockdown by RNA interference. Two cIAP-2-directed siRNAs, siRNA14 and siRNA15, were purchased from Ambion, USA. Transfection with cIAP-2-directed siRNA15 abrogated the expression of H_2O_2-induced cIAP-2 expression (Figure 14). cIAP-2 silencing, mediated by siRNA15, caused significant levels of cell death under oxidative stress, as evidenced by Hoechst/PI staining (Figure 15). Further, appearance of the 89 kDa fragment of cleaved PARP was monitored in cIAP-2-silenced cells to check the occurrence of apoptosis. Full-length PARP is a 116 kDa protein involved in the repair of DNA, in differentiation and in chromatin structure formation. However, during apoptosis this protein is cleaved by caspase-3, and possibly other caspases, into an 89 kDa fragment, which is considered a

hallmark of apoptosis (Gobeil *et al*., 2001). No PARP cleavage was observed in cardiac fibroblasts exposed to 25 µM H_2O_2, which was in agreement with the absence of uptake of PI under these conditions. However, in cIAP-2-silenced cells exposed to H_2O_2, marked cleavage of PARP was observed (Figure 16), with siRNA15. SiRNA14 was found to be less effective than siRNA15 in mediating cIAP-2 silencing (Figure 14) and also in resultant PARP cleavage (Figure 16).

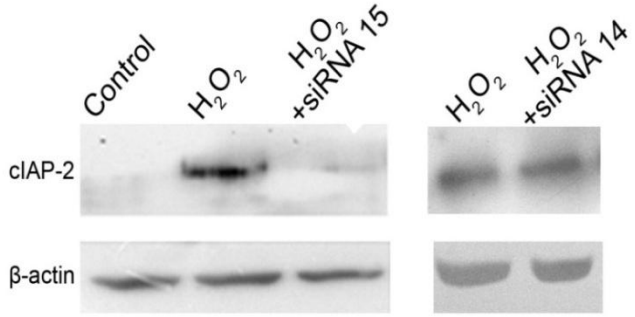

Figure 14: siRNA- mediated knockdown of cIAP-2 in cardiac fibroblasts exposed tooxidative stress

Cardiac fibroblasts were incubated with Ambion cIAP-2 pre-designed Silencer-Select siRNA 14 or siRNA15 (5 pmol) and Lipofectamine (2 µl) for 19 h and then subjected to H_2O_2 treatment. Western blotting confirmed knockdown of cIAP-2 expression by siRNA 15. β-actin served as loading control. Representative blot from one of three experiments is shown.

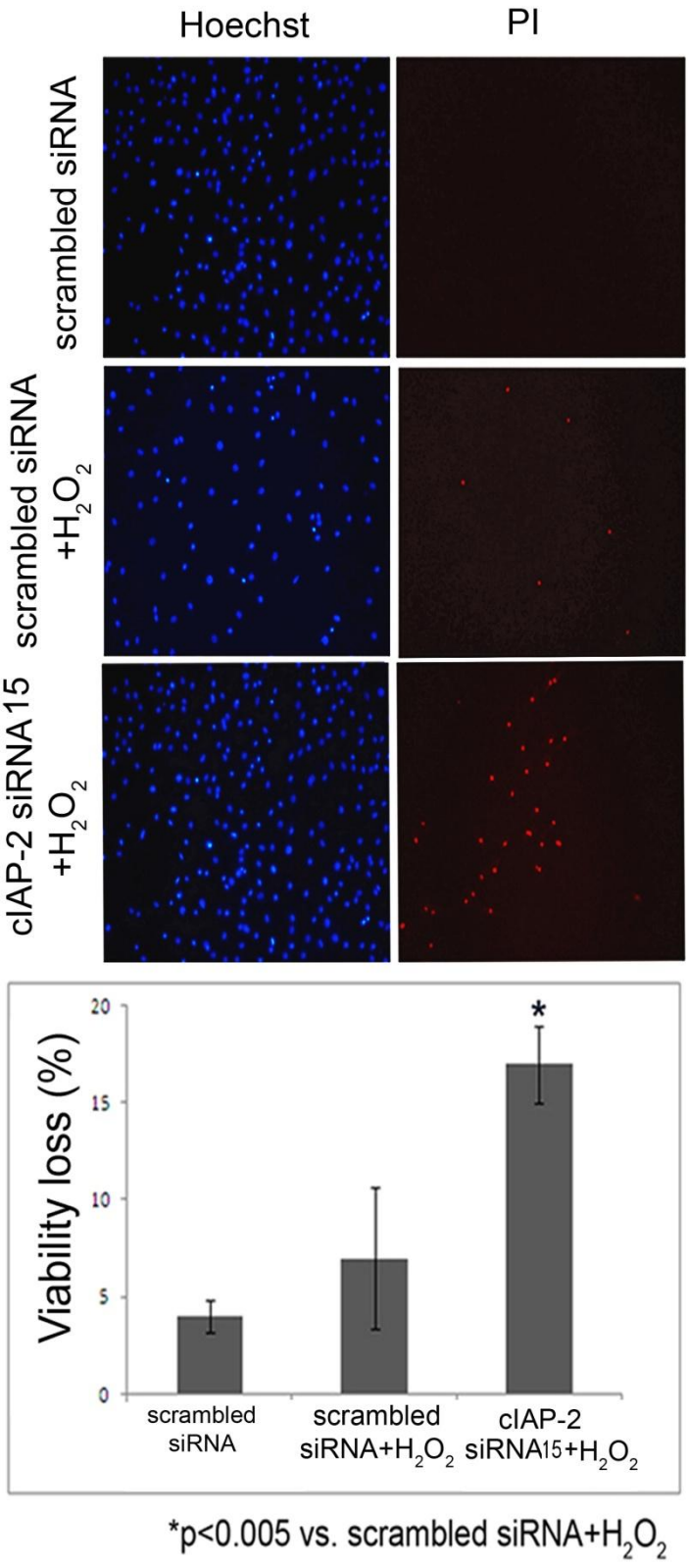

Figure 15: cIAP-2 protects cardiac fibroblasts from oxidative stress

Following cIAP-2 knockdown using siRNA 15, cells were exposed to H_2O_2 treatment for 3 h and stained with Hoechst 33342/PI. cIAP-2 knockdown significantly enhanced cell death in response to oxidative stress. Values are expressed as Mean+/-SD. A minimum of 250 cells was counted per dish. Representative fluorescent micrographs from one of three experiments are shown.

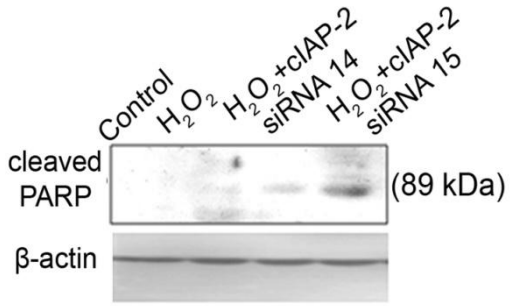

Figure 16: cIAP-2 silencing induces apoptosis in cardiac fibroblasts exposed to oxidativestress

Levels of cleaved PARP in cell lysates prepared from cIAP-2 siRNA 14- and 15-treated cells exposed to oxidative stress were assessed by Western blot analysis, using monoclonal anti-cleaved PARP antibody. β-actin served as loading control. cIAP-2 knockdown caused marked increase in cleaved PARP levels (89 kDa fragment, characteristic of apoptosis) and the effect was more pronounced with siRNA 15.A representative profile from one of two experiments is shown.

1V.7 Regulation of cIAP-2 expression

Subsequent experiments addressed the regulation of cIAP-2 induction in cardiac fibroblasts exposed to H_2O_2. NF-κB is known to mediate up-regulation of both pro- and anti-apoptotic proteins, depending on the cell type and the stress stimulus (Sarnico *et al*., 2009). This study examined the role of NF-κB in cell survival and cIAP-2 expression in cardiac fibroblasts under conditions of oxidative stress.

1V.7.1 Nuclear translocation of NF-κB in response to H_2O_2

To begin with, the activation status of NF-κB was assessed by EMSA using nuclear extracts from cardiac fibroblasts following 30 and 60 minutes of H_2O_2 treatment. As shown in Figure 17, H_2O_2 induced nuclear translocation of NF-κB.

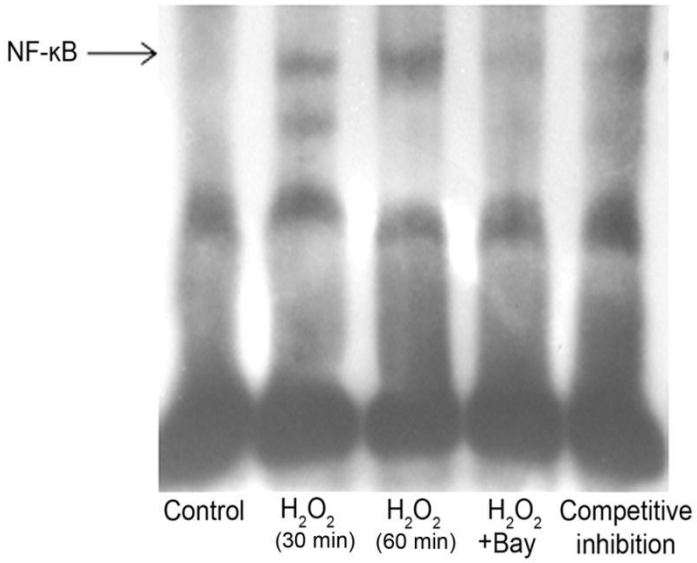

Figure 17: H_2O_2 induces NF-κB translocation

Confluent cardiac fibroblast cultures in M199 were serum-deprived for 12 h followed by H_2O_2 treatment for 30 and 60 min in serum-free M199. Nuclear extracts, prepared using NEPER extraction kit, were incubated with biotinylated primers for NF-κB and the LightShift Chemiluminescent EMSA kit components. DNA binding activity of NF-κB was observed in response to H_2O_2 at both 30 and 60 min, which was significantly attenuated upon pre-treatment with Bay 11-7085 (4 µM). NF-κB binding was significantly reduced in the presence of wild type oligos due to competition. A representative profile from one of three experiments is shown.

1V.7.2 Competition assay

The specificity of NF-κB for the putative NF-κB binding site was established by the competition assay using wild-type oligonucleotides containing binding site for NF-

κB in 200-fold excess. EMSA was perfomed with nuclear extracts incubated with biotin-labeled oligo and an excess of wild-type NF-κB oligo. As expected, the wild-type oligo competitively reduced the binding of NF-κB to the biotin-labeled oligo (Figure 17), which resulted in diminished band intensity, confirming the specificity of the binding. (Details of supershift assay performed to determine the subunit composition of NF-κB are included under Section IV.12.1.)

Having demonstrated the nuclear localization of NF-κB, experiments were designed to determine whether the transcription factor plays a role in the survival of these cells under conditions of H_2O_2 treatment. The strategy consisted in evaluating the effect of NF-κB inhibition on viability of cardiac fibroblasts under oxidative stress.

1V.7.3 Abrogation of NF-κB activation by Bay 11-7085

Bay 11-7085 is reported to effectively inhibit NF-κB activation in different cell types (Gutierrez *et al*., 2006). Earlier studies from this laboratory had shown that incubation of cardiac fibroblasts with Bay 11-7085 at 2 µM for 24 hours (or 4 µM Bay 11-7085 for 12 hours) did not result in any cell loss under normoxia (Sangeetha, 2009), facilitating analysis of the cells for Bay-induced changes in: a) nuclear import of NF-κB, b) cell viability, and c) the status of anti-apoptotic proteins in cardiac fibroblasts exposed to oxidative stress.

Inhibition of nuclear translocation of NF-κB by Bay 11-7085

Cells were pre-treated with 4 µM Bay 11-7085 for one hour followed by 60 minutes of H_2O_2 treatment in presence of 4 µM Bay 11-7085. Nuclear extracts were then

prepared as described under ‘Methods’ and EMSA was performed. Pre-treatment of cells with Bay 11-7085 resulted in the inhibition of the nuclear import of NF-κB in cells exposed to oxidative stress, as shown in Figure 17.

V.8 NF-κB inhibition promotes apoptosis in cardiac fibroblasts exposed to H_2O_2

To test if NF-κB plays a pro-survival role in cardiac fibroblasts exposed to H_2O_2, the study checked the effect of NF-κB inhibition on cardiac fibroblast viability using Bay11-7085 (4 μM). Annexin/PI uptake revealed that NF-κB inhibition promotes 21% death in cells exposed to H_2O_2 (Figure 18). Appearance of cleaved PARP (89kDa) in NF-κB-inhibited cardiac fibroblasts under oxidative stress confirmed the occurrence of apoptosis (Figure 19).

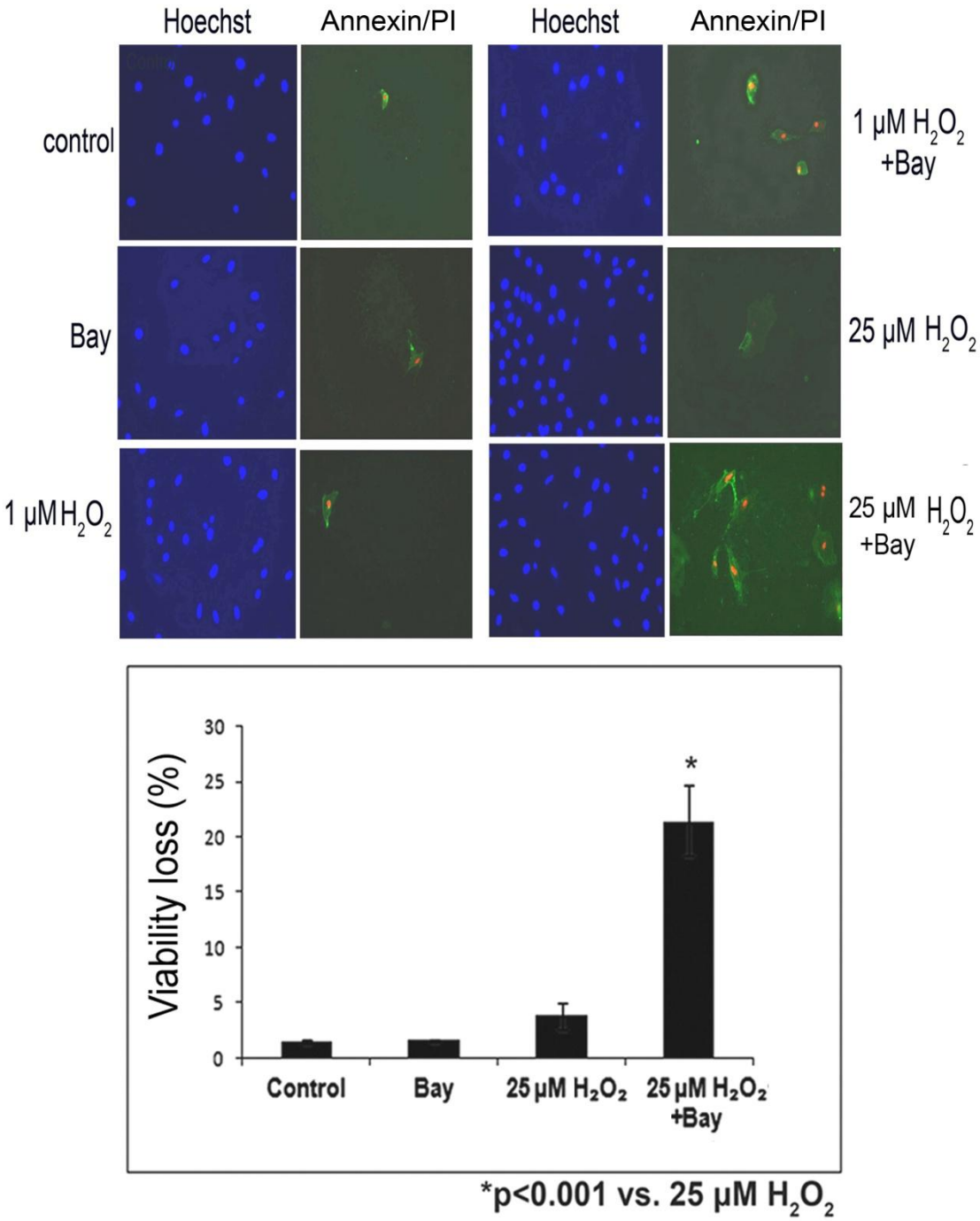

Figure 18: NF-κB protects cardiac fibroblasts from oxidative injury

A marked increase in the number of Annexin and PI-positive cells was observed in NF-κB-inhibited cells exposed to H_2O_2 for 3 h. Values are expressed as Mean± SD. A minimum of 250 cells was counted per dish. Representative fluorescent micrograph from one of five experiments is shown.

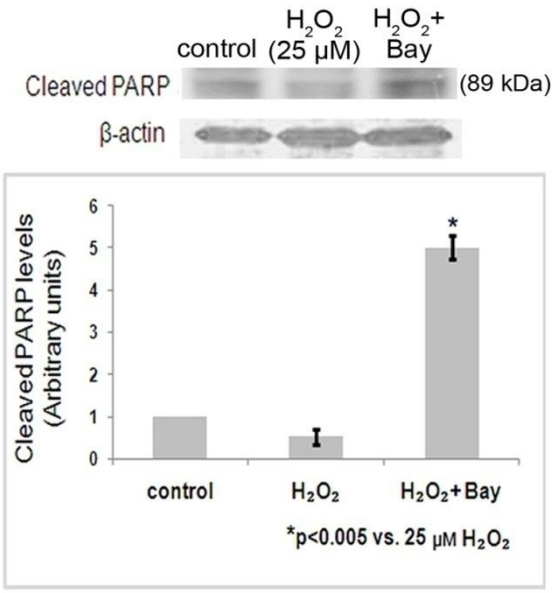

Figure 19: NF-κB inhibition induces apoptosis in cardiac fibroblasts exposed to H_2O_2

Levels of cleaved PARP (89 kDa fragment), assessed by Western blot analysis, were significantly higher in NF-κB-inhibited cardiac fibroblasts exposed to H_2O_2 for 12 h. A representative profile from one of three experiments is shown.

1V.9 Regulation of cIAP-2 by NF-κB in cardiac fibroblasts exposed tooxidative stress

The study showed on the one hand, activation of NF-κB in response to oxidative stress, and on the other, loss of viability upon NF-κB inhibition in H_2O_2-treated cells. As several studies point to a role for NF-κB in transcriptional regulation of cIAP-2, this study checked the involvement of NF-κB in cIAP-2 up-regulation in these cells.

IV.9.1 Real time PCR analysis of cIAP-2 mRNA

Confluent cultures were exposed to H_2O_2 in M199 containing 10% FBS for 6 hours. Total RNA was isolated using Tri-reagent and its purity was ascertained by 1% agarose gel electrophoresis. Appearance of intact 18S and 28S rRNA bands confirmed the intactness of the isolated RNA (Figure 20). To get rid of any genomic DNA contamination, total RNA was subjected to DNase I treatment as per manufacturer's instructions. PCR analysis of RNA samples subjected to DNase I treatment using G3PDH primers revealed no genomic DNA contamination after the treatment (Figure 21). 2 μg of DNase I-treated RNA was reverse transcribed to cDNA with random hexamer primers and M-MLV reverse transcriptase. The cDNA was co-amplified over 40 cycles with primers specific for rat cIAP-2 and 18S rRNA (internal control) by Taqman quantitative real-time polymerase chain reaction (RT-PCR) using the ABI 7900 Sequence Detection System (Applied Biosystems, CA). A significant 3-fold induction in the cIAP-2 mRNA levels, observed in response to H_2O_2, was markedly attenuated upon NF-κB inhibition by Bay 11-7085 (Figure 22). This showed that NF-κB transcriptionally up-regulates cIAP-2 under H_2O_2-mediated oxidative stress.

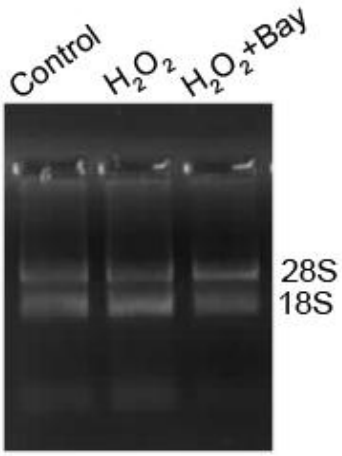

Figure 20: Agarose gel electrophoresis of RNA

RNA, isolated from control, H_2O_2-treated cells and NF-κB-inhibited cells exposed to H_2O_2 as described under 'Methods', was subjected to 1% agarose gel electrophoresis. The presence of intact 28S and 18S bands was documented using Syngene Bio Imaging system.

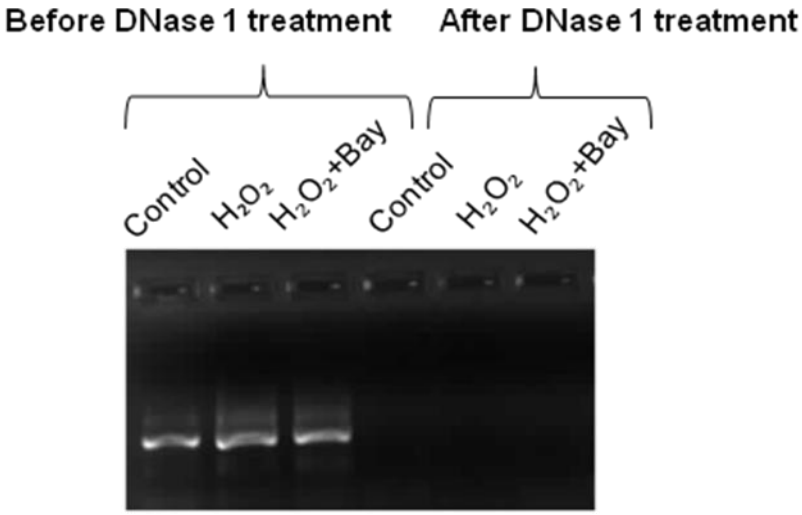

Figure 21: PCR analysis of RNA samples subjected to DNase I treatment

RNA, isolated from control, H_2O_2-treated cells and NF-κB-inhibited cells exposed to H_2O_2 was subjected to DNase I treatment, as per manufacturer's instructions, was subjected to PCR analysis using G3PDH primers. PCR products were analyzed by 1% agarose gel electrophoresis. A representative profile shows no genomic DNA contamination after DNase I treatment.

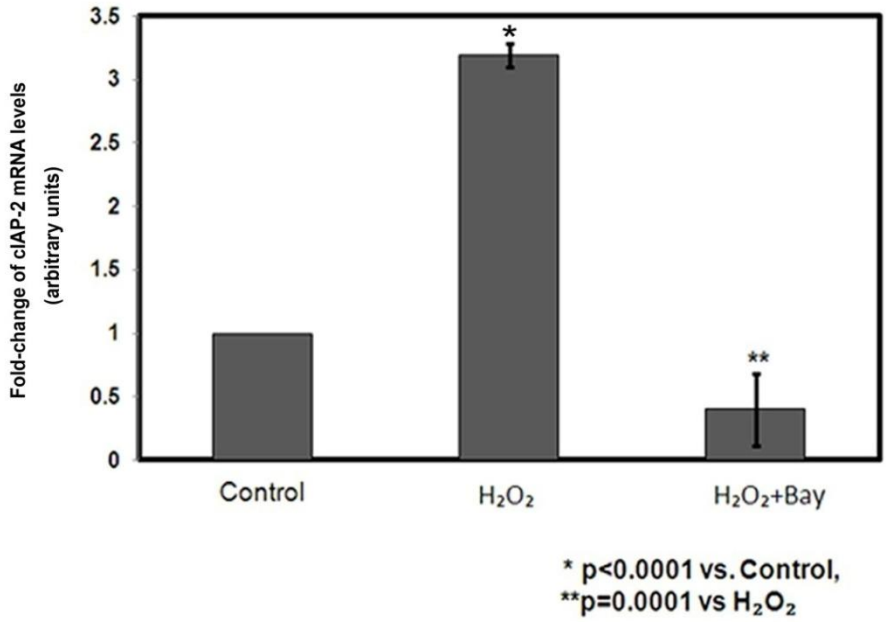

Figure 22: NF-κB inhibition down-regulates cIAP-2 mRNA levels

Confluent cardiac fibroblast cultures in M199 with 10% FBS were exposed to H_2O_2 for 6 h in the presence/absence of 4 µmol/L Bay 11-7085. 2 µg of total isolated RNA was reverse transcribed to cDNA. Relative quantification of cIAP-2 mRNA expression was performed by Real Time PCR analysis using FAM-labelled probes of cIAP-2 (Rn00572734_m1) and 18S rRNA (4333760T) over 40 cycles. H_2O_2 increased cIAP-2 transcript levels markedly while NF-κB inhibition by Bay 11-7085 attenuated the effect. n=3

1V.9.2 Down-regulation of cIAP-2 protein in NF-κB-inhibited cardiac fibroblasts exposed to oxidative stress

Consistent with the real time PCR data, cIAP-2 protein expression was also found to decrease upon NF-κB inhibition (Figure 23).

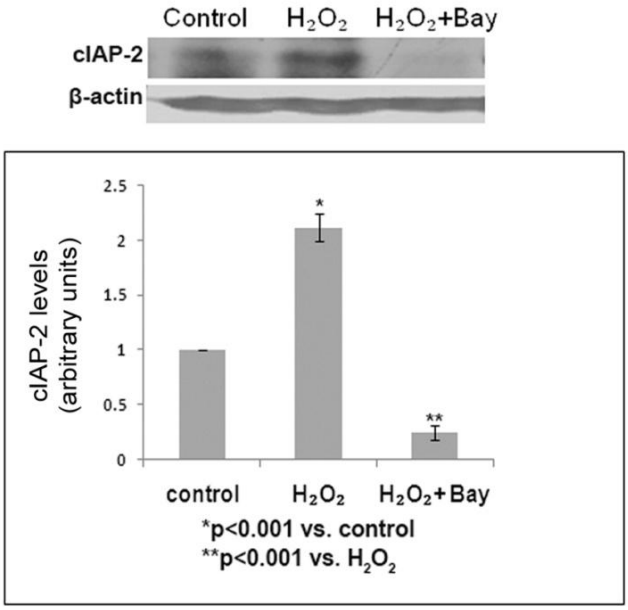

Figure 23: NF-κB inhibition down-regulates cIAP-2 protein levels

Confluent cultures of cardiac fibroblasts in M199 with 10% FBS were treated with 25 µM H_2O_2 for 12 h with and without Bay 11-7085. Western blot analysis revealed that the H_2O_2-induced cIAP-2 is significantly reduced upon NF-κB inhibition. β-actin served as loading control. Values are represented as Mean ± SD of 3 independent experiments and are expressed in arbitrary units. A representative profile from one of three experiments is shown.

Together, evidence that

1) cIAP-2 inhibition leads to apoptosis in cardiac fibroblasts exposed to oxidative stress (Figures 15 & 16), and
2) NF-κB inhibition compromises viability (Figures 18 & 19) and attenuates cIAP-2 expression (Figures 22 & 23) in cardiac fibroblasts under oxidative stress

clearly demonstrate that NF-κB mediates a pro-survival role by up-regulating anti-apoptotic cIAP-2. To confirm the pro-survival role of cIAP-2, subsequent experiments investigated the possibility that forced expression of cIAP-2 would

prevent or attenuate the loss of viability noted in NF-κB-inhibited cardiac fibroblasts exposed to H_2O_2 that do not express cIAP-2 and are susceptible to oxidative stress.

1V.10 cIAP-2 over-expression attenuates viability loss in NF-κB-inhibited cardiac fibroblasts exposed to H_2O_2

Strong constitutive expression of cIAP-2 was induced using the cIAP-2 Native ORF clone- containing pCMV vector in NF-κB-inhibited cardiac fibroblasts exposed to H_2O_2.

1V.10.1 Optimization of turbofectin concentration

Cells were exposed to a range of concentrations of turbofectin (1.5 µl to 6 µl) to determine the optimal concentration at which transfection occurred without significant cell death. PI uptake by cells was not significant upon exposure to 4 µl turbofectin but was much higher upon exposure to 6 µl. An optimal concentration of 3 µl was chosen for further experiments (Figure 24).

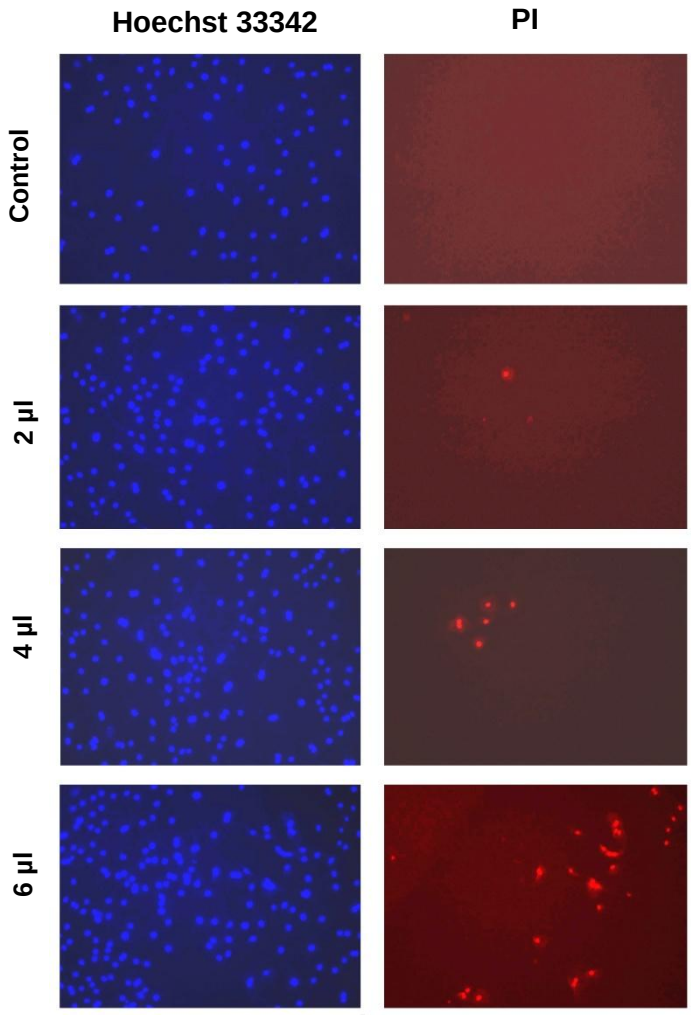

Figure 24: Optimization of turbofectin concentration in cardiac fibroblasts

Cells were exposed to a range of concentrations of turbofectin (1.5 µl to 6 µl) and viability was checked by Hoechst/ PI staining. Turbofectin-induced viability loss was observed at 4 µl onwards.

1V.10.2 Plasmid amplification and screening of kanamycin-resistant clones

The ready-to-transfect cIAP-2 Native ORF clone was amplified by transformation in competent DH5-α strain. As kanamycin resistance was the antibiotic selection marker, kanamycin-resistant clones were selected (Figure 25) and amplified further in LB medium.

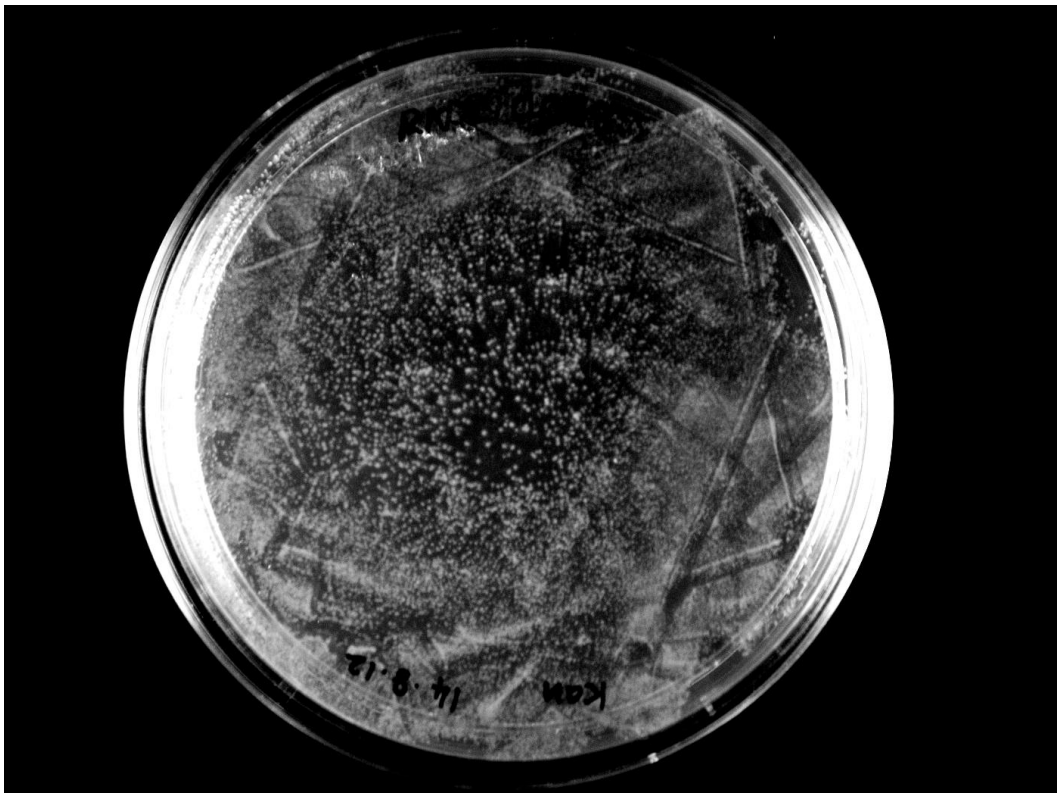

Figure 25: Photograph of kanamycin-resistant clones grown after amplification in kanamycin-containing LB medium

DH5-α strain after transformation with native cIAP-2 ORF clone was grown in kanamycin-containing medium to screen for kanamycin-resistant clones as kanamycin is the antibiotic selection marker.

1V.10.3 Plasmid isolation

pCMV6 plasmid was isolated as described under 'Methods'. Purity was checked spectrophotometrically and by agarose gel electrophoresis (Figure 26). The plasmid was subjected to verification steps using PCR and restriction digestion.

- *PCR amplification of cIAP-2 clone*

Size of the plasmid, isolated using the Qiagen's Plasmid Midi kit was checked by amplification of the cIAP-2 clone using forward and reverse primers supplied with the same kit. The cIAP-2 clone size (1770 bp) was determined on 1.2% agarose gel after amplification (Figure 26).

- *Restriction digestion*

The cIAP-2 clone was integrated in the pCMV6 plasmid at the restriction sites of Sgf-1 and Mlu-1. Single site restriction digestion at Mlu-1 yielded the linearized form of the plasmid (6770 bp), analyzed on 1.2% agarose gel (Figure 26).

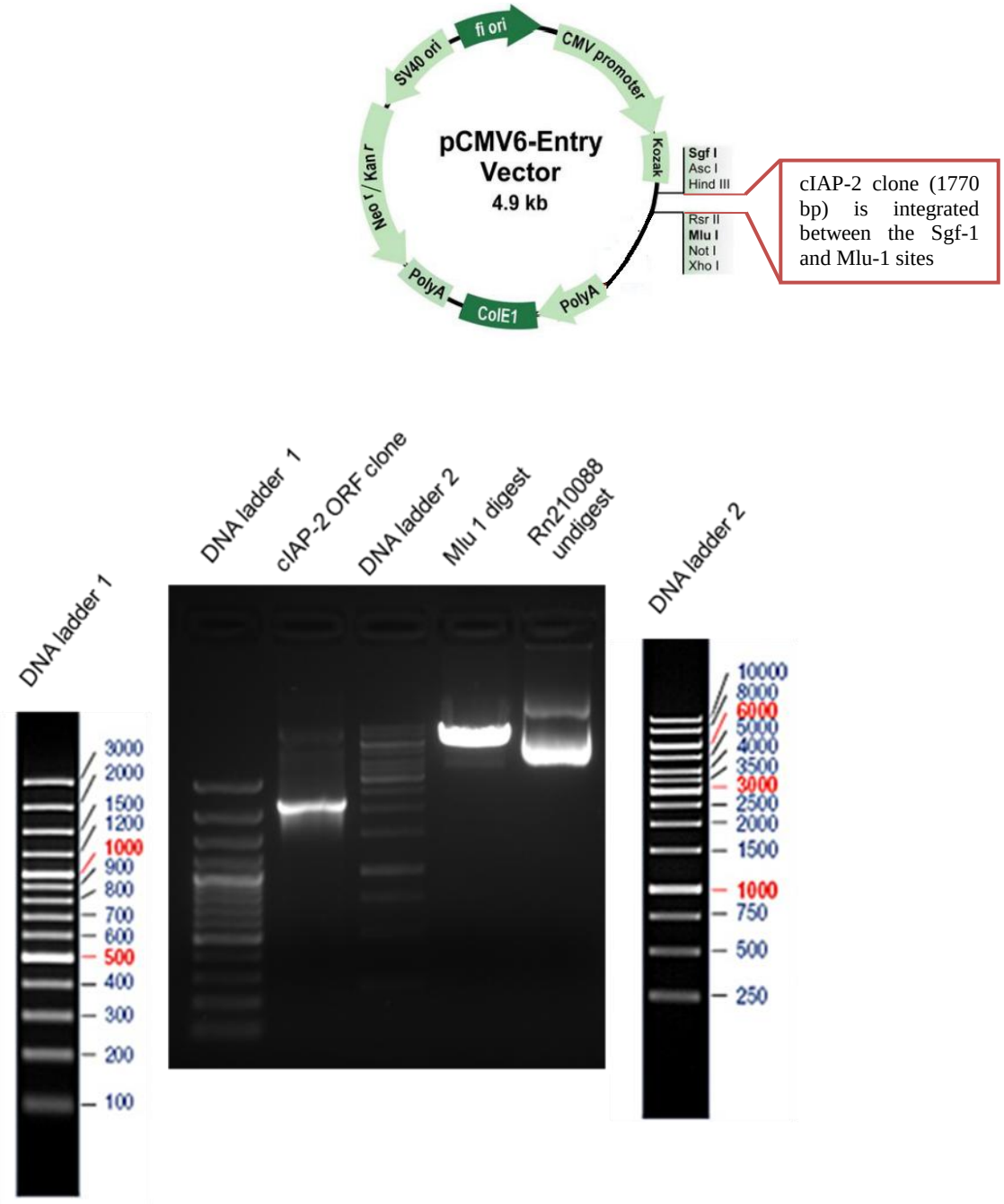

Figure 26: 1.2% agarose gel electrophoresis of PCR product, restriction digest andundigested plasmid

Using forward and reverse primers supplied with the kit, the cIAP-2 clone was amplified by PCR using conditions described under 'Methods' and size (1770 bp) was determined on 1.2% agarose gel (cIAP-2 ORF clone) . Single site restriction digestion at Mlu-1 yielded the linearized form of the plasmid and analyzed on 1.2% agarose gel (6770 bp)(Mlu-1 digest). The size of the undigested circularized plasmid

was determined on 1.2 % agarose gel (~8500 bp)(RN210088). Inset: Plasmid map of the pCMV6 vector containing the cIAP-2 clone, procured from Origene, USA.

IV.10.4 Transfection of cardiac fibroblasts

cIAP-2 over-expression plasmid cocktail was prepared with 1 µg plasmid and 3 µl turbofectin in 100 µl Opti-MEM, which was added to the cultures for incubation in M199+10% FBS for 12 hours. After a recovery period of 19 hours, cells were pre-treated with Bay 11-7085 followed by H_2O_2 treatment. Extensive cell damage was observed in control plasmid (pcI)-transfected cells following treatment duration of 12 hours. However, duration of 4 hours did not result in significant morphological damage. Over-expression of cIAP-2 in Bay-treated cells was confirmed by western blotting (Figure 27).

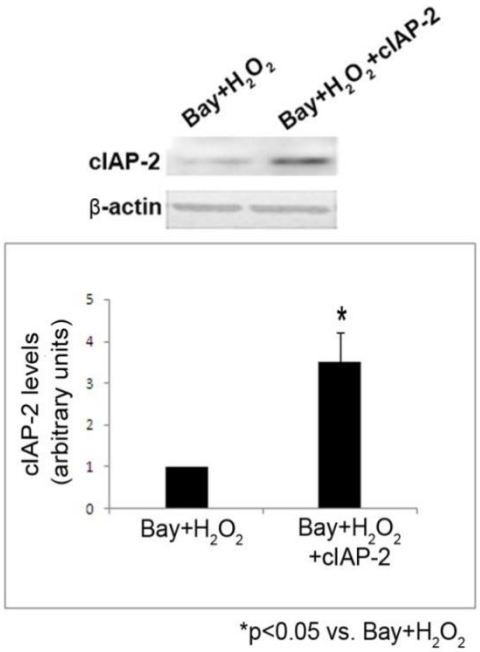

Figure 27: **Constitutive expression of cIAP-2 was achieved using Native ORF clone ofcIAP-2 in a pCMV system**

The ready-to-transfect cIAP-2 plasmid (RN210088) cocktail was prepared by adding 1 µg plasmid and 3 µl turbofectin to 100 µl Opti-MEM, which was added to the cultures for incubation in M199+10% FBS for 4 h. After a recovery period of 15 h, cells were pre-treated with Bay 11-7085 followed by H_2O_2 treatment. Western blotting confirmed over-expression of cIAP-2 under conditions of NF-κB inhibition in cardiac fibroblasts exposed to H_2O_2. A representative profile from one of three experiments is shown.

IV.10.5 cIAP-2 over-expression attenuates viability loss in NF-κB-inhibited cardiac fibroblasts exposed to oxidative stress

The loss of viability observed upon NF-κB inhibition was prevented upon cIAP-2 over-expression, which underscored the importance of NF-κB-dependent cIAP-2 expression in the resistance of cardiac fibroblasts to apoptosis (Figure 28).

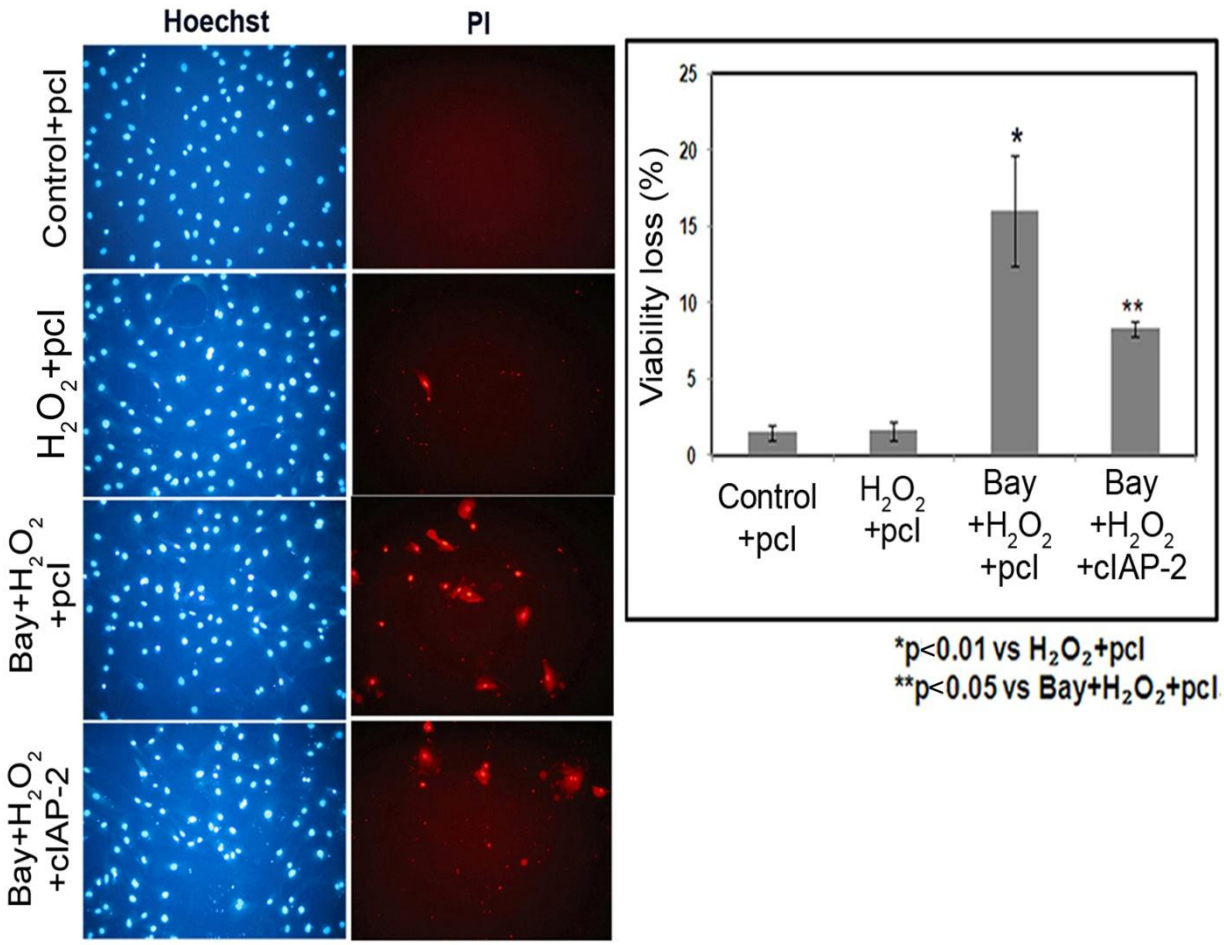

Figure 28: Constitutive expression of cIAP-2 reduces viability loss in NF-κB-inhibited cardiac fibroblasts exposed to oxidative stress

Loss of viability upon NF-κB inhibition, observed by Hoechst/PI staining, was reduced significantly upon cIAP-2 over-expression. Values are expressed as Mean±SD. A minimum of 250 cells was counted per dish. Representative fluorescent micrographs from one of three experiments are shown.

1V.11 ERK1/2 is an upstream mediator of apoptosis resistance in cardiac fibroblasts under oxidative stress

ERK1/2 is known to mediate protective effects in the myocardium (Hausenloy & Yellon, 2003). The present study explored the possibility that ERK1/2 may regulate NF-κB activity and exert a pro-survival role in cardiac fibroblasts exposed to oxidative stress.

1V.11.1 H_2O_2 induces ERK1/2 activation

Treatment of cardiac fibroblasts with H_2O_2 resulted in activation of ERK1/2 as early as 15 minutes, which was sustained upto 12 hours (Figure 29).

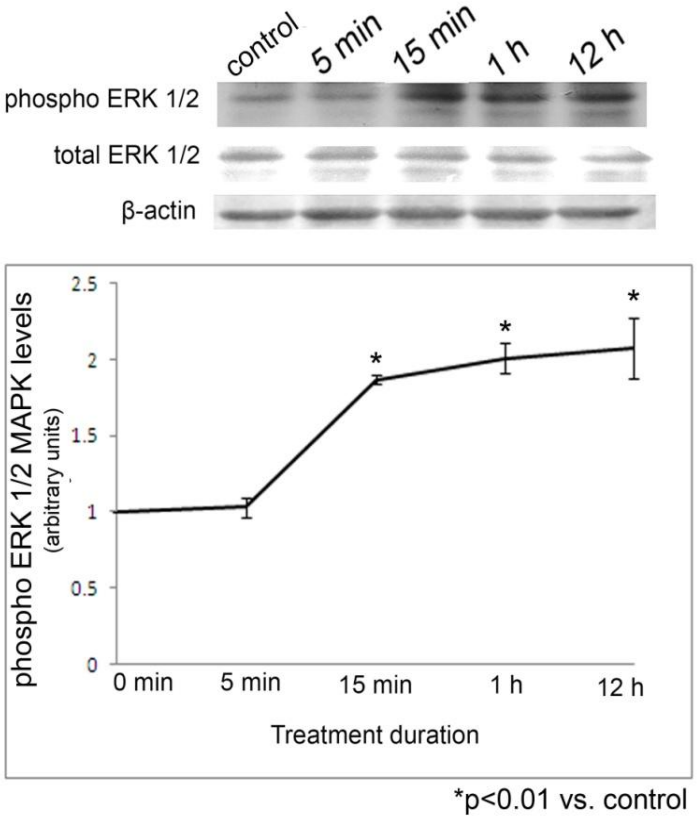

Figure 29: Activation of ERK1/2 in response to H_2O_2

Confluent cultures of cardiac fibroblasts in M199 were serum-deprived for 36 h followed by exposure to H_2O_2 for the indicated durations. Western blot analysis was performed using monoclonal anti-phospho-ERK1/2 antibody. ERK1/2 activity, normalized to total ERK1/2 levels, peaked at 15 min, which was sustained upto 12 h. A representative profile from one of two experiments is shown.

1V.11.2 ERK1/2 inhibition compromises cardiac fibroblast viability under oxidativestress

ERK1/2 inhibition by PD 98059 was found to significantly compromise viability of cardiac fibroblasts exposed to H_2O_2, which indicated that ERK1/2 may have a pro-survival role in these cells under conditions of oxidative stress (Figure 30).

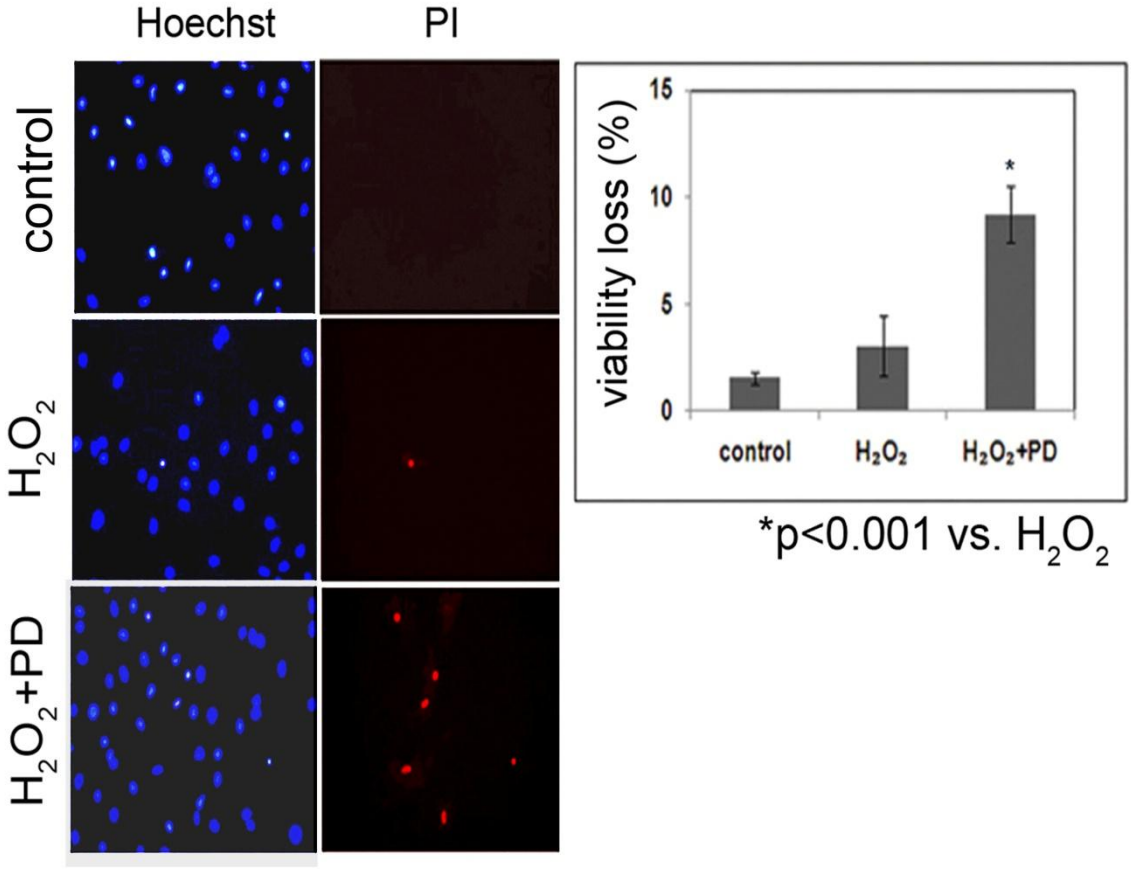

Figure 30: ERK1/2 inhibition induces cell death in cardiac fibroblasts exposed to H_2O_2

A marked increase in the number of PI-positive cells was observed in cells exposed to H_2O_2 for 3 h in the presence of PD 98059 (10 µM). Values are expressed as Mean± SD. A minimum of 250 cells was counted per dish. Representative fluorescent micrographs from one of three experiments are shown.

1V.11.3 ERK1/2 inhibition down-regulates cIAP-2 and promotes cell death in cardiac fibroblasts under oxidative stress

To determine if the pro-survival role of ERK1/2 is mediated by cIAP-2, expression levels of cIAP-2 were checked in ERK1/2-inhibited cells exposed to H_2O_2. Significant reduction of cIAP-2 levels in ERK1/2-inhibited cells (Figure 31)

demonstrated that ERK1/2 is a positive regulator of cIAP-2 in cardiac fibroblasts. Together, the data suggested that ERK1/2-mediated up-regulation of cIAP-2 may, at least in part, underlie cardiac fibroblast survival under oxidative stress.

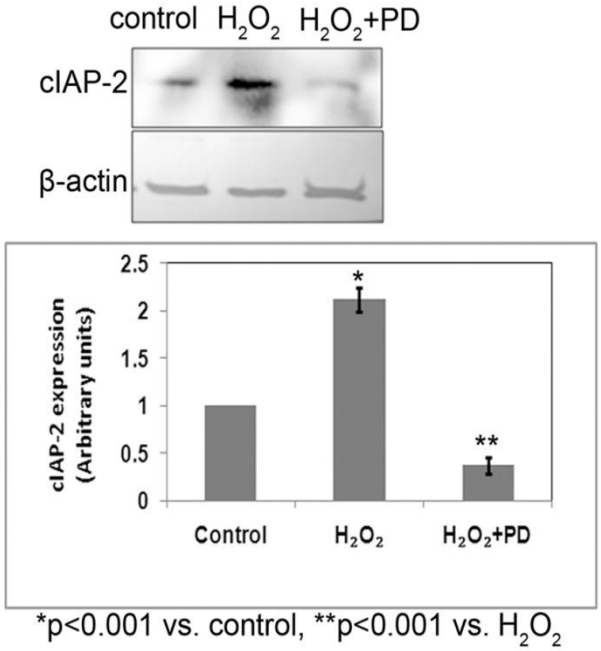

Figure 31: Down-regualtion of cIAP-2 levels in ERK1/2-inhibited cells upon exposure to oxidative stress

Confluent cultures of cardiac fibroblasts in M199 with 10% FBS were treated with 25 µM H_2O_2 for 12 h with and without PD 98059. Western blot analysis showed that ERK1/2 inhibition significantly reduces cIAP-2 induction in cells exposed to H_2O_2 for 12 h. A representative profile from one of three experiments is shown.

IV.12 ERK1/2 is an upstream mediator of NF-κB activation in cardiac fibroblasts

IV.12.1 Attenuation of H_2O_2-induced NF-κB activity upon ERK1/2 inhibition

Since ERK1/2 was found to influence cardiac fibroblast survival and cIAP-2 expression, the study examined if these effects were mediated via activation of NF-

κB. Consistent with such a postulation, H_2O_2-induced NF-κB activation was significantly inhibited in ERK1/2-inhibited cardiac fibroblasts (Figure 32).

Super shift assay

Super-shift assay was performed to ascertain the subunit composition of active NF-κB in cardiac fibroblasts. Nuclear extracts with active NF-κB were separately incubated for 1 hour with biotin-labelled NF-κB consensus sequence and antibodies against the p65 and p50 sub-units. The p50 and p65 antibodies bound to NF-κB, resulting in the assembly of a ternary complex consisting of NF-κB, the bound antibody and the biotin-labelled oligo. The electrophoretic mobility of the ternary complex was understandably lower than that of the NF-κB-biotin-labelled-oligo complex without any bound antibody (Figure 32), which showed that active NF-κB in rat cardiac fibroblasts is a p65/p50 heterodimer.

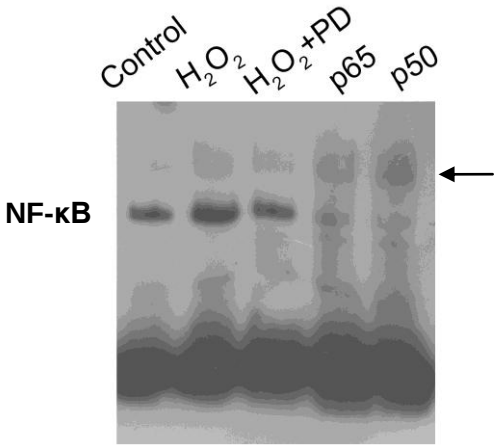

Figure 32: ERK1/2 MAPK regulates NF-κB activation in cardiac fibroblasts

Confluent cardiac fibroblast cultures in M199 were serum-deprived for 12 h followed by H_2O_2 treatment for 1 hour in the presence/ absence of PD 98059 (10 μM). Electrophoretic mobility shift assay showed that the nuclear translocation of

NF-κB observed in response to H_2O_2 is significantly reduced upon ERK1/2 inhibition. Super-shift assay was performed using antibodies against p65 and p50 subunits. Arrow corresponds to the shifted p65 and p50 NF-κB bands. A representative profile from one of two experiments is shown.

IV.12.2 Inhibition of ERK1/2 attenuated H_2O_2-induced IκBα degradation

In unstimulated cells, NF-κB dimmer is retained in the cytosol by its binding to IκB, which masks its nuclear localization signal. Upon activation, IκB undergoes degradation setting the dimer free to translocate to nucleus. p65-containing heterodimers of NF-κB, as observed in the study, are generally activated by the classical pathway, involving mainly degradation of IκBα (Oeckinghaus *et al*., 2011). In this regard, it was observed that H_2O_2 promoted degradation of IκBα, indicating the involvement of IκBα-degradation in activation of NF- κB (Figure 33). Inhibition of ERK1/2 attenuated H_2O_2-induced IκBα degradation, indicating that IκBα-mediated NF-κB activation may be ERK1/2-dependent (Figure 33), possibly by the classical pathway that is mostly responsible for activation of p65-containing heterodimers (Oeckinghaus *et al*., 2011).

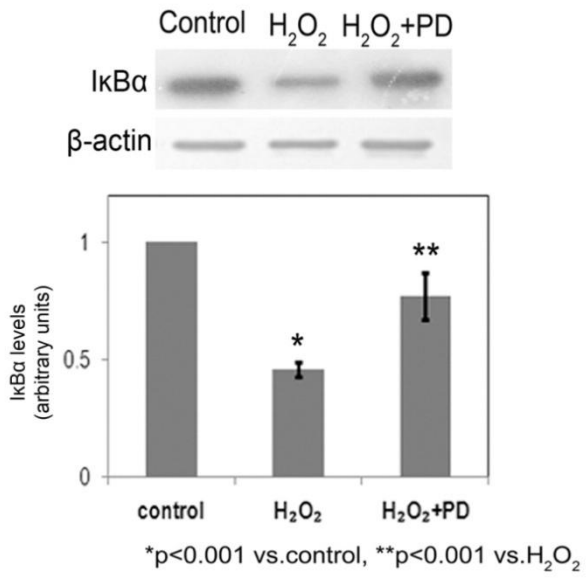

Figure 33: ERK1/2 MAPK inhibition down-regulates H_2O_2-induced IκBα degradation incardiac fibroblasts

Confluent cardiac fibroblast cultures in M199 were serum-deprived for 12 h followed by exposure to H_2O_2 for 1 h. Cytosolic levels of total IκBα were assessed by Western blot analysis, using IκBα polyclonal anti-antibody. β-actin served as loading control. Significant reduction in IκBα expression was observed in response to H_2O_2, which was partially reversed upon ERK1/2 inhibition using PD 98059 (10 μM). A representative profile from one of three experiments is shown.

IV.13 Inhibition of p38 MAPK did not compromise viability of cardiac fibroblasts exposed to H_2O_2

To determine if p38 MAPK, a stress kinase, is involved in cardiac fibroblastresistance to oxidative stress cells were exposed to H_2O_2 under conditions of p38 MAPK inhibition using SB203850 (10 μM) and viability was examined. Absence of cell death upon p38 MAPK inhibition precluded a pro-survival role for p38 MAPK. (Figure 34).

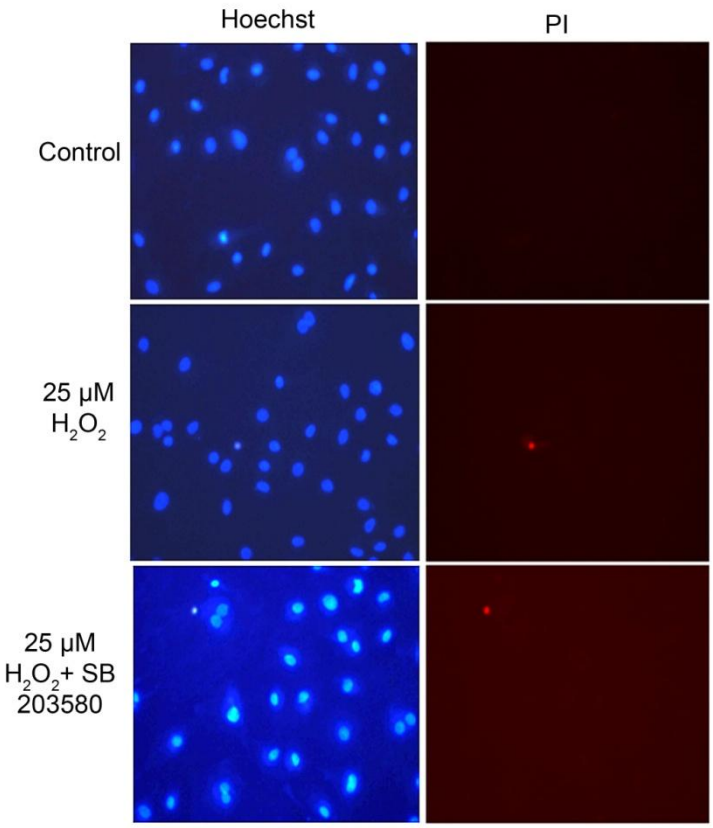

Figure 34: p38 MAPK inhibition does not compromise viability in H_2O_2-treated cardiacfibroblasts

No increase in the number of PI-positive cells was observed in cardiac fibroblasts exposed to 25 µM H_2O_2 for 3 h in the presence of p38 MAPK inhibitor, SB 203580 (10 µM). A minimum of 250 cells was counted per dish. Representative fluorescent micrographs from one of three experiments are shown.

V. Discussion

An integral component of the pathogenesis of heart failure is cardiac remodeling, which encompasses the responses of cardiac cells to diverse etiologies of heart failure such as myocardial infarction, pressure overload (aortic stenosis, hypertension), inflammatory heart muscle disease (myocarditis) and volume overload (valvular regurgitation) (Cohn *et al*., 2000, Palaniyandi *et al*., 2009). Such responses include myocyte hypertrophy and apoptosis, inflammation and fibrosis, which result in progressive decline of cardiac function. Whereas myocyte hypertrophy may be associated with both adaptive and pathological remodeling, cardiac fibrosis is invariably associated with adverse myocardial remodeling. Studies on the mechanisms of heart failure have traditionally focused on the role of myocytes as the cause of heart failure or on the inadequate perfusion of coronary muscles as in ischemic heart disease (Brown *et al*., 2005). Investigations in recent years have, however, stressed the role of the interstitium in the pathogenesis of heart failure. Cardiac fibrosis may manifest either as replacement fibrosis or reactive fibrosis (Weber *et al*., 2013). Replacement fibrosis occurs in response to myocyte loss whereas reactive fibrosis occurs in the absence of myocyte loss, which leads to myocyte apoptosis and further replacement fibrosis to form a vicious loop (Krenning *et al.,* 2010). The enhanced deposition of ECM components that results compromises ventricular compliance and reduces cardiac contractility. Cardiac fibroblast hyperplasia and resistance to apoptosis that underlie disproportionate stromal expansion contribute to the progression of heart failure.

V. 1 Cardiac fibroblast resistance to apoptosis

Apoptosis plays a principal role in the pathogenesis of ventricular dysfunction (Foo *et al.*, 2005). Several pro-apoptotic stimuli like TNF-α, IL-8 and oxidative stress prevail in the myocardium under pathological conditions. Although cardiomyocytes are susceptible to pro-death signals, cardiac fibroblasts are relatively resistant to these factors, which facilitates their role in wound healing following myocyte loss under stress situations. Additionally, post-tissue repair, myofibroblasts are found to persist long after the completion of tissue healing (Souders *et al*., 2009, Krenning *et al*., 2010). The persistence of activated cardiac fibroblasts in the mature infarct scar may be attributed to resistance to apoptotic stimuli like Fas, TGF-β1 and Ang II (Van den Borne *et al*., 2010). Resistance to death signals may, in the short-term, enable these cells to play a central role in tissue repair following myocyte loss but, in the long-term, facilitate their persistence in the infarct scar, resulting in disproportionate stromal growth and pump dysfunction. Elucidation of the mechanisms that regulate cardiac fibroblast numbers is therefore vital for understanding the pathogenesis of left ventricular remodeling following myocardial injury. Surprisingly, the factors and mechanisms that underlie cardiac fibroblast resistance to apoptosis are largely unknown.

V.1.1 Cardiac fibroblast resistance to apoptosis - *in vitro* observations

Addressing the molecular basis of cardiac fibroblast resistance to apoptosis, Mayorga *et al.*, 2004 probed the response of pro- and anti-apoptotic members of the Bcl-2 family of proteins and XIAP, a member of the IAP family of proteins, in fibroblasts of cardiac and non-cardiac origin upon exposure to diverse apoptotic stimuli. The

study found constitutive levels of XIAP in both cardiac and non-cardiac fibroblasts. However, Bcl-2 is selectively expressed in cardiac but not non-cardiac fibroblasts and plays a predominant role in cardiac fibroblast resistance to staurosporine, etoposide, serum deprivation and simulated ischemia (Mayorga *et al*., 2004). Given the plethora of pro-death signals that can prevail in the diseased heart, it is reasonable to postulate that cardiac fibroblast survival may involve multiple mechanisms. In this context, recent work from our laboratory had shown that NF-κB affords protection to cardiac fibroblasts exposed to hypoxia (Sangeetha *et al*., 2011). Additionally, the study also provided co-rrelational evidence that NF-κB may exert its pro-survival role via anti-apoptotic protein, cIAP-2.

In an attempt to delineate the mechanisms conferring survival advantage upon cardiac fibroblasts, this study aimed at understanding cardiac fibroblast response to oxidative stress. Oxidative stress is implicated in several disease states such as ischemia/reperfusion injury, hypertension and congestive heart failure (Mak & Newton, 2001). Myocytes are found to be susceptible to oxidative stress and *in vitro* studies show the occurrence ofMPT and cytochrome *c* release in cardiomyocytes in response to H_2O_2-induced oxidative stress (Lisa *et al*., 2001). However, cardiac fibroblasts are reported to be resistant to H_2O_2 (Zhang *et al*., 2001).

V.1.2 Molecular mechanisms underlying cardiac fibroblast resistance to oxidativestress

Cells exposed to exogenously added H_2O_2 constitute a widely used *in vitro* model to study oxidant-dependent cellular responses. Schroder *et al*., 2007 showed that exogenously added H_2O_2 may trigger similar signaling pathways as H_2O_2 produced endogenously (Schroder *et al.*, 2007).

The present study showed that cardiac fibroblasts are more resistant to oxidative stress than pulmonary fibroblasts at all concentrations of H_2O_2 used. Whereas significant viability loss was observed in pulmonary fibroblasts, cardiac fibroblasts showed hardly any death at 25 µM H_2O_2. Of note, H_2O_2 in this concentration range is reported to mediate oxidative injury in multiple cell types. For instance, 30 µM H_2O_2 induced apoptosis in cultured cortical neurons (Whittermore *et al.*, 1995) and 15 µM H_2O_2 caused 60% cell death in HL60 cells (DiPietrantonio*et al*., 1999). Additionally, Zhang *et al.*, 2001 have shown that, compared to cardiac myocytes, cardiac fibroblasts are relatively refractory to oxidative stress owing to differential expression of anti-apoptotic Bcl-2 and pro-apoptotic Bax (Zhang *et al.*, 2001).

V.2 Constitutive expression of Bcl-2 in cardiac fibroblasts, which remainsunaltered upon exposure to oxidative stress

Consistent with earlier reports (Zhang *et al*., 2001, Mayorga *et al.*, 2004), this study found constitutive levels of Bcl-2 in cardiac fibroblasts, which remained unaffected upon exposure to oxidative stress. The Bcl-2 family of anti-apoptotic proteins

protects against the mitochondria-dependent death pathway by sequestering pro-apoptotic Bid from activating Bax/Bak and blocks them from forming pores in the outer mitochondrial membrane and prevents release of proapoptotic Smac/DIABLO/AIF/cytochrome c into the cytoplasm (Crow *et al*., 2004). It is interesting to note that in most tissues Bcl-2 is repressed after birth but this study demonstrates that, in cardiac fibroblasts, constitutive expression of Bcl-2 is observed in the adult as well.

V.3 Oxidative stress induces cIAP-2 in cardiac fibroblasts

In addition to Bcl-2, the study also probed the role of another anti-apoptotic protein belonging to the Inhibitor of apoptosis family of proteins, cIAP-2, in cardiac fibroblasts in response to oxidative stress. Significant up-regulation of cIAP-2 in cardiac fibroblasts exposed to H_2O_2-mediated oxidative stress (Figure 12) was found, which upon silencing by RNA interference, induced apoptosis, as evidenced by increased PI uptake and PARP cleavage (Figures 15 & 16). In striking contrast to cardiac fibroblasts, cIAP-2 was not induced in pulmonary fibroblasts exposed to H_2O_2. Admittedly, the absence of a cIAP-2-mediated protective mechanism in pulmonary fibroblasts could potentially contribute to their susceptibility to oxidative damage. However, it is important to recognize that cell survival and cell death are complex processes and the susceptibility of pulmonary fibroblasts to oxidative damage may perhaps not be attributable exclusively to the absence of cIAP-2. The molecular basis of pulmonary fibroblast susceptibility to ambient stress was clearly beyond the scope of this study. Pulmonary fibroblasts were used here only to test the relative resistance of cardiac fibroblasts to H_2O_2.

IAPs play a dynamic role in regulating apoptosis by directly inhibiting active caspases, caspases-3, -7 and -9, to suppress both mitochondria-dependent and -independent apoptosis (Hunter *et al*., 2007). A substantial body of biochemical, structural and *in vivo* data show that IAPs, particularly cIAP-2, may inhibit apoptosis in caspase-independent manners as well (Srinivasula & Ashwell, 2008). cIAP-2 may bind to IAP-binding motif (IBM)-containing proteins like Smac/DIABLO, a pro-apoptotic factor, and thus sequester it for proteasomal degradation (Hu *et al*., 2003). cIAP-2 up-regulation is known to mediate apoptosis resistance in many cell types like 3T3 fibroblasts and primary cultures of human umbilical vein endothelial cells (Mahoney *et al*., 2008).

Expression of the members of the IAP family is tightly regulated with respect to developmental stage, cell type and stress conditions. Among the members of the IAP family of proteins, expression of survivin is restricted to the embryonic stages of development in normal tissues (Ambrosini *et al*., 1997) and is also reported to have a role in cytokinesis by its association with mitotic spindle apparatus (LaCasse *et al*., 1998). On the other hand, constitutive levels of XIAP as in cardiac fibroblasts (Mayorga *et al*., 2004), is generally considered to play a "housekeeping" role by preventing apoptosis in healthy cells (Hunter *et al*., 2007). XIAP resists cell death by up-regulating anti-oxidant gene expression and controlling intracellular ROS levels (Ulrike *et al*., 2008). It is tempting to speculate that markedly up-regulated ROS levels upon exogenously added H_2O_2 induce cIAP-2 when the intrinsic stress

exceeds the apoptotic threshold within which anti-apoptotic Bcl-2 and XIAP may play significant roles.

It is noteworthy that, in an earlier study from this laboratory (Sangeetha *et al*., 2011), hypoxia was found to induce cIAP-2 expression whereas Bcl-2 expression remained unaffected. Although the contribution of ROS under conditions of hypoxia is controversial (Zuo & Clanton, 2005) and intracellular ROS was not measured in hypoxic cells in that study, the observations reported here seem consistent with the speculation that the anti-apoptotic mechanisms triggered in hypoxic cardiac fibroblasts could be ROS-mediated. Anyway, the findings support the postulation that cIAP-2 may be a dynamic regulator of apoptosis in cardiac fibroblasts, induced under conditions of ambient stress wherein the anti-apoptotic action of constitutively expressed Bcl-2 may be inadequate.

The pro-survival role of cIAP-2 under oxidative stress may be particularly important since oxidative stress is reported to increase TNF-α production and TNF-α can induce apoptosis by the extrinsic pathway, which is inhibited by cIAP-2 (Varfolomeev *et al*., 2007). Apart from their role in apoptosis inhibition, several lines of evidence point to roles for IAPs in morphogenesis, heavy metal homeostasis and in survival-related signaling involving other pro-survival factors. In this regard, cIAP-2 is reported to turn on NF-κB and MAPKs (Varfolomeev *et al*., 2012), which can potentially contribute to its protective action. MALT (mucosa-associated lymphoid tissue) lymphoma is a condition that arises due to cIAP-2 gene rearrangements, leading to the formation of fusion protein between cIAP-2 and

MALT1. This chimeric-fusion product mediates cIAP-2-driven constitutive activation of NF-κB (Oeckinghaus *et al*., 2007), thus forming a feedback loop for the transcriptional control of NF-κB on cIAP-2 promoter.

V.4 Oxidative stress-activated NF-κB in cardiac fibroblasts promotessurvival by up-regulating cIAP-2

In looking for the regulation of cIAP-2, this study focused on NF-κB, a redox-sensitive stress-activated transcription factor known to be involved in multiple functions like immune response, inflammation, embryonic development, cell cycle and apoptosis (Mattson & Meffert, 2006). In response to H_2O_2 nuclear translocation of NF-κB was observed as early as 30 minutes (Figure 17), and it was a p65/p50 heterodimer (Figure 32). Notably, Xu *et al*., 2006 demonstrated differential kinetics of IκBα- and IκBβ-degradation resulting in NF-κB activation upon cytokine stimulation. IκBα degradation occurs rapidly leading to early activation of NF-κB while IκBβ degradation is associated with delayed activation of NF-κB (Xu *et al*., 2006). The findings presented here are consistent with IκBα-degradation-mediated early activation of NF-κB.

This study showed that NF-κB abrogation under conditions of oxidative stress causes marked apoptosis in cardiac fibroblasts and significant down-regulation of cIAP-2 protein and mRNA levels (Figures 22 & 23). Importantly, over-expression of cIAP-2 in NF-κB-inhibited cells prevented viability loss under oxidative stress. In tandem, these findings showed that NF-κB-dependent transcriptional regulation of cIAP-2

mediates cardiac fibroblast survival under conditions of oxidative stress. The link between NF-κB and cIAP-2 is evident from the earlier studies that demonstrated, by deletion analysis, two putative consensus NF-κB binding sites on the 5' flanking region surrounding the cIAP-2 transcription start site required for TNF-α-induced-cIAP-2 promoter activation (Hong *et al*., 2000). In p65-silenced glioma cell lines, TNF-α-induced cIAP-2 was significantly attenuated, showing that cIAP-2 could be a transcriptional target of NF-κB (Zhao *et al*., 2011).

Interestingly, Jin & Lee, 2006 showed enhanced occurrence of apoptosis upon cIAP-2 knockdown in nocodazole-mediated-G_2/M arrested cells, which pointed to a survival role for cIAP-2 in mitotically-arrested cells. Further, the cIAP-2 promoter was shown to possess a bipartite CDE (cell cycle-dependent element)/CHR (cell cycle gene homology region) element that mediates cIAP-2 gene activation in G_2/M phase (Jin & Lee, 2006). It is tempting to postulate on the basis of these observations that H_2O_2 may trigger G_2/M arrest, as observed in human lens epithelial B3 cells (Seomun *et al*., 2005), and associated peak in cIAP-2 expression that in turn facilitates survival. Further, the transient growth arrest may mediate integration of multiple mechanisms into a co-ordinated survival response. In the phase of arrest, cIAP-2 can induce NF-κB activation (Varfolomeev *et al*., 2012) that up-regulates its array of target survival genes. Once the cell is fully equipped with the plethora of survival factors, negative auto-regulatory feedback mechanisms may be up-regulated, which lead to NF-κB inactivation, followed by cell cycle progression with protection against pro-apoptotic stimuli (Lee & Collins, 2001). These observations suggest an alternative pathway of cIAP-2-mediated cell survival apart from the

findings of the present study that indicate cell survival mediated by an NF-κB-activated cIAP-2 up-regulation and consequent inhibition of caspase-dependent death signaling.

V.5 Oxidative stress-induced ERK1/2 activation up-regulates NF-κB-mediated cIAP-2 expression

Oxidative stress induces activation of serine/threonine kinases called mitogen-activated protein kinases (MAPK) like ERK1/2, JNK/SAPK, PI3K/Akt and p38 MAPK (Kyriakis & Avruch, 1996, Aikawa *et al*., 1997, Mielke & Herdegen, 2000, Ono & Han, 2000). This study attempted to examine upstream regulators of NF-κB and identified ERK1/2 as an important regulator. Phosphorylation of ERK1/2 was found to peak at 15 minutes of H_2O_2 exposure, which remained persistent for 12 hours (Figure 29). ERK1/2 inhibition increased cell death in cardiac fibroblasts exposed to oxidative stress (Figure 30), pointing to a pro-survival for ERK1/2. However, inhibition of p38 MAPK did not significantly compromise cell viability upon exposure to oxidative stress (Figure 34), showing that p38 MAPK may not have a pro-survival role under these conditions.

Down-regulation of NF-κB activation (Figure 32) and IκBα degradation (Figure 33) under ERK1/2-inhibited conditions underscored the relationship between ERK1/2 and NF-κB. In this context, the 90 kDa ribosomal S6 kinase (pp90rsk) has been identified as a downstream target of ERK-activated signaling pathway (Ghoda *et al.*, 1997). Upon activation, pp90rsk phosphorylates IκBα on Ser-32 and triggers its

degradation by ubiquitination (Ghoda *et al*., 1997) and activates NF-κB by the classical pathway. Apart from IκB-degradation-mediated pathway, NF-κB may also be activated by phosphorylation of p65 by ERK (Jefferies & O'Neill, 2000). ERK-mediated NF-κB induction is reported to regulate cell cycle-related GADD45β (Wang *et al*., 2005), iNOS and COX-2 (Jiang *et al*., 2004).

Further, expression of cIAP-2 was found to be down-regulated upon ERK1/2 inhibition (Figure 29), which clearly showed that ERK1/2-activated NF-κB-mediated signaling is involved in cIAP-2 up-regulation. It is pertinent to point out that ERK1/2 can mediate both pro- and anti-apoptotic effects, depending on its interacting partners that may vary with stimuli and cell type (Mebratu & Tesfaigzi, 2009). For example, it is reported to mediate neuronal death upon spinal cord injury in a setting of ischemia-reperfusion but, in striking contrast to our data, ERK1/2 inhibition leads to cIAP-2 up-regulation that contributes to neuronal survival (Lu *et al.*, 2010). A role for ERK1/2 in mediating cell death in renal proximal tubule epithelial cells upon exposure to ROS has also been demonstrated (Ramachandiran *et al*., 2001). On the other hand, ERK1/2 signaling is reported to be protective as well (Mebratu *et al*., 2009). Downstream molecules that orchestrate the survival signals induced by ERK activation vary with cell type and the nature of pro-apoptotic stimuli. ERK has been shown to mediate survival by phosphorylation and consequent degradation of several pro-apoptotic factors of the Bcl-2 family of proteins like Bim, Bad and Bax (Zha *et al*., 1996, Tsuruta F *et al*., 2002, Tay *et al*., 2012). ERK1/2 is also found to down-regulate XAF1 (X-linked IAP-associated Factor 1), an XIAP-inhibitory protein, and hence up-regulate XIAP indirectly (Yu *et al*., 2007). Notably, ERK1/2 is known to

inhibit caspase-3 activation in haematopoietic cells (Terada *et al.*, 2000) but the underlying mechanism is still unknown. It seems likely from the present study that the inhibition of caspase activity could be via cIAP-2 induction.

This study provides evidence of a linear relationship between ERK1/2, NF-κB and cIAP-2 in cardiac fibroblasts under oxidative stress that culminates in a survival response. Of note, previous studies show the involvement of ERK1/2 in survival by post-translational modification and inactivation of pro-apoptotic factors (Zha *et al*., 1996, Tsuruta F *et al*., 2002, Tay *et al*., 2012). But this study, for the first time, provides evidence of transcriptional regulation of anti-apoptotic cIAP-2 by ERK1/2 via IκBα phosphorylation, degradation and consequent NF-κB activation. Additionally, this is the first demonstration of the regulatory role of ERK1/2 in cIAP-2 expression, which translates into a cell survival mechanism under conditions of ambient stress.

Figure 35: Schematic representation of the major findings of the study

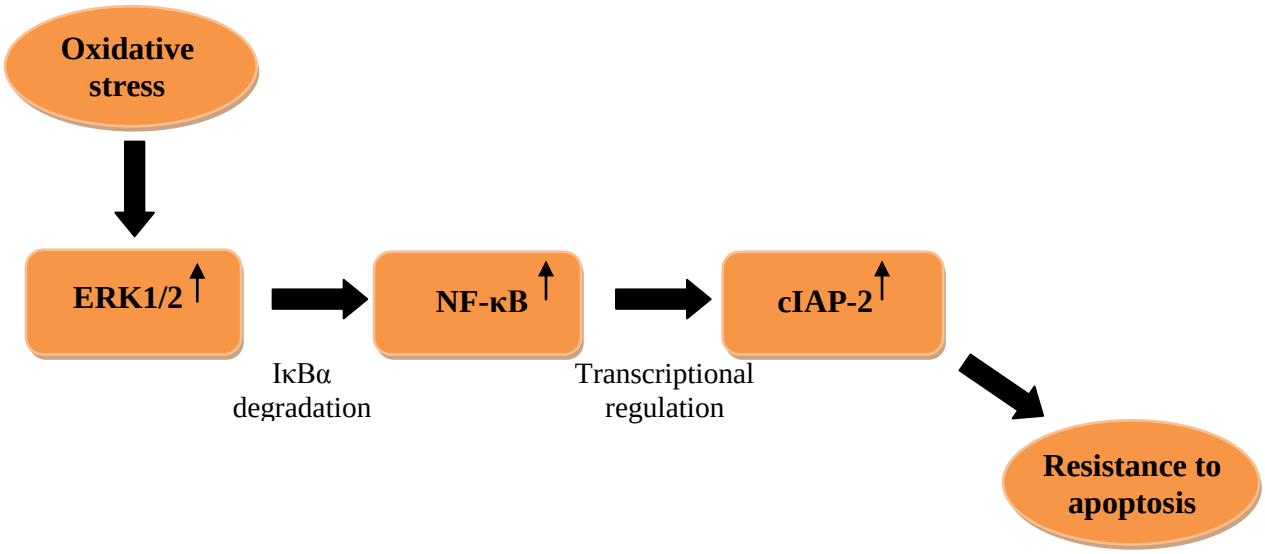

Proposed mechanism of cIAP-2-mediated cardiac fibroblast resistance to oxidative stress

V.6 Significance of the study

The resistance of cardiac fibroblasts to apoptosis has important implications in pathological states of the myocardium. Though resistance to apoptosis may facilitate a role in tissue healing *post injury*, persistence of cardiac fibroblasts in the mature infarct scar, associated with enhanced collagen turnover, leads to adverse myocardial remodeling, which is a major determinant of heart failure. Identification of factors that contribute to apoptosis resistance, therefore, is a desirable clinical goal. Using a combination of approaches, including knockdown and knock-in techniques, this study demonstrates for the first time that ERK1/2-mediated NF-κB-activated cIAP-2

up-regulation plays a pro-survival role in cardiac fibroblasts exposed to ambient stress.

V.7 Limitations of the study and future directions

Although the relationship between NF-κB and cIAP-2 is well-documented by gain-of-function and loss-of-function approaches, the study does not provide confirmatory evidence of direct transcriptional control of the cIAP-2 gene by NF-κB, which needs to be ascertained through promoter binding assay. Apart from Annexin/PI staining and PARP cleavage, measurement of caspase activity would further confirm occurrence of apoptosis.

Future investigations must ascertain if cardiac-specific knockdown of cIAP-2 in an *in vivo* model of myocardial inury would prevent or minimize excessive fibrous tissue formation and pump dysfunction. It is important to recognize that survival mechanisms in cells may involve multiple factors including, but possibly not limited to, Bcl-2 and cIAP-2. Therefore, the involvement of other factors that contribute to cardiac fibroblast resistance to apotosis under conditions of ambient stress warrants scrutiny.

VI. Summary and Conclusions

The resistance of cardiac fibroblasts to diverse death signals in the diseased myocardium may, in the short term, equip cardiac fibroblasts to orchestrate tissue healing but, in the long term, may mediate fibrotic myocardial remodeling that would significantly compromise pump function. Cardiac fibroblasts are reported to be resistant to diverse apoptotic insults like staurosporine, hypoxia, nutrient deprivation and oxidative stress. However, factors conferring resistance to apoptosis remain largely unidentified. Therefore, the goal of the present study was to identify survival mechanisms recruited in cardiac fibroblasts exposed to oxidative stress, which is associated with several cardiac pathologies.

Major findings of the study

- Cardiac fibroblasts are more resistant to oxidative stress-mediated injury than pulmonary fibroblasts
- Cardiac fibroblasts express constitutive levels of Bcl-2, which remain unchanged upon exposure to H_2O_2-mediated oxidative stress
- cIAP-2 is up-regulated in cardiac fibroblasts exposed to H_2O_2
- cIAP-2 knockdown by RNA interfernce causes significant apoptosis in cardiac fibroblasts exposed to oxidative stress
- NF-κB is activated in response to H_2O_2 and its inhibition causes apoptosis
- cIAP-2 mRNA and protein levels are down-regulated in NF-κB-inhibited cells exposed to H_2O_2

- Forced expression of cIAP-2 in NF-κB-inhibited cardiac fibroblasts reverses cell death significantly

- H_2O_2 induces ERK1/2 activation and its inhibition promotes cell death cIAP-2 is down-regulated in ERK1/2 -inhibited cells exposed to H_2O_2

- ERK1/2 inhibition attenuates NF-κB activation in H_2O_2-treated cells

To conclude, this study identifies cIAP-2 as a major effector of apoptosis resistance in cardiac fibroblasts exposed to oxidative stress and shows that its expression is regulated by ERK1/2-dependent NF-κB signaling. These observations suggest a novel mechanism of regulation of cIAP-2 by upstream ERK1/2, which translates into a cell survival mechanism under conditions of ambient stress.

VI. References

Aikawa R, Komuro I, Yamazaki T, Zou Y, Kudoh S, Tanak M, Shiojima I, Hiro Y, Yazaki Y (1997) Oxidative stress activates extracellular signal-regulated kinases through Src and Ras in cultured cardiac myocytes of neonatal rats. *J Clin Invest* 100: 1813–1821.

Ambrosini G, Adida C, Altieri D (1997) A novel anti-apoptosis gene, survivin, expressed in cancer and lymphoma. *Nat Med* 3:917–921.

Amerongen MJ, Bou-Gharios G, Popa ER, Ark J, Petersen AH, Dam GM, Luyn MJA, Harmsen MC (2008) Bone marrow-derived myofibroblasts contribute functionally to scar formation after myocardial infarction *J Pathol* 214: 377–386.

Bagnoli M, Canevari S, Mezzanzzanica D (2010) Cellular FLICE-inhibitory protein (c-FLIP) signaling: A key regulator of receptor-mediated apoptosisin physiological context and cancer. *Int J Biochem Cell Biol* 42: 210-213.

Banerjee I, Yekkala K, Borg TK, Baudino TA (2006) Dynamic Interactions between myocytes, fibroblasts and extracellular matrix. *Ann N Y Acad Sci* 1080: 76–84.

Baudino TA, Carver W, Giles W, Borg TK (2006) Cardiac fibroblasts: friend or foe? *Am J Physiol Heart Circ Physiol* 291: H1015–H1026.

Beere HM (2004) 'The stress of dying': the role of heat shock proteins in the regulation of apoptosis. *J Cell Sci* 117: 2641-2651.

Blankesteijn WM, Essers-Janssen YP, Verluyten MJA, Daemen MJAP, Smits JFM (1997) A homologue of Drosophila tissue polarity gene frizzled is expressed in migrating myofibroblasts in the infracted rat heart. *NatMed* 3: 541-544.

Bolli R, Li QH, Tang XL, Guo Y, Xuan YT, Rokosh G, Dawn B (2007) The late phase of preconditioning and its natural clinical application—gene therapy. *Heart Fail Rev* 12:189–199.

Bosman FT, Stamenkovic I (2003) Functional structure and composition of the extracellular matrix. *J Pathol* 200: 423-428.

Bottcher R, Niehrs C (2005). Fibroblast growth factor signaling during early vertebrate development.*Endocinol Rev* 26: 63–77.

Bowers SL, Banerjee I, Baudino TA (2009). The extracellular matrix: at the center of it all. *J Mol Cell Cardiol* 48: 474-482.

Bradford MM (1976) A rapid and sensitive method for the quantitation of microgram quantities of protein utilizing the principle of protein-dye binding.*Anal Biochem* 72: 248-254.

Breckenridge DG, Germain M, Mathai JP, Nguyen M, Shore GC (2003) Regulation of apoptosis by endoplasmic reticulum pathways. *Oncogene* 22:8608–8618.

Bruey JM, Ducasse C, Bonniaud P, Ravagnan L, Susin SA, DiazLatoud C, Gurbuxani S, Arrigo AP, Kroemer G, Solary E, Garrido C (2000). Hsp27 negatively regulates cell death by interacting with cytochrome c. *Nat Cell Biol* 2: 645-652.

Brown L, Chan V, Fenning A (2005)Targets for pharmacological modulation of cardiac fibrosis In: Interstitial fibrosis in heart failure, Springer, New York, pp. 275-310.

Brown RD, Ambler SK, Mitchell MD, Long CS (2005) The cardiac fibroblast: therapeutic target in myocardial remodeling and failure. *Annu Rev Pharmacol Toxicol* 45: 657-87.

Burguillos MA, Deierborg T, Kavanagh E , Persson A , Hajji N,Quintanilla AG, Cano J, Brundin P, Englund E , Venero JL, Joseph B (2011). Caspase signalling controls microglia activation and neurotoxicity. *Nature* 472: 319-325.

Cagnol S, Chambard JC (2010). ERK and cell death: Mechanisms of ERK-induced cell death – apoptosis, autophagy and senescence. *FEBS J* 277: 2–21.

Camelliti P, Borg TK, Kohl P (2005) Structural and functional characterization of cardiac fibroblasts.*Cardiovasc Res* 65: 40 –51.

Chen F, Castranova V, Shi X, Demers LM (1999) New insights into the role of nuclear factor-kappaB, a ubiquitous transcription factor in the initiation of diseases. *Clin Chem* 45: 7-17.

Chen Z, Chua CC, Ho YS, Hamdy RC, Chua BH. (2001) Overexpression of Bcl-2 attenuates apoptosis and protects against myocardial I/R injury in transgenic mice. *Am J Physiol Heart Circ Physiol* 280: H2313–H2320.

Cheung EC, Slack RS (2004) Emerging role for ERK as a key regulator of neuronal apoptosis.*Sci STKE* 251: PE45.

Cohn JN, Ferrari R, Sharpe N *(2000*) Concepts and clinical implications: a consensus paper from an international forum on cardiac remodeling (on Behalf of an International Forum on Cardiac Remodeling Cardiac remodeling) *J Am Coll Cardiol* 35: 569-582.

Corda S, Samuel JL, Rappaport L (2000) Extracellular matrix and growth factors during heart growth. *Heart Fail Rev* 5: 119–130.

Crow MT, Mani K, Nam YJ, Kitsis RN (2004). The mitochondrial death pathway and cardiac myocyte apoptosis.*Circ Res* 95: 957-70.

Cucoranu I, Clempus R, Dikalova A, Phelan PJ, Ariyan S, Dikalov S, Sorescu D (2005) NADPH oxidase 4 mediates transforming growth factor-β1–induced differentiation of cardiac fibroblasts into myofibroblasts. *Circ Res* 97: 900–907.

Dan HC, Sun M, Kaneko S, Feldman RI, Nicosia SV, Wang HG, Tsang BK, Cheng JQ (2004) Akt phosphorylation and stabilization of X-linked inhibitor of apoptosis protein (XIAP). *J Biol Chem* 279: 5405–5412.

Datta SR, Dudek H, Tao X, Masters S, Fu H, Gotoh Y, Greenberg ME (1997) Akt phosphorylation of Bad couples survival signals to the cell-intrinsic death machinery. *Cell* 91: 231–241.

Davidson SM, Duchen MR (2006) Effects of NO on mitochondrial function in cardiomyocytes: pathophysiological relevance. *Cardiovasc Res* 71: 10–21.

Deshpande NN, Sorescu D, Seshiah P Ushio-Fukai M, Akers M, Yin Q, Griendling KK (2002) Mechanism of hydrogen peroxide–induced cell cycle arrest in vascular smooth muscle.*Antioxid Redox Signal* 4: 845– 854.

Desmouliere A, Geinoz A, Gabbiani F, Gabbiani G (1993) Transforming growth factor-beta 1 induces alpha smooth muscle actin expression in granulation tissue myofibroblasts and in quiescent and growing cultured fibroblasts. *J Cell Biol* 122: 103–11.

DiPietrantonio AM, Hsieh T, Wu JM (1999) Activation of caspase 3 in HL-60 cells exposed to H_2O_2. *Biochem Biophys Res Commun* 255: 477-482.

Domina AM, Vrana JA, Gregory MA, Hann SR, Craig RW (2004) MCL1 is phosphorylated in the PEST region and stabilized upon ERK activation in viable cells, and at additional sites with cytotoxic okadaic acid or taxol. *Oncogene* 23: 5301 – 5315.

Dudley SC, Hoch NE, McCann LA, Honeycutt C, Diamandopoulos L, Fukai T, Harrison DG, Dikalov SI, Langberg J (2005). Atrial fibrillation increases production of superoxide by the left atrium and left atrial appendage: role of the NADPH and xanthine oxidases. *Circulation* 112: 1266–1273.

Dueber EC, Schoeffler AJ, Lingel A, Elliott JM, Fedorova AV, Giannetti AM, Zobel K, Maurer B, Varfolomeev E,Wu P, Wallweber HJA, Hymowitz SG, Deshayes K, Vucic D, Fairbrother WJ (2011) Antagonists induce a conformational change in cIAP1 that promotes autoubiquitination. *Science* 334: 376–380.

Earnshaw WC, Martins LM, Kaufmann SH (1999) Mammalian caspases: structure, activation, substrates and functions during apoptosis. *Annu Rev Biochem* 68: 383-424.

Eghbali M, Blumenfeld OO, Seifter S, Buttrick PM, Leinwand LA, Robinson TF, Zern MA,Giambrone MA (1989). Localization of types I, III and IV collagen mRNAs in rat heart cells by in situ hybridization. *J Mol Cell Cardiol* 21: 103−113.

Empel VPM, Windt LJ (2005) Myocyte hypertrophy and apoptosis: a balancing act. *Cardiovasc Res* 67: 21–29.

Ferrari R, Bachetti T, Confortini R, Opasich C, Febo O, Corti A, Cassani G, Visioli O (1995) Tumor necrosis factor soluble receptors in patients with various degrees of congestive heart failure. *Circulation* 92:1479–1486.

Finkel T, Holbrook NJ (2000) Oxidants, oxidative stress and the biology of ageing *Nature* 408: 239-247

Flesch M, Margulies KB, Mochmann HC, Engel D, Sivasubramanian N, Mann DL (2001) Differential regulation of mitogen-activated protein kinases in the failing human heart in response to mechanical unloading. *Circulation* 104: 2273–2276.

Foo RSY, Mani K, Kitsis RN (2005) Death begets failure in the heart. *J Clin Invest* 115: 565–571.

Frantz S, Hu K, Bayer B, Gerondakis S, Strotmann J, Adamek A, Ertl G, Bauersachs J (2006) Absence of NF-kappaB subunit p50 improves heart failure after myocardial infarction. *Faseb J* 20: 1918-20.

Freund C, Schmidt-Ullrich R, Baurand A, Dunger S, Schneider W, Loser P, El-Jamali A, Dietz R, Scheidereit C, Bergmann MW (2005) Requirement of nuclear factor-kappaB in angiotensin II- and isoproterenol-induced cardiac hypertrophy in vivo. *Circulation*. 111: 2319 –2325.

Fujioka S, Schmidt C, Sclabas GM, Li Z, Pelicano H, Peng B, Yao A, Niu J, Zhang W, Evans DB, Abbruzzese JL, Huang P, Paul J, Chiao PJ (2004) Stabilization of p53 is a novel mechanism for proapoptotic function of NF-κB. *J Biol Chem* 279: 27549-275459.

Gabbiani G (1998). Evolution and clinical implications of the myofibroblast concept.*Cardiovasc Res* 38: 545−548.

Garcia, J, Ye Y, Arranz V, Letourneux C, Pezeron G, Porteu F (2002) IEX-1: a new ERK substrate involved in both ERK survival activity and ERK activation. *EMBO J.* 21: 5151 – 5163.

Ghoda L, Lin X, Greene WC (1997). The 90-kDa ribosomal S6 kinase (pp90rsk) phosphorylates the N-terminal regulatory domain of IκBα and stimulates its degradation *in vitro.J Biol Chem* 272: 21281–21288.

Ghosh S, Karin M. (2002). Missing pieces in the NF-κB puzzle. *Cell* 109: S81-S96.

Gobeil S, Boucher CC, Nadeau D, Poirier GG (2001) Characterization of the necrotic cleavage of poly (ADP-ribose) polymerase (PARP-1): implication of lysosomal proteases. *Cell Death Differ* 8: 588- 94.

Goldsmith EC, Hoffman A, Morales MO, Potts JD, Price RL, McFadden A, Rice M, Borg TK (2004) Organization of fibroblasts in the heart. *Dev Dyn* 230: 787–794.

Gordon JW, Shaw JA, Kirshenbaum LA (2011) Multiple facets of NF-κB in the heart: To be or not to NF-κB. *Circ Res* 108:1122-1132.

Griendling KK, FitzGerald GA (2003) Oxidative stress and cardiovascular Injury: Part I-Basic mechanisms and *in vivo* monitoring of ROS *Circulation* 108:1912-1916.

Grieve DJ, Shah AM (2003) Oxidative stress in heart failure. *Eur Heart J* 24: 2161-2163.

Gugasyan R, Christou A, O'Reilly LA, Strasser A, Gerondakis S (2006) Bcl-2 transgene expression fails to prevent fatal heptocyte apoptosis induced by endogenous TNF-α in mice lacking RelA. *Cell Ceath Differ* 13: 1235-1237.

Gurtner GC, Werner S, Barrandon Y, Longaker MT (2008) Wound repair and regeneration. *Nature* 453:314–321.

Hacker H, Karin M (2006).Regulation and function of IKK and IKK-related kinases.*Sci STKE* 357: p.re13

Hamid T, Guo SZ, Kingery JR, Xiang X, Dawn B, Prabhu SD (2011). Cardiomyocyte NF-κB p65 promotes adverse remodelling, apoptosis, and endoplasmic reticulum stress in heart failure. *Cardiovasc Res* 89:129 –138.

Harvey PR, Rosenthal N (1999).*Heart Development.*Academic Publishers, New York.

Hatano N, Mori Y, Oh-hora M, Kosugi A, Fujikawa T, Nakai N, Niwa H, Miyazaki J, Hamaoka T, Ogata M (2003) Essential role for ERK2 mitogen-activated protein kinase in placental development. *Genes Cells* 8: 847 – 856.

Hausenloy D, Yellon D (2007) Reperfusion injury salvage kinase signalling: taking a RISK for cardioprotection. *Heart Fail Rev* 12: 217–234.

Hess ML, Manson NH (1984) Molecular oxygen: friend and foe. The role of the oxygen free radical system in the calcium paradox, the oxygen paradox and ischemia/reperfusion injury.*J Mol Cell Cardiol* 16:969 –985.

Ho JQ, Asagiri M, Hoffmann A, Ghosh G (2011) NF-κB potentiates caspase independent hydrogen peroxide induced cell death. *PLoS One* 6: e16815.

Hong SY, Yoon WH, Park JH, Kang SG, Ahn JH, Lee TH (2000) Involvement of two NF-κB Binding Elements in Tumor Necrosis Factor α, CD40-, and Epstein-Barr Virus Latent Membrane Protein 1-mediated induction of the Cellular Inhibitor of Apoptosis Protein 2 Gene. *J Biol Chem* 24: 18022–18028.

Hu S, Yang X (2003) Cellular inhibitors 1 and 2 act as ubiquitin ligases for the apoptosis inducer Smac/DIABLO.*J Biol Chem* 278: 10055-10060.

Huang B, Yang XD, Lamb A, Chen LF (2010) Posttranslational modifications of NF-κB: Another layer of regulation for NF-κB signaling pathway. *Cellular Signalling* 22: 1282–1290.

Huebert RC, Li Q, Adhikari N, Charles NJ, Han X, Ezzat MK, Grindle S, Park S, Ormaza S, Fermin D, Miller LW, Hall JL (2004) Identification and regulation of Sprouty1, a negative inhibitor of the ERK cascade, in the human heart. *Physiol Genomics* 18: 284–289.

Hunter AM, LaCasse EC, Korneluk RG (2007) The inhibitors of apoptosis (IAPs) as cancer targets. *Apoptosis* 12: 1543–68.

Ichijo H, Nishida E, Irie K , Dijke P, Saitoh M, Moriguchi T, Takagi M, Matsumoto K, Miyazono K, Gotoh Y (1997) Induction of apoptosis by ASK1, a mammalian MAPKKK that activates SAPK/JNK and p38 signaling pathways. *Science* 275: 90–94.

Jefferies CA, O'Neill LAJ (2000) Rac1 regulates interleukin 1-induced nuclear factor κB activation in an inhibitory protein κBα-independent manner by enhancing the ability of the p65 subunit to transactivate gene expression. *J Biol Chem*275: 3114–3120.

Jiang X and Wang X (2004) Cytochrome c-mediated apoptosis. *Annu Rev Biochem* 73:87–106

Jiang B, Xu S, Hou X, Pimentel DR, Brecher P, Cohen RA (2004) Temporal control of NF-κB activation by ERK differentially regulates interleukin-1β-induced gene expression. *J Biol Chem* 279: 1323–29.

Jin HS, Lee TH (2006) Cell cycle-dependent expression of cIAP2 at G2/M phase contributes to survival during mitotic cell cycle arrest. *Biochem J* 399: 335–342.
Kakkar R, Lee RT (2010) Intramyocardial fibroblast-myocyte communication. *Circ*

*Res*106:47-57.

Kam PCA, Ferch NI (2000). Apoptosis: mechanisms and clinical implications *Anaesthesia*, 55: 1081-1093.

Kanekar S, Hirozanne T, Terracio L, Borg TK (1998). Cardiac fibroblasts: form and function. C*ardiovasc Pathol* 7:127–133.

Kehat I and Molkentin JD (2010) Molecular pathways underlying cardiac remodeling during pathophysiological stimulation. *Circulation* 122: 2727-2735.

Kerr JF (1971) Shrinkage necrosis: a distinct mode of cellular death.*J Pathol* 105:13–20.

Keyes WM, Sanders EJ (2002) Regulation of apoptosis in the endocardial cushions of the developing chick heart*Am J Physiol Cell Physiol* 282: C1348–C1360.

Klionsky DJ (2005) The molecular machinery of autophagy: unanswered questions. *J Cell Sci* 118: 7–18.

Konstam MA, Kramer DG, Patel AR, Maron MS, Udelson JE (2011) Left ventricular remodeling in heart failure current concepts in clinical significance and assessment
JAm Coll Cardiol: Cardiovascular Imaging 4: 98 –108.

Kovacs K, Hanto K, Bognar Z, Tapodi A, Bognar E, Kiss G, Szabo A, Rappai G, Kiss T, Sumegi B, Gallyas F (2009) Prevalent role of Akt and ERK activation in cardioprotective effect of Ca^{2+} channel- and beta-adrenergic receptor blockers. *Mol Cell Biochem* 321: 155–164.

Kracikova M, Akiri G, George A, Sachidanandam R, Aaronson A (2013) A threshold mechanism mediates p53 cell fate decision between growth arrest and apoptosis. *Cell Death Differ* 20: 576-588.

Kratsios P, Huth M, Temmerman L, Salimova E, Banchaabouchi MA, Sgoifo A, Manghi M, Suzuki K, Rosenthal N, Mourkiot F (2010) Antioxidant Amelioration of Dilated Cardiomyopathy Caused by Conditional Deletion of NEMO/IKKγ in Cardiomyocytes. *Circ Res* 106:133-144.

Krenning G, Zeisberg EM, Kalluri R (2010) The origin of fibroblasts and mechanism of cardiac fibrosis *J Cell Physiol* 225: 631–637.

Kumaran C, Shivakumar K (2002) Calcium- and superoxide anion-mediated mitogenic action of substance P on cardiac fibroblasts.*Am J Physiol Heart Circ Physiol* 82: H1855–H1862.

Kurland JF, Voehringer DW, Meyn RE (2003) The MEK/ERK Pathway acts upstream of NF-κB1 (p50) homodimer activity and Bcl-2 expression in a Murine B-

Cell Lymphoma Cell Line MEK INHIBITION RESTORES RADIATION-INDUCED APOPTOSIS. *J Biol Chem* 278: 32465–32470.

Kyriakis JM, Avruch J (1996) Protein kinase cascades activated by stress and inflammatory cytokines. *Bioessays* 18:567–577.

LaCasse EC, Baird S, Korneluk RG, MacKenzie AE (1998) The inhibitors of apoptosis (IAPs) and their emerging role in cancer. *Oncogene* 17: 3247-3259.

Lee RT, Collins T (2001) Nuclear Factor-kB and Cell Survival IAPs Call for Support.*Circ Res* 88:262-264.

Leslie NR, Downes CP (2002) PTEN: The down side of PI 3-kinase signalling. *Cell Signal* 14: 285–295.

Levkau B, Garton KJ, Ferri N, Kloke K, Nofer JR, Baba HA, Raines EW, Breithardt G (2001) XIAP induces cell-cycle arrest and activates nuclear factor-kappaB : new survival pathways disabled by caspase-mediated cleavage during apoptosis of human endothelial cells. *Circ Res* 88:282–90.

Liang C, Zhang M, Sun SC (2006) β-TrCP binding and processing of NF-κB2/p100 involve its phosphorylation at serines 866 and 870. *Cell Signal*18: 1309-1317.

Lijnen P, Paparella I, Petrov V, Semplicini A, Fagard R. (2006) Angiotensin II-stimulated collagen production in cardiac fibroblasts is mediated by reactive oxygen species. *J Hypertens*24:757-66.

Lin A, Karin M (2003) NF-κB in cancer: a market target. *Semin Cancer Biol* 13: 107-14.

Lisa FD, Menabo R, Canton M, Barile M, Bernardi P (2001) Opening of the mitochondrial permeability transition pore causes depletion of mitochondrial and cytosolic NAD^+ and is a causative event in the death of myocytes in postischemic reperfusion of the heart *J Biol Chem* 276: 2571-2575.

Livak KJ and Thomas D. Schmittgen TD (2001).Analysis of Relative Gene Expression Data Using Real Time Quantitative PCR and the $2^{-\Delta\Delta C}{}_T$ Method.*Methods* 25: 402–408.

Looi YH, Grieve DJ, Siva A, Walker SJ, Anilkumar N, Cave AC, Marber M, Monaghan MJ, Shah AM (2008) Involvement of Nox2 NADPH oxidase in adverse cardiac remodeling after myocardial infarction. *Hypertension* 51:319–325.

Lopez J, Wicky JS, Tenev T, Tautureau GJP, Hinds MG, Francalanci F, Wilson R, Broemer M, Santoro MM, Day CL, Meier O (2011) CARD-mediated autoinhibition of cIAP1's E3 ligase activity suppresses cell proliferation and migration. *Mol Cell* 42: 569–583.

Lu K, Liang CL, Liliang PC, Yang CH, Cho CL, Weng HC, Tsai YD, Wang KW, Chen HJ. (2010) Inhibition of extracellular signal-regulated kinases 1/2 provides neuroprotection in spinal cord ischemia/reperfusion injury in rats: relationship with the nuclear factor-κB-regulated antiapoptotic mechanisms. *J Neurochem*114:237–246.

Lorenzo HK, Susin SA (2004) Mitochondrial effectors in caspase-independent cell death *FEBS Lett* 557:14-20.

Luo X, Budihardjo I, Zou H, Slaughter C, Wang X (1998) Bid, a Bcl-2 interacting protein, mediates cytochrome c release from mitochondria in response to activation of cell surface death receptors. *Cell* 94:481–490.

Mace PD, Shirley S, Day CL (2010) Assembling the building blocks: structure and function of inhibitor of apoptosis proteins. *Cell Death Differ* 17: 46–53.

Mahoney DJ, Cheung HH, Mrad RL, Plenchette S, Simard C. (2008) Both cIAP-1 and cIAP-2 regulate TNFα-mediated NF-κB activation. *Proc Natl Acad Sci USA* 33: 11778-11783.

Mak S, Newton GE (2001) The oxidative stress hypothesis of congestive heart failure: radical thoughts. *Chest* 120: 2035–2046.

Mallat Z, Philip I, Lebret M, Chatel D, Maclouf J, Tedgui A (1998) Elevated levels of 8-iso-prostaglandin $F_{2\alpha}$ in pericardial fluid of patients with heart failure: A potential role for *in vivo* oxidant stress in ventricular dilatation and progression to heart failure. *Circulation* 97: 1536–1539.

Mani K (2008) Programmed cell death in cardiac myocytes: strategies to maximize post-ischemic salvage. *Heart Fail Rev* 13:193–209.

Martinon F, Tschopp J (2004) Inflammatory Caspases: Linking an Intracellular Innate Immune System to Autoinflammatory Diseases. *Cell* 117: 561–574.

Martinon F, Tschopp J (2007) Inflammatory caspases and inflammasomes: master switches of inflammation *Cell Death Differ* 14: 10–22.

Matsuzawa A, Saegusa K, Noguchi T, Sadamitsu C, Nishitoh H, Nagai S, Koyasu S, Matsumoto K, Takeda K, Ichijo H (2005) ROS-dependent activation of the TRAF6-ASK1-p38 pathway is selectively required for TLR4-mediated innate immunity. *Nat Immunol* 6: 587–592.

Mattson MP, Meffert MK (2006) Roles for NF-κB in nerve cell survival, plasticity and disease. *Cell Death Differ* 13: 852–860.

Mayorga M, Bahi N, Ballester M, Comella JX, Sanchis D (2004) Bcl-2 is a key factor for cardiac fibroblast resistance to programmed cell death. *J Biol Chem* 279: 34882- 34889.

Mebratu Y, Tesfaigzi Y (2009) How ERK1/2 activation controls cell proliferation and cell death is subcellular localization the answer? *Cell Cycle* 8:1168–1175.

Mielke K, Herdegen T (2000) JNK and p38 stress kinases-degenerative effectors of signal-transduction-cascades in the nervous system. *Prog Neurobiol* 61:45–60.

Mike S, Yee HL, Ajay MS (2007) Oxidative stess and redox signaling in cardiac hypertrophy and heart failure. *Heart* 93: 903-907.

Minamino T, Kitakaze M (2010) ER stress in CVD. *JMol Cell Cardiol* 48:1105-1110.

Montaigne D, Hurt C, Neviere R (2012) Mitochondria death/survival signaling pathways in cardiotoxicity induced by anthracyclines and anticancer-targeted therapies. *Biochemistry Research International* Hindawi Publishing Corporation.

Misra A, Haudek SB, Knuefermann P, Vallejo JG, Chen ZJ, Michael LH, Sivasubramanian N, Olson EN, Entman ML, Mann DL (2003) NF-κB protects the adult cardiac myocyte against ischemia-induced apoptosis in a murine model of acute myocardial infarction. *Circulation* 108: 3075-3078.

Misra MK, Sarwat M, Bhakuni P, Tuteja R, Tuteja N (2009) Oxidative stress and ischemic myocardial syndromes. *Med Sci Monit* 15: 209-219.

Nag A. (1980) Study of non-muscle cells of the adult mammalian heart: a fine structural analysis and distribution. *Cytobios* 28:41– 61.

Niwa K, Inanami O, Yamamori T, Ohta T, Hamasu T, Karino T, Kuwabara M (2002) Roles of protein kinase C delta in the accumulation of P53 and the induction of apoptosis in H_2O_2-treated bovine endothelial cells. *Free Radic Res* 36:1147–1153.
Norberg E, Gogvadze V, Ott M, Horn M, Uhlen P, Orrenius S,Zhivotovsky B (2008) An increase in intracellular Ca^{+2} is required for the activation of mitochondrial calpain to release AIF during cell death. *Cell Death Differ* 15: 1857–1864.

Oeckinghaus A, Hayden MS, Ghosh S (2011) Crosstalk in NF-κB signaling pathways.*Nat Immunol*12: 695-708.

Ono K, Han J (2000) The p38 signal transduction pathway: activation and function. *Cell Signal* 12:1–13.

Osorio-Fuentealba C, Valdés JA, Riquelme D, Hidalgo J, Hidalgo C, Carrasco MA (2009) Hypoxia stimulates via separate pathways ERK phosphorylation and NF-κB activation in skeletal muscle cells in primary culture. *J Appl Physiol* 106: 1301-10.

Palaniyandi SS, Sun L, Ferreira JCB, Mochly-Rosen D (2009) Protein kinase C in heart failure: a therapeutic target? *Cardiovasc Res* 82: 229–239.

Pandey P, Farber R, Nakazawa A, Kumar S, Bharti A, Nalin C, Weichselbaum R, Kufe D, Kharbanda S (2000). Hsp27 functions as a negative regulator of cytochrome c-dependent activation of procaspase-3. *Oncogene* 19: 1975-1981.

Pardo OE, Lesay A, Arcaro A, Lopes R, Ng BL, Warne PH, McNeish IA, Tetley TD, Lemoine NR, Mehmet H, Seckl MJ, Downward J (2003) Fibroblast Growth Factor 2-mediated translational control of IAPs blocks mitochondrial release of Smac/DIABLO and apoptosis in small cell lung cancer cells. *Mol Cell Biol* 23: 7600-7610.

Perkins, N.D. (2006). Post-translational modifications regulating the activity and function of the nuclear factor kappa B pathway.*Oncogene* 25: 6717-6730.

Pest SM, Tomkinson AE, Lee EYHP (2003) The human checkpoint Rad protein, Rad 17 is chromatin-associated throughout the cell cycle, localizes to DNA replication sites, and interacts with DNA polymerase ε. *Nucleic Acids Res* 31: 5568–5575.

Porter KE and Turner NA. (2009) Cardiac fibroblasts: at the heart of myocardial remodeling. *Pharmacol Ther* 123: 255-278.

Ramachandiran S, Huang Q, Dong J, Lau SS, Monks TJ (2002) Mitogen-activated protein kinases contribute to reactive oxygen species-induced cell death in renal proximal tubule epithelial cells. *Chem Res Toxicol* 15: 1635–1642.

Rasola A, Sciacovelli M, Chiara F, Pantic B, Brusilow WS, Bernardi P (2009) Activation of mitochondrial ERK protects cancer cells from death through inhibition of the permeability transition. *Proc Natl Acad Sci USA* 107: 726-731.

Ray PD, Huang BW, Tsuji Y (2012) Reactive oxygen species (ROS) homeostasis and redox regulation in cellular signaling. *Cell Signal* 24: 981–990.

Rheaume E, Cohen LY, Uhlmann F, Lazure C, Alam A, Hurwitz J, Sekaly RP and Denis F. (1997). The large subunit of replication factor C is a substrate for caspase-3 in vitro and is cleaved by a caspase-3-like protease during Fas-mediated apoptosis. *EMBO J* 16: 6346 - 6354.

Rodriguez A, Chen P, Oliver H, Abrams JM (2002) Unrestrained caspase-dependent cell death caused by loss of Diap1 function requires the Drosophila Apaf-1 homolog, Dark. *EMBO J*. 21: 2189–2197.

Rose BA, Force T, Wang Y *(*2010) Mitogen-activated protein kinase signaling in the heart: angels versus demons in a heart-breaking tale. *Physiol Rev* 90: 1507–1546.

Sabri A, Hughie HH, Lucchesi PA (2003) Regulation of hypertrophic and apoptotic signaling pathways by reactive oxygen species in cardiac myocytes.*Antioxid Redox Signaling* 5:731–740.

Santos DGB, Resende MF, Mill JG, Mansur AJ, Krieger JE, Pereira AC (2010) NF-κB polymorphism is associated with heart function in patients with heart failure. *BMC Med Genetics* 11:89.

Sarnico I, Lanzillotta A, Benarese M, Alghise M, Baiquera C, Battistin L, Spano PF, Pizzi M(2009) NF-κB dimers in the regulation of neuronal survival. *Int Rev Neurobiol* 85: 351-62.

Sakahira H, Enari M, Nagata S (1998) Cleavage of CAD inhibitor in CAD activation and DNA degradation during apoptosis. *Nature* 391: 96-99.

Salvesen GS, Duckett CS. IAP proteins: blocking the road to death's door. *Nat Rev Mol Cell Biol* 2002; 3: 401-10.

Sangeetha M (2009) NF-κB plays a role in cardiac fibroblast survival under hypoxia. PhD Thesis.Sree Chitra Tirunal Institute for Medical Sciences and Technology.

Sangeetha M, Malini SP, Linda P, Edward GL, Shivakumar K (2011) NF-κB inhibition compromises cardiac fibroblast viability under hypoxia. *Exp Cell Res* 317: 899-909.

Sanna MG, Correia SJ, Ducrey O, Lee J, Nomoto K, Schrantz N, Deveraux QL, Ulevitch RJ (2002) IAP supression of apoptosis involves distinct mechanisms: the TAK1/JNK1 signaling cascade and caspase inhibition. *Mol Cell Biol* 22:1754–66.

Scaffidi C, Schmitz I, Krammer PH, Peter ME (1999) The role of c-FLIP in modulation of CD95-induced apoptosis.*J Biol Chem*274: 1541-1548.

Scarlatti F, Granata R, Meijer AJ, Codogno P. (2009) Does autophagy have a license to kill mammalian cells? *Cell Death Differ* 16: 12–20.

Schroder E, Eaton P (2008) Hydrogen peroxide as an endogenous mediator and exogenous tool in cardiovascular research: issues and considerations *Curr Opin Pharmacol* 8:153-159.

Schweichel JU, Merker HJ (1973) The morphology of various types of cell death in prenatal tissues. *Teratology* 7: 253–266.

Shi Y (2004) Caspase activation, inhibition, and reactivation: A mechanistic view. *Protein Sci*13:1979–1987.

Shiozaki EN, Chai J, Rigotti DJ, Riedl SJ, Li P, Srinivasula SM, Alnemri ES, Fairman R, Shi Y (2003) Mechanism of XIAP-mediated inhibition of caspase-9. *Mol Cell* 11:519–27.

Schimmer AD (2004) Inhibitor of Apoptosis Proteins: Translating basic knowledge into clinical practice. *Cancer Res* 64: 7183–7190.

Seomun Y, Kim JT, Kim HS, Park JY, Joo CK (2005) Induction of p21 Cip1-mediated G2/M arrest in H_2O_2-treated lens epithelial cells. *Mol Vision* 11:764-774.

Shimizu S, Eguchi Y, Kosaka H, Kamiike W, Matsuda H, Tsujimoto Y (1995) Prevention of hypoxia-induced cell death by Bcl-2 and Bcl-X_L. *Nature* 374:811-813.

Shivakumar K, Sollott SJ, Sangeetha M, Sapna S, Ziman B, Wang S, Lakatta EG (2008) Paracrine effects of hypoxic fibroblast-derived factors on the MPT-ROS threshold and viability of adult rat cardiac myocytes, *Am J Physiol Heart Circ Physiol* 294: H2653–H2658.

Silke J and Meier P (2013) Inhibitor of apoptosis proteins–modulators of cell death and inflammation.*Cold Spring Harb Perspect Biol* doi: 10.1101

Spinale FG (2007) Myocardial matrix remodeling and the matrix metalloproteinases: influence on cardiac form and function. *Physiol Rev* 87: 1285–1342.

Souders CA, Bowers SLK, Baudino TA (2009) Cardiac fibroblasts: the renaissance cell. *Circ Res* 105: 1164–1176.

Srinivasula MS, Ashwell JD (2008) IAPs: What's in a name? *Mol Cell* 30:123-135.

Stone JR, Yang S (2006) Hydrogen peroxide: a signalling messenger. *Antioxid Redox Signal* 8: 243–270.

Su HF, Samsamshariat A, Fu J, Shan YX, Chen YH, Piomelli D, Wang PH (2006) Oleylethanolamide activates Ras-Erk pathway and improves myocardial function in doxorubicin-induced heart failure. *Endocrinology* 147: 827–834.

Szegezdi E, Logue SE, Gorman AM, Samali A (2006) Mediators of endoplasmic reticulum stress-induced apoptosis. *EMBO Rep* 7:880–885.

Tait SWG, Green DR (2010) Mitochondria and cell death: outer membrane permeabilization and beyond. *Nature Reviews Mol Cell Biol* 11: 621–632.

Takeda N, Manabe I, Uchino Y, Eguchi K, Matsumoto S, Nishimura S, Shindo T, Sano M, Otsu K, Snider P, Conway SJ, Nagai R (2010) Cardiac fibroblasts are

essential for the adaptive response of the murine heart to pressure overload.*J Clin Invest* 120: 254–65.

Tang G, Minemoto Y, Dibling B, Purcell NH, Li Z, Karin M, Lin A (2001) Inhibition of JNK activation through NF-κB target genes. *Nature* 414:313–317.

Tay KH, Jin L , Tseng HY, Jiang CC, Ye Y, Thorne RF, Liu T, Guo ST, Verrills NM, Hersey P, Zhang XD (2012) Suppression of PP2A is critical for protection of melanoma cells upon endoplasmic reticulum stress *Cell Death Dis* 3: e337 doi:10.1038/cddis.2012.79.

Temme A, Rieger M, Reber F, Lindemann D, Weigle B, Diestelkoetter-Bachert P, Ehninger G, Tatsuka M, Terada Y, Rieberet EP (2003) Localization, dynamics, and function of survivin revealed by expression of functional survivinDsRed fusion proteins in the living cell. *Mol Biol Cell* 14:78–92.

Terada K, Kaziro Y, Satoh T (2000) Analysis of Ras-dependent signals that prevent caspase-3 activation and apoptosis induced by cytokine deprivation in hematopoietic cells. *Biochem Biophys Res Commun* 267:449 – 455.

Testa M, Yeh M, Lee P, Fanelli R, Loperfido F, Berman JW, LeJemtel TH (1996) Circulating levels of cytokines and their endogenous modulators in patients with mild to severe congestive heart failure due to coronary artery disease or hypertension. *J Am Coll Cardiol* 28:964–971.

Thorburn A (2004) Death receptor-induced cell killing.*Cell Signal* 16: 139 – 144.

Thum T, Gross,Fiedler J, Fischer T, Kissler S, Bussen M, Galuppo P, Just S, Rottbauer W, Frantz S, Castoldi M, Soutschek J, Koteliansky V, Rosenwald AM, Basson MA, Licht JD, Pena JTR, Rouhanifard SH, Muckenthaler MU, Tuschl T, Martin GR, Bauersachs J, Engelhard S (2008) MicroRNA-21 contributes to myocardial disease by stimulating MAP kinase signalling in fibroblasts. *Nature* 456: 980-984.

Tsuruta F, Masuyama N, Gotoh Y (2002) The phosphatidylinositol 3-kinase (PI3K)–Akt pathway suppresses Bax translocation to mitochondria. *J Biol Chem* 277:14040 – 14047.

Van den Borne SWM, Javier D, Matthijs BW, Verjans J, Hofstra L, Narula J (2010) Myocardial remodeling after infarction: the role of myofibroblasts. *Nat Rev Cardiol* 7: 30–37.

Varfolomeev E, Blankenship JW, Wayson SM, Fedorova AV, Kayagaki N, Garg P, Zobel K, Jasmin N. Dynek JN, Elliott LO, Heidi J.A. Wallweber HJA, Flygare JA, Fairbrother WJ, Deshayes K, Vishva M. Dixit VM, Vucic D (2007) IAP antagonists induce autoubiquitination of c-IAPs, NF-κB activation, and TNFα-dependent apoptosis. *Cell* 131: 669–681.

Varfolomeev E, Goncharov T, Maeccker H, Zobel K, Komuves LG, Deshayes K, Vucic D. (2012) Cellular inhibitors of apoptosis are global regulators of NF-κB and MAPK activation by members of the TNF family of receptors. *Sci Signal* 216: p.ra22.

Verhagen AM, Coulson EJ, Vaux D (2001) Inhibitor of apoptosis proteins and their relatives: IAPs and other BIRPs. *Genome Biology* 2: 3009.1–3009.10.

Visconti RP and Markwald RR (2006) Recruitment of new cells into the postnatal heart: potential modification of phenotype by periostin. *Ann N Y Acad Sci* 1080:19-33.

Walker CA and Spinale FG (1999) The structure and function of the cardiac myocyte: a review of fundamental concepts. *J Thorac Cardiovasc Surg* 118: 375-382.

Wang T, Hu YC, Dong S, Fan M, Tamae D, Ozeki M, Gao Q, Gius D, Li JJ (2005) Co-activation of ERK, NF-κB and GADD45β in response to ionizing radiation *J Biol Chem* 280: 12593-12601.

Weber KT (1989).Cardiac interstitium in health and disease: the fibrillar collagen network. *J Am Coll Cardiol* 13: 1637-1652.

Weber KT, Sun Y, Katwa LC, Cleutjens JP (1995) Connective tissue: a metabolic entity? *J Mol Cell Cardiol* 27: 107-20.

Weber KT, Sun Y, Bhattacharya SK, Ahokas RA, Gerling IC (2013) Myofibroblast-mediated mechanisms of pathological remodelling of the heart. *Nat Rev Cardiol* 10: 15–26.

Wencker D, Chandra M, Nguyen K, Miao W, Garantziotis S, Factor SM, Shirani J, Armstrong RC, Kitsis RN (2003) A mechanistic role for cardiac myocyte apoptosis in heart failure. *J Clin Invest* 111:1497-1504.

Wessels A and Perez-Pomares JM (2004) The epicardium and epicardially derived cells(EPDCs) as cardiac stem cells. *Anat Rec A Discov Mol Cell Evol Biol* 276:43-57.

Whittermore ER, Loo DT, Watt JA, Cotman CW (1995). A detailed analysis of H_2O_2-induced cell death in primary neuronal culture. *Neuroscience* 67: 921-932.

Willingham MC. Fluorescence labeling of intracellular antigens of attached or suspended tissue-culture cells. In: Immunocytochemical methods and protocols, Humana press, pp-113-129.

Wirawan E, Berghe TV, Lippens S, Agostinis P , Vandenabeele P (2012) Autophagy: for better or for worse. *Cell Research* 22:43-61.

Wu D, Chen B, Parihar K, He L, Fan C, Zhang J, Liu L, Gillis A, Bruce A, Kapoor A, Tang D (2006) ERK activity facilitates activation of the S-phase DNA damage checkpoint by modulating ATR function. *Oncogene* 25: 1153–1164.

Xu S, Bayat H, Hou X, Jiang B (2006) Ribosomal S6 kinase-1 modulates interleukin-1β-induced persistent activation of NF-κB through phosphorylation of IκBα *Am J Physiol Cell Physiol* 291: C1336–C1345.

Yu LF, Wang J, Zou B, Lin MC, Wu YL, Xia HH, Sun YW, Qing Gu Q, He H, Lam SK, Kung HF, Wong BCY (2007) XAF1 mediates apoptosis through an extracellular signal-regulated kinase pathway in colon cancer. *Cancer* 109: 1996−2003.

Zelarayan L, Renger A, Noack C, Zafiriou M-P, Gehrke C, van der Nagel R, Dietz R, de Windt L, Bergmann MW (2009) NF-κB activation is required for adaptive cardiac hypertrophy. *Cardiovasc Res*.84: 416–424.

Zha J, Harada H, Yang E, Jockel J, Korsmeyer SJ (1996) Serine phosphorylation of death agonist Bad in response to survival factor results in binding to 14-3-3 not Bcl-X_L. *Cell* 87: 619 – 628.

Zhang X, Azhar G, Nagano K, Wei JY (2001) Differential vulnerability to oxidative stress in rat cardiac myocytes versus fibroblasts *J Am Coll Cardiol* 38:2055–2062.

Zhang Y, Tocchetti CG, Krieg T, Moens AL (2012) Oxidative and nitrosative stress in the maintenance of myocardial function. *Free Radical Biol Med* 53: 1531–1540.

Zhao L, Eghbali-Webb M (2001) Release of pro- and anti-angiogenic factors by human cardiac fibroblasts: effects on DNA synthesis and protection under hypoxia in human endothelial cells. *Biochim Biophys Acta* 1538: 273-282.

Zhao X, Laver T, Hong SW, Twitty GB, DeVos A, DeVos M, Benveniste EN, Nozell SE (2011) An NF-κB p65-cIAP2 link is necessary for mediating resistance to TNF-α-induced cell death in gliomas. *J Neurooncol* 102: 367-381.

Zhimin Lu, Shuichin Xu (2006) ERK1/2 MAPK in Cell Survival and Apoptosis. Critical Review.*IUBMB Life* 58:621-631.

Zuo L, Clanton TL (2005) Reactive oxygen species formation in the transition to hypoxia in skeletal muscle. *Am J Physiol Cell Physiol* 289: C207-C216.

List of Publications

- **Linda Philip**, K Shivakumar (2013) cIAP-2 protects cardiac fibroblasts from oxidative damage: An obligate regulatory role for ERK1/2 MAPK and NF-κB. *J Mol Cell Cardiol* doi: 10.1016/j.yjmcc.2013.06.009

- M Sangeetha, Malini S Pillai, **Linda Philip**, Edward G Lakatta, K Shivakumar (2011) NF-κB inhibition comprises cardiac fibroblast viability under hypoxia. *Exp Cell Res* 317: 899-909.